Iiro Pitkälä

SHEAR ZONES AND STRUCTURAL ANALYSIS OF THE LOIMAA AREA, SW FINLAND

Geologian pro gradu –tutkielma

Turku 2019

University of Turku
Faculty of Science and Engineering
Department of Geography and Geology

PITKÄLÄ, IIRO: Shear zones and structural analysis of the Loimaa area, SW Finland

MSc thesis, 72 pages
40 ECTS, Geology
Supervisors: Pietari Skyttä, Markku Väisänen and Jaakko Kara
June 2019

The study area is located in the western part of the Häme belt, where deformation has partitioned into folded- and sheared domains. The N-S and the ENE-WSW striking shear zones form the most prominent structures. In areas with lesser shear zone deformation, the regional scale synforms and antiforms can be distinguished. The main goals of this study are: (i) to map the structural features, determine their evolution and draw a structural map within the study area, (ii) determine the kinematics of the two major shear zones and their correlation with other nearby shear zones, (iii) determine the relationship between the shear zones and folds, (iv) determine the age and temperature of the shearing. Three regional-scale folded areas can be distinguished in addition to the two shear zones. These folds and shear zones are inferred to characterize separate deformation phases of the same orogenic event. The folds are parts of the continuous fold chain which has formed due to NW directed compression prior to the shear zones. In the central area the shear zone deformation merges with the fold structures, which has caused a very complex crustal structure. Both of the shear zones characterize mainly oblique dip-slip shear sense under ductile conditions. The west-side-up shear sense seems dominant within the N-S striking shear zone, while in ENE-WSW shear zone it is the south-side-up. The N-S striking shear zone could have merged with the Kynsikangas and Kolinummi shear zones due to the reactivation of shearing forming one major shear zone. The ENE-WSW striking shear zone is interpreted to be a part of the Hämeenlinna shear zone in its western part. Based on the dynamic quartz recrystallization the deformation temperature in the N-S striking shear zone is estimated between 480°C and 530°C, while in the ENE-WSW striking shear zone it is 420-480°C in the east and 300-380°C in the west. The attempted age determination of the N-S shearing was performed with U-Pb zircon geochronology from a syntectonic granite, from which at least three zircon populations were found. The youngest of these yielded weighted average and upper intercept ages of c. 1.87 Ga. However, all the populations are regarded inherited from the source.

Keywords: shear zone, shear sense, structural geology, fold, mylonite

Turun yliopisto
Luonnontieteiden ja tekniikan tiedekunta
Maantieteen ja geologian laitos

PITKÄLÄ, IIRO: Shear zones and structural analysis of the Loimaa area, SW Finland

Pro gradu -tutkielma, 72 sivua
40 op, geologia
Ohjaajat: Pietari Skyttä, Markku Väisänen ja Jaakko Kara
Kesäkuu 2019

Tutkimusalue sijaitsee Häme-vyöhykkeen läntisessä osassa, missä deformaatio on jakautunut hiertyneisiin ja poimuttuneisiin rakennekokonaisuuksiin. N-S- ja ENE-WSW-suuntaiset hiertovyöhykkeet muodostavat alueen huomattavimmat rakenteet. Syn- ja antiformit ovat kartalla erotettavissa alueilla joihin hiertodeformaatio ei ole vaikuttanut suuresti. Tämän tutkimuksen päätavoitteet ovat: (i) kartoittaa kallioperän rakenteet, päätellä niiden synty ja piirtää alueen rakennegeologinen kartta, (ii) määrittää kahden hiertovyöhykkeen kinematiikka sekä niiden yhteys muihin lähellä sijaitseviin hiertovyöhykkeisiin, (iii) määrittää hiertovyöhykkeiden ja poimujen välinen yhteys, (iv) määrittää hiertovyöhykedeformaation ikä ja lämpötila. Kahden hiertovyöhykkeen lisäksi voidaan erottaa kolme karttatason poimualuetta. Poimujen ja hiertovyöhykkeiden päätellään edustavan saman vuorijonopoimutuksen eri vaiheita. Poimut kuuluvat samaan poimuketjuun, joka on syntynyt ennen hiertovyöhykkeitä NW-suuntaisen kompression aiheuttamana. Hiertovyöhykkeiden deformaatio on kohdannut poimurakenteet ja aiheuttanut monimutkaiset rakenteet tutkimusalueen keskiosaan. Molempien hiertovyöhykkeiden liikkeiden päätellään olevan pääosin vinoa ”dip-slip” -tyylin liikettä duktiileissa olosuhteissa. N-S-suuntaisella hiertovyöhykkeellä länsilohko on kohonnut ylöspäin, kun taas ENE-WSW-suuntaisella hiertovyöhykkeellä etelälohko. N-S-suuntainen hiertovyöhyke saattaa olla yhdistynyt Kynsikankaan ja Kolinummen hiertovyöhykkeiden kanssa muodostaen yhtenäisen hiertovyöhykkeen hiertodeformaation uudelleenaktivoitumisen seurauksena. ENE-WSW-suuntaisen hiertovyöhykkeen päätellään kuuluvan Hämeenlinnan hiertovyöhykkeen läntiseen osaan. Kvartsin dynaamisen uudelleenkiteytymisen perusteella päätellään N-S-suuntaisen hiertovyöhykkeen deformaatiolämpötilan olleen 480-530°C, kun taas ENE-WSW-suuntaisen hiertovyöhykkeen 420-480°C idässä ja 300-380°C lännessä. N-S-suuntaisen deformaation ikä yritettiin määrittää zirkonien U-Pb-iänmääritysmenetelmällä syntektonisesta graniitista, josta löydettiin ainakin kolme zirkonipopulaatiota. Nuorimman populaation painotetuksi keskiarvoiäksi ja yläleikkausiäksi määritettiin n. 1.87 Ga. Kaikkien populaatioiden arvellaan kuitenkin periytyneen vanhemmista lähteistä.

Asiasanat: hiertovyöhyke, hiertoliike, rakennegeologia, poimu, myloniitti

Table of contents

1. Introduction 1
1.1 Orogenic gold and shear zones 1
1.2 Gold in the Häme belt and its relation to the present project 2
2. Geological setting of the study area 4
2.1 Fennoscandian shield 4
2.2 The Svecofennian orogeny 5
2.3 The Häme belt 7
2.4 Main lithological features within the Loimaa area 10
2.5 Shear zones 11
3. Methods 12
3.1 Field work 12
3.2 Thin sections 14
3.3 Age determination of the N-S shear zone deformation 14
3.4 Geophysical maps 15
4. Results 15
4.1 Overview of the area 15
4.1.1 Structural data 17
4.2 Alastaro shear zone 18
4.2.1 D1 subarea 19
4.2.2 D2 subarea 21
4.2.3 D3 subarea 24
4.2.4 D4 subarea 27
4.3 Kankaanranta shear zone 30
4.4 Regional fold patterns 36
4.4.1 Oripää fold 36
4.4.2 Alastaro fold 40
4.4.3 North fold 42
5. Microscale kinematics 46
5.1 Alastaro SZ 47
5.2 Kankaanranta SZ. 51
6. Alastaro shear zone U-Pb zircon analysis 54
7.Discussion 59
7.1 Geometry and kinematics of the studied shear zones 59
7.2 Folds and their relation to the shearing observed in this study 60
7.3 Correlation with the existing models of crustal evolution in SW Finland 63
7.3.1 Correlation of the Alastaro and Kankaanranta shear zones with other known major shear zones 63
7.3.2 Temperature and timing of deformation 64
7.3.3 Inferred tectonic model 65
7.4 The sources of error 67
8. Conclusions 67
9. Acknowledgements 68
References 69

1. Introduction

1.1 Orogenic gold and shear zones

Orogenic gold deposits are the most common and important type of gold deposits in Finland. Most significant deposits have formed in the late Archaean and during the final stages of the Svecofennian orogeny (Ojala 2008). Globally, deposits in Phanerozoic sedimentary rocks are also important (Groves 1998). Orogenic gold deposits have formed by fluid migration at tectonic plate margins during continental collision or accretion and, therefore, in compressional or transpressional environments. When classified by P/T conditions during ore formation, epizonal (<6 km), mesozonal (6-12 km) and hypozonal (>12 km) subtype nomenclature are in use (Gebre-Mariam *et al.* 1995; Groves *et al.* 1998; Goldfarb *et al.* 2005). Orogenic gold occurs in rocks with different metamorphic grade, but according to global observations the greenschist facies rocks are the most common host rocks (Groves *et al.* 1998). However, the metamorphic grade of the Archaean host rocks varies from prehnite-pumpellyite to lower granulite facies (Groves 1993). For example, the hypozonal orogenic gold deposits often occur in mid-amphibolite or lower-granulite facies rocks (Gebre-Mariam *et al*. 1995; Groves 1998). Orogenic gold is structurally controlled and occurs commonly in quartz vein systems. These vein systems have formed when gold-transferring aqueous carbonic fluids have ascended along channels. The channels have been formed during shearing and faulting in the later stages of orogenies. These mineralisations are syn- to post-tectonic in relation to peak metamorphism. Mineralisations occur usually in second or third order structures, within or near major deformation zones (McCuaig & Kerrich 1998). Typical gold-bearing quartz veins contain 3-5% sulfide minerals and up to 5-15% carbonate minerals. The greenschist facies host rocks sometimes contain albite, white mica, chlorite, scheelite and tourmaline minerals. In addition to Au, variable enrichments in As, B, Bi, Hg, Sb, Te are common in quartz veins. Slightly higher concentrations of W, Cu, Pb and Zn can also occur in these veins compared to the surrounding barren rocks (Groves 1998).

Shear zones are high deformation zones, with planar or curviplanar shape. Their length to width ratio is more than 5 : 1. In these zones deformation has transected the surrounding rocks of lower strain. Shear zone deformation type can be divided to ductile, brittle, semi-brittle and brittle-ductile depending on P/T conditions, strain degree and rock composition/strength (Ramsay & Huber 1987). Ductile shear zones are continuous

deformation zones, with progressive increase of strain towards the core, while brittle shear zones are discontinuous sharp physical rupture dominated zones. Brittle shear zones are also known as fault zones. Ductile shear zones are dominated by plastic structures formed by ductile flow, such as folds and grain asymmetries, while brittle shear zones are characterized by typical brittle deformation structures, such as fractures and grain breaking or rotation (Fossen & Cavalcante 2017). The brittle-ductile transition zone is located approximately at a depth of 10-15 km within the lithosphere (Fossen 2010). Semi-brittle shear zones are characterized by pressure solutions and cataclastic flow. In brittle-ductile shear zone, the ductility and fragility are both represented at approximately equal amounts. Many shear zones contain both types of deformation and therefore, the classification is based on the more frequent structures (Fosse & Cavalcante 2017; Homberg *et al*. 2017). The gold controlling structures within shear zones are variable because of the difference in elasticity (brittle-ductile) and shear type (dip-slip, strike-slip and oblique slip), which causes the fluid channels to form along very complex secondary structures (Groves 1998).

1.2 Gold in the Häme belt and its relation to the present project

Interest towards mineral exploration, especially towards gold, has grown in southern Finland because of the increasing number of gold occurrences, prospects and mines in the Uusimaa, Häme, Pirkanmaa and Tampere belts. The Geological Survey of Finland (GTK) has had a main role in finding new possible economical gold deposits in the area, especially during two main gold exploration projects, which were running between 1998-2002 and 2003-2007 (Grönholm & Kärkkäinen 2012). However, the geoscientific research concerning gold bearing ores and other economically valuable mineralisations in southern Finland has remained active until this day. Gold reserves in the Häme belt have been estimated to be approximately 170 t, whereof 70 t would occur in the orogenic gold deposits such as the Jokisivu deposit and the rest (100 t) would occur in porphyric mineralisations. However, the known reserves in the Häme belt are only 11 t and they have been found from the orogenic type of deposits. The estimates indicate that 80 % of orogenic gold in the Häme belt is yet to be found. Off course, these estimates are not very precise, but rather directional. New geological data are expected to support companies in their investments and exploration projects within the Häme area. The regional authorities and residents of the municipalities will gain insights into the status of these projects. At

the moment, only the Jokisivu gold mine and the carbonate mines in Vampula are operating (Tiainen *et al*. 2017).

GTK started a two-year collaborative project with the University of Turku (UTU) in 2017. First part of fieldwork was made during summer 2017 and the second fieldwork period was organized in summer 2018. Purpose of the project is to continue the geological mapping of the Häme belt in order to form a better understanding of the structural and lithological features within the area and also their linkages to gold mineralisations. The project aims to study the structure, chemical composition, geological evolution and mineral occurrences, and will provide new important tools for choosing new targets in the area for future exploration, from the gold exploration point of view. Another main objective was to train new geoscientist within a project closely related to economical ore geology. In the first year the project involved staff members from GTK and UTU and two MSc students and one PhD student from UTU. The project had three main objectives: (1) structural mapping of the major N-S and ENE-WSW trending shear zones to characterize their kinematic features, (2) structural and lithological mapping of the Uunimäki gold mineralisation and its linkage to structural evolution of the Häme Belt and (3) geochemical characterization of the mafic intrusions in the Häme Belt. This MSc thesis focuses on the first object, structural geology.

Three municipalities are located within the study area: Loimaa, Huittinen and Oripää. The major focus is on the N-S and ENE-WSW striking shear zones, which are the two major structural features in the western Häme belt. Before the two-month-long field season the shear zones were identified using geophysical survey data and previous field observations. These shear zones are assumed to represent the late Svecofennian E-W and N-S directed shearing within the southern Finland described by Väisänen & Skyttä (2007). Several map-scale folds were also identified from the geophysical survey data. Observations from aeromagnetic and lithological maps were supported with field observations. Tectonic measurements, stereographic projections and oriented thin sections are used in this study to form an understanding of the structural features and their evolution. In addition to the oriented samples, a sample for dating the shear activity was also collected from the N-S shear zone.

This study introduces the results, which are interpreted from the data collected during the field season in June and July of 2017. The results of this study encompasses structural map of the study area, kinematics of the two shear zones, nature of the major map-scale

folds and U-Pb zircon age for the syntectonic granite, which was interpreted to represent the age of the N-S shearing within the study area.

2. Geological setting of the study area

2.1 Fennoscandian shield

Eastern and northern Europe and western Russia belong to the Precambrian East European craton (e.g. Vaasjoki *et al*. 2005) which consists of three domains (Fig. 1): Fennoscandia, Sarmatia and Volgo-Uralia (Gorbatschev & Bogdanova 1993). Bedrock of Finland covers approximately one third of the Fennoscandian shield, which can be split to four different areas, which are the Archean, the Svecofennian, the Sveconorwegian and the Transscandinavian Igneous Belt (TIB). TIB is a collection of plutonic intrusions between the Svecofennian and Sveconorwegian provinces (Vaasjoki *et al*. 2005).

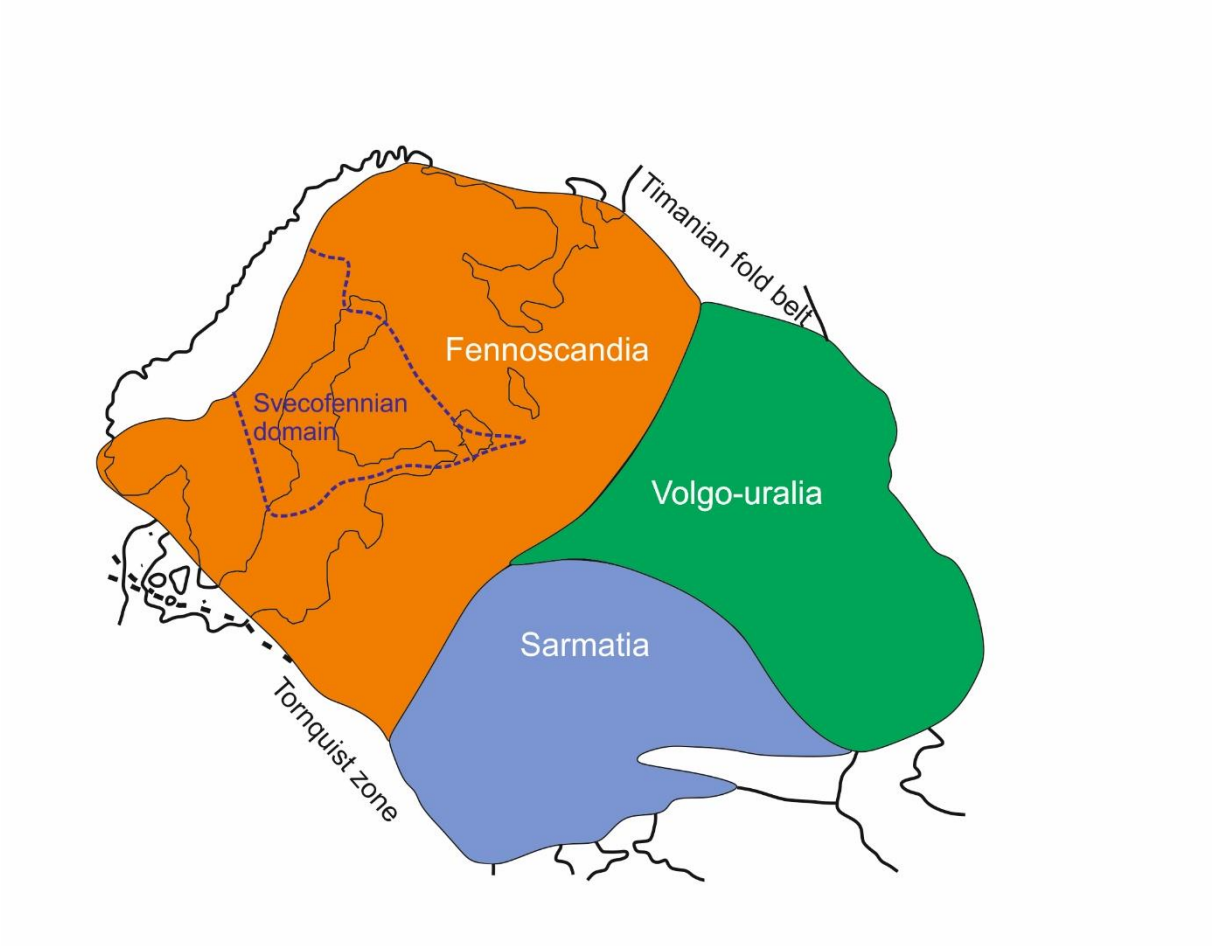

Fig. 1. The three crustal segments of the East European craton and location of the Svecofennian domain. Modified after Gorbastchev & Bogdanova (1993)

2.2 The Svecofennian orogeny

Central part of the Fennoscandian shield consists of Paleoproterozoic ~1.93-1.80 Ga rocks forming the Svecofennian domain, which covers the southern and central parts of Finland (Lahtinen *et al*. 2005). In its entirety the Svecofennian domain covers an area of 800 km by 800 km in Finland and Sweden (Kähkönen 2005). The Svecofennian domain in Finland can be divided into several subdomains (Fig. 3): the Vaasa Complex, the Central Finland Granitoid Complex and the Savo, Tampere, Pirkanmaa, Häme and Uusimaa belts. The Paleoproterozoic rocks of the Svecofennian domain are bordered from the Archean rocks of the Karelian craton by the complex NW-SE striking suture zone (Nironen *et al*. 2016). Key points of the two models, which explain the formation of the Svecofennian orogeny are summarised below and their differences between 1.91 Ga and 1.85 Ga are visualized in Fig. 2.

Lahtinen *et al*. (2005) suggest a four-stage orogenic evolution with five different partially overlapping orogenic events, in which the Paleoproterozoic rocks were formed. Rifting of the Karelian craton started at 2.5-2.4 Ga, which is substantiated by the anorthositic and other basic intrusions in northernmost Fennoscandia. These rocks were formed during rifting (Daly *et al*. 2001; Lahtinen *et al*. 2005), which finally evolved to continental breakup at around 2.06 Ga. The collision of the Kola and Karelian cratons (the **Lapland-Kola orogeny**), collision of the Karelian craton with both the Norrbotten craton and the Keitele microcontinent and also the docking of the Bothnia microcontinent (the **Lapland-Savo orogeny**) were included in the microcontinent accretion stage. After this the newly-formed Archean-Paleoproterozoic complex collided with the Bergslagen microcontinent starting the **Fennian orogeny**. The Häme belt is interpreted to have formed at ~1.89 – 1.87 Ga of this stage. The model proposes two ongoing subduction zones in the south and west. The crust in the boundaries of the subduction zones underwent an extension, which started around 1.86 Ga. This event was followed by oblique collision between Fennoscandia and Sarmatia at 1.84-1.80 Ga, which is known as the **Svecobaltic orogeny**. The Svecobaltic orogeny was divided into two different convergent environments by a major crustal shear zone: in the southwest to a retreating Andean-type subduction zone and in the southeast to a transpressional regime. The central and northern parts of the western edge of the Fennoscandian Shield were modified by the collision with Amazonia at 1.82-1.80 Ga during the **Nordic orogeny.** Even after the orogenic stabilization at 1.79 – 1.77 Ga, the Gothian orogeny modified the southwestern boundary of the

Fennoscandian shield at 1.73-1.55 Ga. The orogenic evolution can thus be divided to four stages: (A) microcontinent accretion stage at 1.92-1.87 Ga, (B) continental extension stage at 1.86-1.84 Ga, (C) continent-continent collision stage at 1.84-1.79 Ga and (D) orogenic collapse and stabilization stage at 1,79-1,77 Ga (Lahtinen *et al*. 2005).

According to Hermansson *et al*. (2008), there was only one subduction zone during all tectonic phases throughout the Svecofennian orogeny, which was situated in the northwest in relation to the major continent. The back-arc extension, which was caused by the subduction hinge retreat at 1.91–1.89 Ga is characterized by eruption of both mafic and felsic lavas and formation of clastic sedimentary rocks. The hinge migration started to cease at approximately between 1.89 and 1.87 Ga and concurrently started to change direction resulting in less voluminous extension. At this time the voluminous calc-alkaline arc magmatism took place. The 1.89-1.87 Ga interval also represents the time of plutonic activity in the Häme belt. Subsequently, the compression dominated the back-arc basin between 1.87 and 1.86 Ga and was caused by the intensified hinge travel. Extensional phase was followed at 1.86 Ga, when the hinge retreat started again causing a bimodal magmatism and second depositional phase for the clastic sedimentary rocks. The model does not go into details with events younger than this, but intruding suite of subvolcanic rocks is interpreted at 1.86-1.85 Ga during the ceasing of the aforementioned deformation. Also, one or more major deformation events are suggested to have taken place after this, possibly after 1.83 Ga.

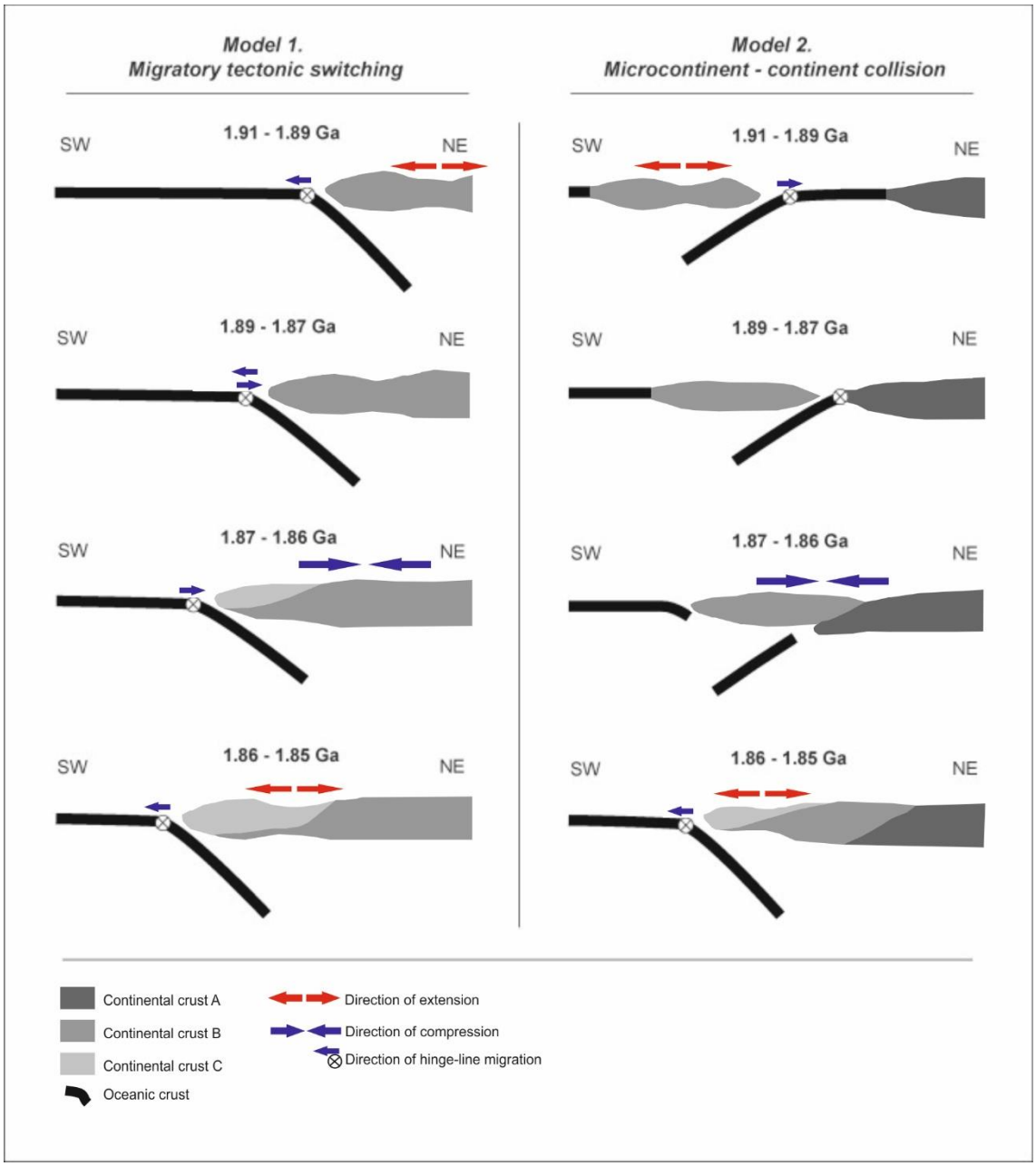

Fig. 2. Differences between the migratory tectonic switching model (Hermansson *et al*. 2008) and the microcontinent - continent collision model (Lahtinen *et al*. 2005) at 1,91-1,85 Ga. Continental crusts A-C represent different lithotectonic units in central Sweden. Modified after Hermansson *et al*. (2008).

2.3 The Häme belt

The Häme belt is located in the middle of the Fennoscandian shield or more precisely in the Paleoproterozoic Svecofennian domain in SW Finland (Lahtinen 1996). Most of the rocks in the Häme belt have formed during the magmatic arc stage of the orogeny (e.g. Väisänen *et al*. 2002; Kähkönen 2005; Lahtinen *et al*. 2005; Saalmann *et al*. 2009). The Häme belt is also located between the Uusimaa belt in the north and the Pirkanmaa belt in the south (Fig. 3). Together the Häme belt and Uusimaa belt form the Southern

Svecofennian Arc Complex (SSAC), which is intervened by sedimentary basins (Kähkönen 2005). The Pirkanmaa belt is located in the boundary area between the SSAC and the Central Svecofennian Arc Complex (CSAC) and is proposed to be within a suture zone of these arcs in between the Tampere belt and the Häme belt, but the exact location of the suture zone is not known (Lahtinen 1994; Lahtinen 1996; Väisänen *et al*. 2002; Saalman *et al.* 2009). The Pirkanmaa belt represents the accretionary complex, which accreted to a continental nucleus of the Keitele microcontinent (Lahtinen *et al.* 2005; Saalmann *et al.* 2009), while the Häme belt most likely characterizes the volcanic arc magmatism at 1.90-1.88 Ga, when an oceanic plate was subducted towards the south, north of the combined Tavastia island arc and the Bergslagen microcontinent (Lahtinen *et al*. 2005).

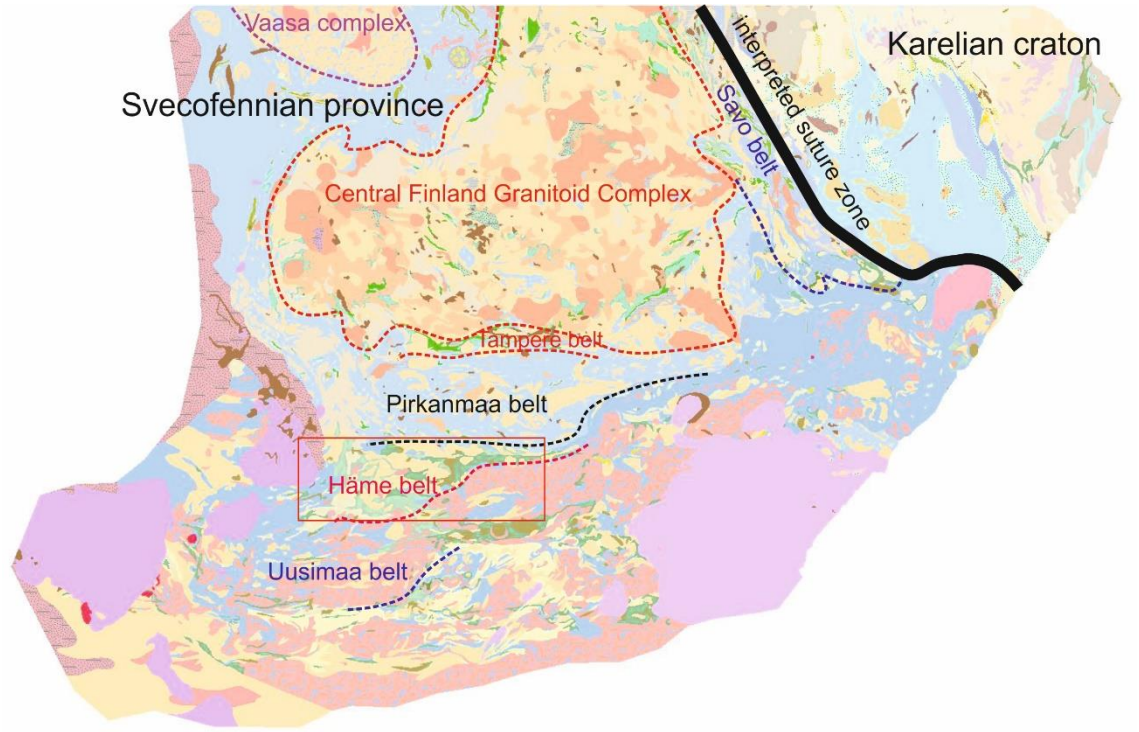

Fig. 3. Location of the Häme belt and locations/coarse outlines of other major belts and complexes within the Svecofennian domain in southern and central Finland. The black line represents the interpreted suture zone between the Svecofennian domain and the Archean Karelian craton. Modified after Korsman *et al*. (1997).

The Häme belt characterizes equal amounts of supracrustal and plutonic rocks. The granodiorites and granites are more common than diorites or gabbros, the most common is the deformed granodiorite. However, the voluminous granodiorites and granites are usually associated with gabbros and diorites. Some granitoid intrusions are peraluminous (A/CNK $\geq$ 1.0), while intrusions surrounding them have mainly lower aluminium

contents (A/CNK ≤ 1.0). These intrusions and their diorite and gabbro associations are surrounded by metavolcanic and sedimentary rocks. (Mäkitie *et al*. 2016). Volcanic rocks are the most common supracrustal rocks of the Häme belt (Sipilä & Kujala 2014). Their compositions vary between basaltic and rhyolitic, andesites being the most common. The uralite and plagioclase porphyritic basaltic lavas, which grade into andesites in some parts, are a typical feature of the Häme belt (Kähkönen 2005). Hakkarainen (1994) divided volcanic rocks into the Häme and Forssa suites. Sipilä & Kujala (2014) classified the volcanic rocks of the belt using the Finstrati-classification, and divided them to four groups known as the Loimaa, Renkajärvi, Forssa and the Nuutajärvi suites. Rocks of the Loimaa suite are mainly banded hornblende gneisses and amphibolites, and they have experienced higher grade of metamorphism than rocks within the Forssa suite (Nironen 1999; Sipilä & Kujala 2014). Andesitic rocks are the most common in the Forssa suite, even though the compositions vary from basaltic to rhyolitic. Basaltic volcanic rocks are most common next to the Forssa gabbro. These volcanic rocks are characterized by calc-alcaline affinities. In the Renkajärvi suite, mafic volcanic rocks are dominant. Percentage of intermediate rocks increases on upper stratigraphic levels. In some areas there are also felsic volcanic rocks, which occur as thin interlayers in mafic volcanic rocks. Unlike in the other areas, the felsic volcanic rocks are the most common in the Nuutajärvi suite. Some intermediate and mafic volcanic rocks occur only in the western and northern part of the Nuutajärvi suite. The turbiditic pelites are the most abundant. The epiclastic sediments and carbonatites are quite rare compared to other areas within the Svecofennides (Sipilä & Kujala 2014). Most of the aforementioned plutonic and supracrustal rocks are metamorphosed in amphibolite facies conditions (Hakkarainen 1994). Some sedimentary rocks are migmatized, especially within the Nuutajärvi suite. Still, primary structures are quite well preserved within some pelitic sedimentary and felsic volcanic rocks (Sipilä & Kujala 2014).

After 1998, seven different types of prominent mineral deposits have been identified in the Häme belt by GTK: the VMS-type Zn-Cu-Pb/Ag ores, porphyry Cu-Au ores, orogenic Au ores, Ni-Cu and Fe-Ti ores in gabbroic intrusions, LCT-pegmatites and Vampula carbonate rocks (Tiainen *et al*. 2017). Shear zones with different ages might structurally control the emplacement of the orogenic Au deposits (Saalmann *et al*. 2009, Saalmann *et al*. 2010, Mertanen & Karell 2011; Mertanen & Karell 2012). Rasilainen & Eilu (2016) used three-phased model by the USGS upgraded by Singer and Menzie (2010) and

mathematically estimated the amount of the undiscovered Cu, Zn, Ni and Au mineralisations to be approximately 17,5 t in the Häme Belt.

2.4 Main lithological features within the Loimaa area

The study area is located in the western part of the Häme belt (Fig. 4), which contains plutonic and supracrustal rocks at about equal amounts. Medium-grained equigranular tonalites and granodiorites are the most common plutonic rocks of the study area. In places they bear mafic enclaves and most likely represent the oldest plutonic rocks of the study area and the whole Häme belt (Nironen 1999). The U-Pb dating of the Uunimäki gabbro yielded and age of 1891±5 Ma, which makes it one of the oldest plutonic rocks within the belt in addition to the tonalities and granodiorites (Leskelä 2019). Intermediate and mafic volcanic rocks are predominant in the farthest southeast. Layered intermediate and felsic tuffites also become more common in the southernmost part. Migmatitic gneisses are common in the central part and also in the western part (Nironen 1999). Most of the mineral assemblages within the study area are suggesting an upper amphibolite facies metamorphism with slightly variating P-T conditions (Hakkarainen 1994; Nironen 1999; Hölttä & Heilimö 2017).

Granitoids are much more common than mafic plutonic rocks in the study area, which is a notable feature throughout the whole Häme belt (Mäkitie *et al*. 2016). In places the large quarz diorite intrusions differentiate into tonalite, so that they likely represent the same intrusion. The magnetite-bearing granite southwest of Alastaro causes a high positive anomaly to the aeromagnetic map. The granite has undergone varying degrees of deformation and grain size variates from fine-grained to pegmatitic. The granite contains tonalitic and gneissic xenoliths and expresses one of the highest positive magnetic anomalies in southern Finland (Nironen 1999). Granodiorites and tonalites are dominant rocks in the eastern and southeastern parts of the study area. These rocks are rich in biotite and contain lots of granitic veins and schist fragments (Mäkitie *et al*. 2016). Different sized pegmatitic to aplitic veins are very common in the area and they cross-cut both the host granite and the xenoliths. In the southwest the large 160 km^2 Pöytyä batholith (or Pöytyä granodiorite) consists mainly of granodiorite, porphyric granite and tonalite. Major part of the pluton is equigranular, medium-grained and the composition grades between granodiorite and tonalite. The central part consists of porhyritic granite. The

Oripää granite in western part of the area is pegmatitic in most parts and brecciates a medium-grained pervasively foliated tonalite (Nironen 1999).

Volcanic rocks in the study area belong to the Loimaa suite, which mainly consists of hornblende gneiss and amphibolites (Sipilä & Kujala 2014). A metavolcanic hornblende gneiss occurs in many parts and has massive uralite porphyritic interlayers, especially in the northeastern part. Common metasedimentary rocks in the central part are migmatitic K-feldspar-cordierite and some garnet-cordierite gneisses. In places assimilation has been so intense during migmatization, that it is hard to distinguish ortogneiss from paragneiss (Nironen 1999).

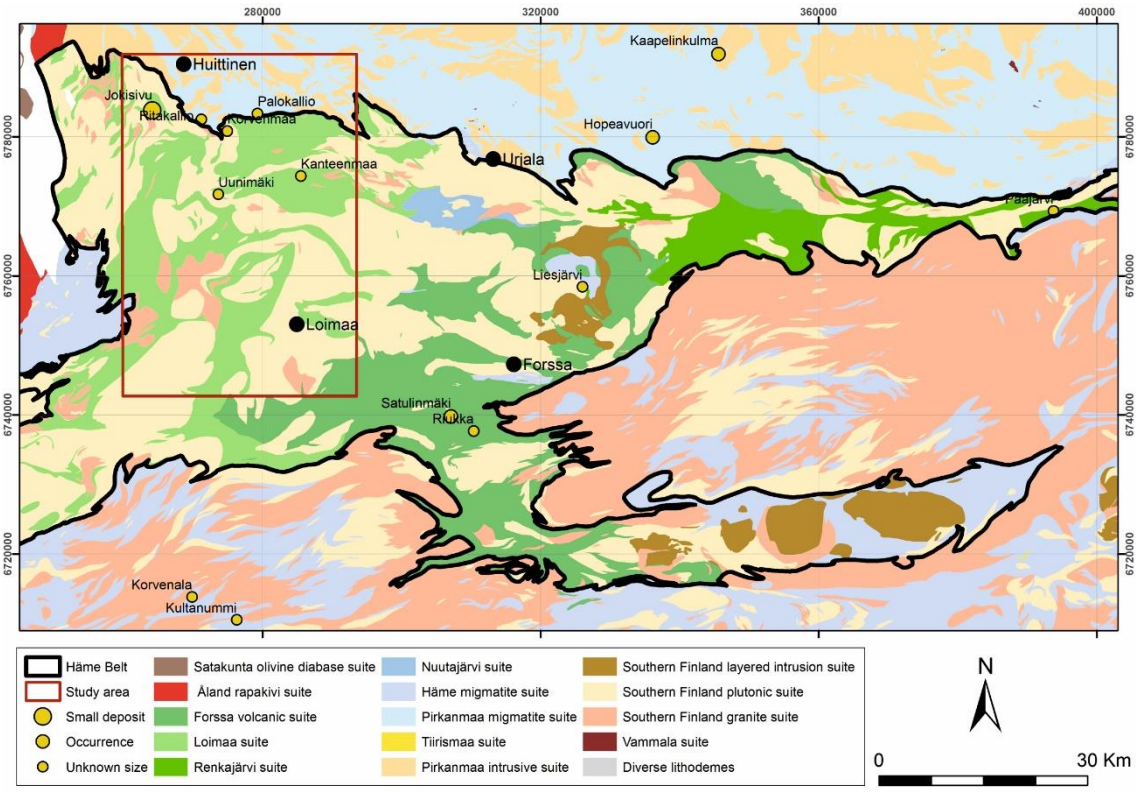

Fig. 4. Lithological units of the Häme belt and location of the study area (modified after Korsman *et al*. (1997) and gold deposits and prospects after Tiainen *et al*. (2017).

2.5 Shear zones

The N-S and ENE-WSW striking shear zones form two most prominent structural patterns in the study area. They are clearly visible as negative magnetic anomalies in the low-altitude aeromagnetic maps. Shear zone deformation is displayed by mylonites in proximity to the area of most intense shearing and further away by penetratively foliated plutonic and volcanic rocks. Orientations of these two shear zones correlate with the 1.84-

1.81 Ga shear zone network presented in Väisänen and Skyttä (2007). Nironen (1999) classified the N-S shear zone as a brittle structure.

3. Methods

3.1 Field work

A two months bedrock mapping period was organized during June and July 2017 within the Loimaa, Huittinen and Oripää areas. Participants from the UTU were two MSc students, Tuomas Leskelä and myself, a PhD student Jaakko Kara and two UTU staff members Pietari Skyttä and Markku Väisänen. The bedrock mapping was performed by the MSc students and PhD student while the staff members provided supervision. The main focus of the mapping was put into the N-S and ENE-WSW striking main shear zones and the Uunimäki gold prospect, which is located approximately in the intersection of the two shear zones.

A total of 484 bedrock observations (locations in Fig. 5) were recorded during the field season, from which 200 observation points were collected by myself. The rest were collected by Tuomas Leskelä and Jaakko Kara. The observations points were GPS-localized to EUREF-FIN-TM35FIN coordinate system with the GPS equipped Panasonic Toughbook field laptops provided by GTK. EUREF-FIN-TM35FIN is based on Universal Transverse Mercator projection and uses the GRS80 as a geodetic datum. The observations were linked to the KAPALO database used by GTK using the GIS-software ArcMap. All examined outcrops had their rock type, grain size, colour of the erosion surface, structural features and other features of interest recorded. To help the later recollection of the outcrops, a total of 345 field photos were taken and several outcrop sketches were drawn.

The main emphasis of the bedrock observations was on the tectonic measurements. Different planar and linear structures were measured from outcrops which include foliations, lineations, fold axes, axial surfaces, faults and in some outcrops, fractures and veins. The Freiberg geological compass was used and the data were declination corrected adding 7° to the measurements. A total of 32 oriented samples from rocks with mylonitic or sheared properties were collected using a hammer and wedge. The north arrow, horizontal line, cardinal direction of both sides of the sample and orientation of the lineation were drawn to the samples to preserve information of the original orientation.

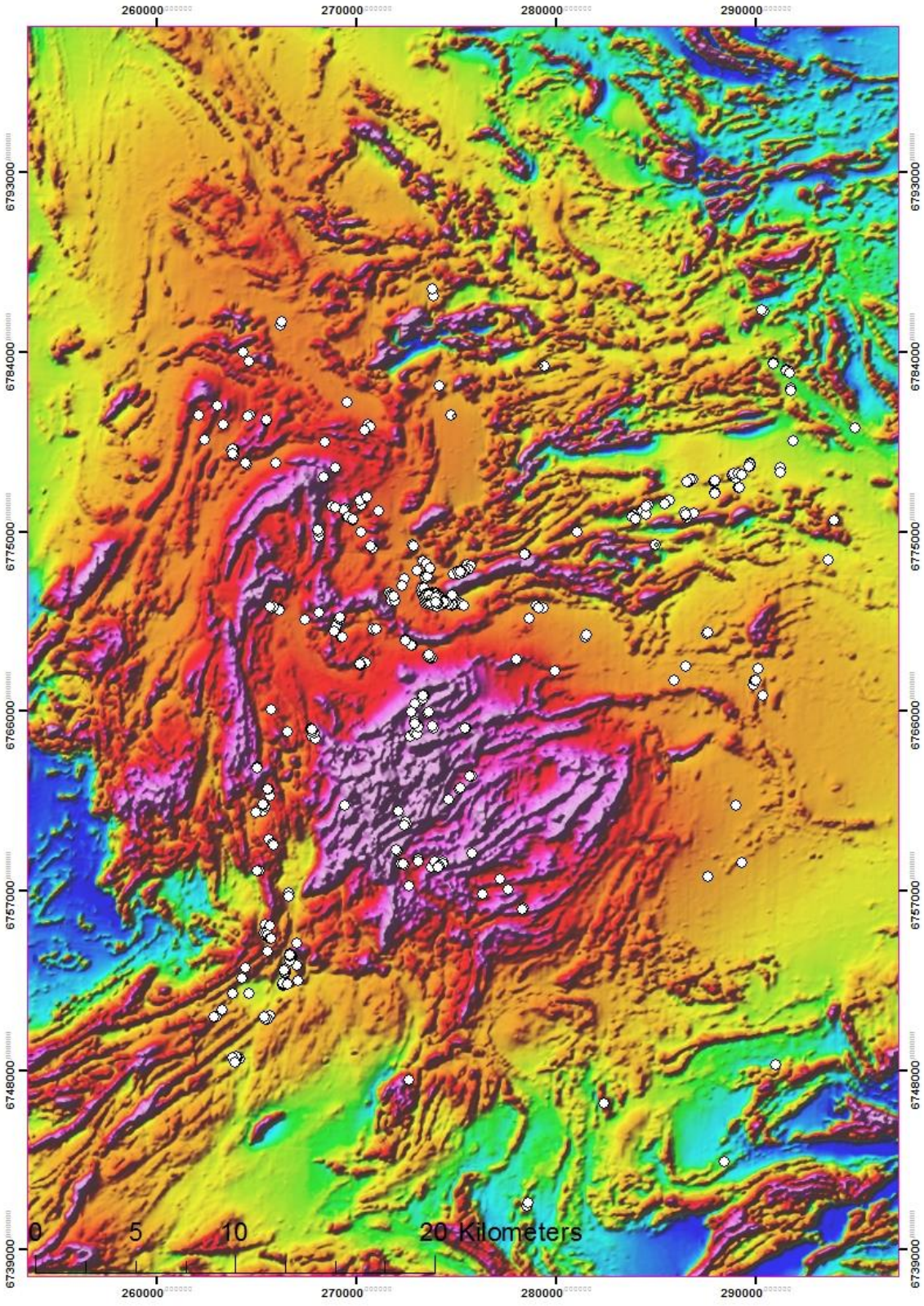

Fig. 5. Distribution of the field observations (white circles with black outlines) on pseudocoloured aeromagnetic anomaly map with shading towards NW. Map provided by GTK.

3.2 Thin sections

A total of 36 thin sections were made from oriented samples for kinematic analysis of the two studied shear zones. Samples were prepared and sawed by the author for the thin section production. MSc Niklas Tenovuo made all the thin sections in the facilities of the University of Turku. Thin sections were studied with polarized light microscope.

3.3 Age determination of the N-S shear zone deformation

A granite sample (IJPI-2017-35.1) was collected for geochronology. After the granite was crushed, the rock powder was panned and the heavy fraction was then separated with a hand magnet, heavy liquid and the Franz isodynamic magnetic separator. After this the best zircons were selected by hand picking and placed on a double-sided tape. The grains were mounted in epoxy resin and then sectioned and polished. Monazite was not found.

The BSE (Back-Scattered Electron) images were prepared for the zircons to target the spot analysis sites. The BSE imaging was done with a scanning electron microscope at Top Analytica Ltd. in Turku. With the help of the BSE images the grains with less core/rim zoning, weathering and micro fractures were selected. The analyses were performed in the Finnish Geosciences Research Laboratory at the Geological Survey of Finland, Espoo. The used instrument was Nu plasma AttoM single collector ICPMS connected to Photon Machine Excite laser ablation system (LAMS), which had a beam diameter of 15 μm, pulse frequency of 5 Hz and beam energy density of 2,5 J/cm^2. Due to 5 Hz pulse frequency the spot size diameter was 25 μm. The U-Pb analysis used three standards. Two of them were the Paleoproterozoic in-house standard A382 (1876±2) from a pyroxene bearing granite and Archean standard A1772 (2712±1) from a gabbro (Huhma *et al*. 2012). Third standard was the 609±1 GJ-1 standard (Jackson *et al*. 2004). The standards were run at regular intervals during the analysis at the beginning and end of each analytical session. The standards were used as concordant reference zircons when correcting the data for the background, laser-induced elemental fractionation, mass discrimination and drift in ion counter gains and reducing to the U-Pb isotope ratios.

The Glitter-software was used when performing the raw data reduction (Van Achterberg *et al*. 2001) and the in-house Excel spreadsheet was used in further data reduction for common lead correction and error propagation. For data plotting and age calculations Isoplot software (Excel add-in) was used (Ludwig 2003).

3.4 Geophysical maps

The field work area and some key locations were planned before the field work season. This was done with an aid of low-altitude aeromagnetic geophysical maps. The greyscale and pseudocolour (Fig. 5) versions were both used. The shear zones and folded domains are both visible in these maps. The maps were later used as a support in structural interpretations.

4. Results

4.1 Overview of the area

Structures of the Loimaa area form quite a heterogeneous entity. Figure 6 shows the conducted subdivisions into structurally consistent domains based on geophysics and structural measurements made during the field season. The most significant features of the area are two shear zones in the western and northeastern, and three major fold systems in the northwestern, central and southeastern parts. From A to F, the areas are here after called the North fold (A), the Uunimäki gold prospect (B), the Kankaanranta shear zone (C), the Alastaro shear zone (D1-D4), the Alastaro fold (E) and the Oripää fold (F). The Uunimäki gold prospect (B) is located immediately to the south of the western termination of the Kankaanranta shear zone. The resulting heterogeneous and complex structure of the Uunimäki area is described in more detail by Leskelä (2019).

Overall, the study area is characterized by steeply dipping planar structures. The most notable planar orientation trends are ENE-WSW in the northern part and the N-S and NNW-SSE in the western part. These relate to the zones with the most intense shearing in the study area. The most notable fold patterns in the NW are isoclinal and differentiate into more open type of folding in SE. Lineations and fold axes are mainly moderately or steeply plunging, with horizontal linear structures occurring in some parts. Lineations follow the plunges and azimuths of the nearby fold axes and in some parts also the major statistically defined fold axes of the regional scale folds.

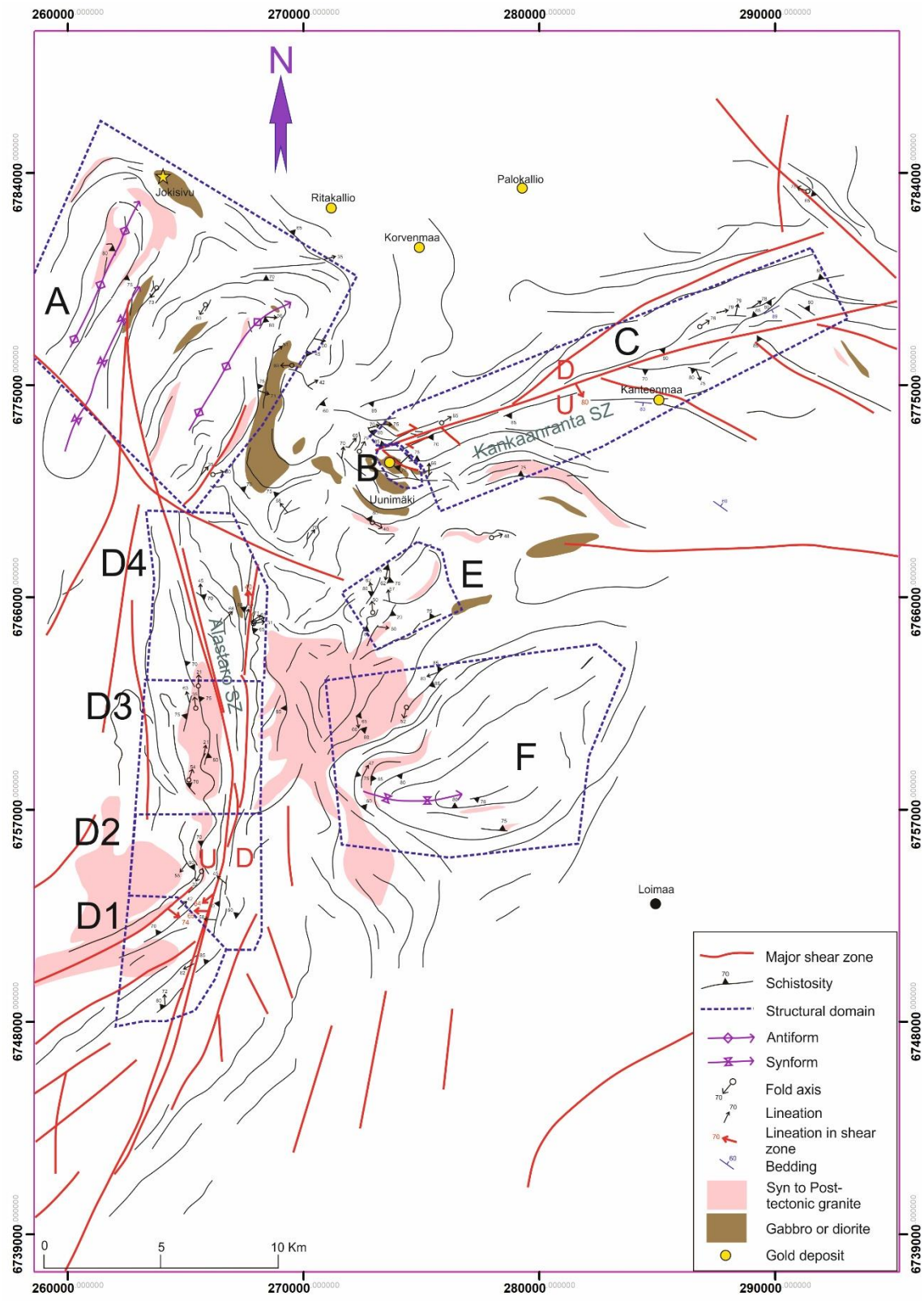

Fig. 6. Structural map of the study area and subdivision into structural domains: A = North fold, B = Uunimäki gold prospect, C = Kankaanranta shear zone, D1-D4 = Alastaro shear zone, E = Alastaro fold, F = Oripää fold. “U” and “D” refer to the up and down movements of the blocks on the opposing sides of the shear zones. Coordinate system is EUREF-FIN-TM35FIN.

4.1.1 Structural data

The structural data is more homogeneous after the subdivision (Figs. 7 & 8), but minor structural diversity still exists within the subareas. The pole to foliation densities are apparently similar in stereographic projections A, E, and F, which all represent the regional scale folds. The subareas within the Alastaro shear zone are characterized by approximately N-S structures, with some variation between the subareas D1-D4, related to the curvature of the shear zone. The structural data from the Kankaanranta shear zone (C) is quite heterogeneous, which is why the subdivision is not needed.

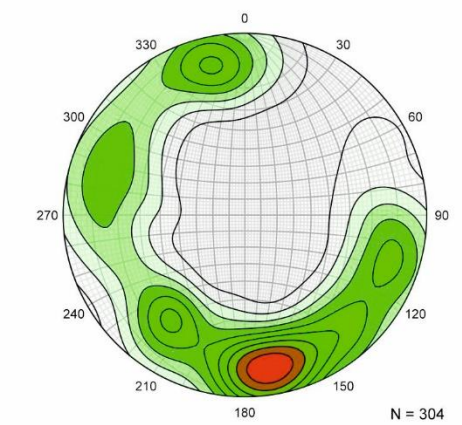

Fig. 7. Contoured pole to foliation densities from the whole study area. Lower hemisphere projection.

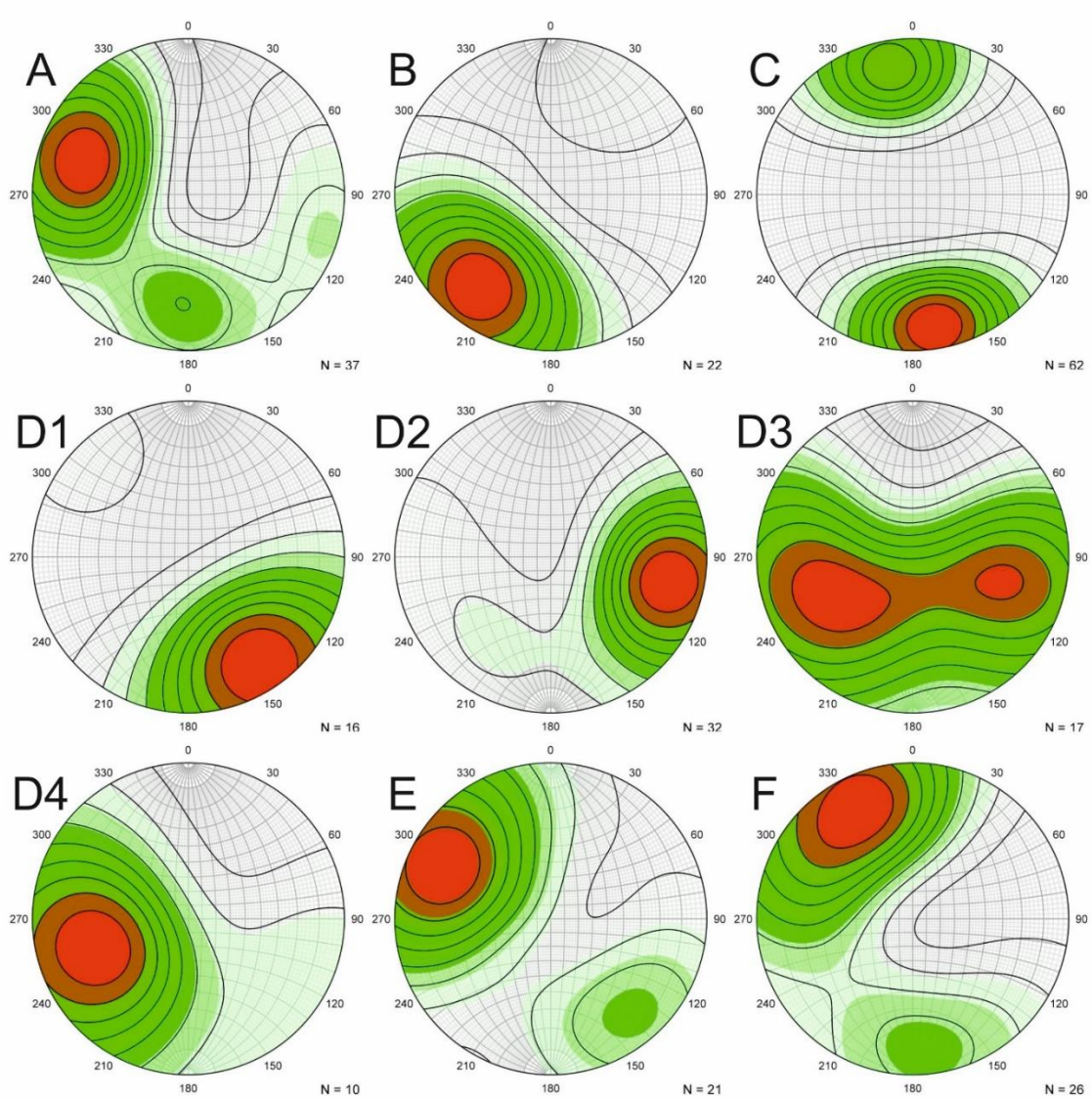

Fig. 8. Contoured pole to foliation densities from each of the subareas A-F: A = North fold, B = Uunimäki gold prospect, C = Kankaanranta shear zone, D1-D4 = Alastaro shear zone, E = Alastaro fold, F = Oripää fold. Lower hemisphere projections.

4.2 Alastaro shear zone

The Alastaro shear zone is a dominant structural feature in the western and southwestern part of the study area. It was subdivided into four subareas (D1-D4) due to variation of the structural data. Dominant planar and linear structures in each of the subareas are moderately to steeply inclined. Areas with most intense shear zone deformation are characterized by mylonitic features. From field observations the Alastaro SZ was interpreted to be a dip-slip feature with west-block up shear sense.

4.2.1 D1 subarea

Subarea D1 (Figs. 6 & 9) occurs within the southernmost part of the Alastaro SZ, where the regionally dominant structural trend is NE-SW striking. Most observations were made from outside the main shear zone and hence reflect the regional NE-SW structural trends. The foliations are NE-SW striking and steeply to subvertically dipping, the measured dips vary between 68° and 86°. The dominant dips are towards NW, which is contrasting to the other parts of the Alastaro SZ subareas (Sections 4.2.2-4.2.4). The dominant set of lineations cluster around vertical orientations but also show some variation in their plunges. In the southernmost part of the D1 area the lineations plunge steeply (72°) towards N whereas in the eastern part the lineations plunge moderately to steeply (52°-84°) towards E, ESE or SE. In the northern part of the subarea, lineations plunge moderately (42°) towards NE. The foliations and lineations within the shear zone are generally a bit steeper than the backround structures within subarea D1.

Penetrative foliation is prevalent but, gneissic banding, schistosity and zonal foliations were also observed from outcrops. Foliation intensity varies between moderate and strong. Lineations are characterized by moderate or strong alignment of minerals or mineral aggregates (Fig. 10A). Locally, the intensely lineated rocks define L-tectonites such as in eastern part of the D1 area (Fig. 10B), contrasting to the typical S- and LS-tectonic nature of the rocks within the Alastaro SZ area. Zonal isoclinal folding in volcanic rocks was observed in the northern and central parts of the D1 area (Fig. 10C-D). In some outcrops the folding occurred alone in pale leucosome veins and vein fragments. These outcrop-scale intrafolial folds occur in intermediate volcanic rock layers in pegmatite host rock. In areas dominated by tonalitic rocks some thin shear bands were observed. In these areas the penetrative foliation in medium-grained tonalite is deflected by pegmatite and leucosome veins.

The shear zone deformation is best represented in the northern part of the D1 area, where strong slickenline lineation has developed within the pervasively foliated, medium-grained quartz-feldspar-gneiss. Slickenlines occur also on a pegmatite vein (Fig. 10E), which is cutting the foliated gneiss but was subjected to the shearing. The slickenline striations plunging moderately (74°) towards SE were caused by the movement of the two rigid bodies under semi-brittle conditions. The lineations have down-dip geometries on slickenside surface, reflecting dip-slip displacements, but no shear sense indicators could be found in the field.

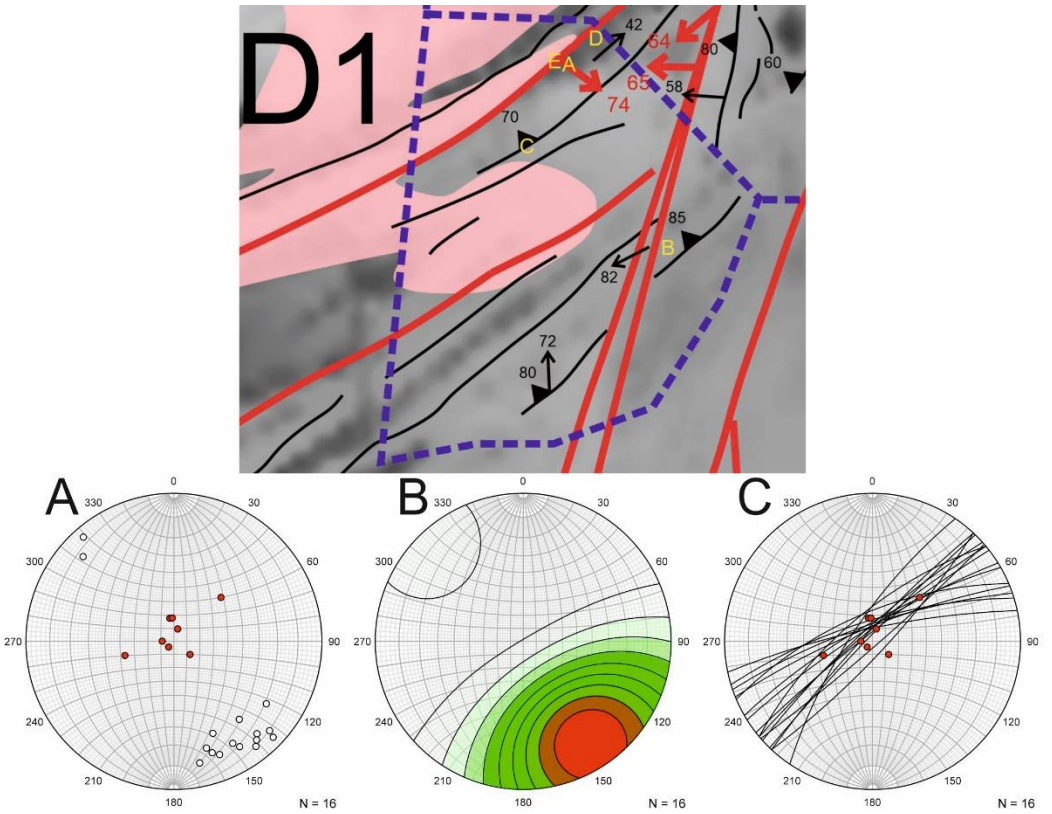

Fig. 9. D1 subarea. Top: An overview and structural interpretation of subarea D1. The letters refer to the field photos in Fig. 10. Greyscale aeromagnetic anomaly map provided by GTK. Below: The lower hemisphere stereographic projections of the structural data. A: White dots = pole to foliation, Red dots = lineations. B: Densities of the pole to foliation. C: Black lines = foliation as great circles, Red dots = lineations.

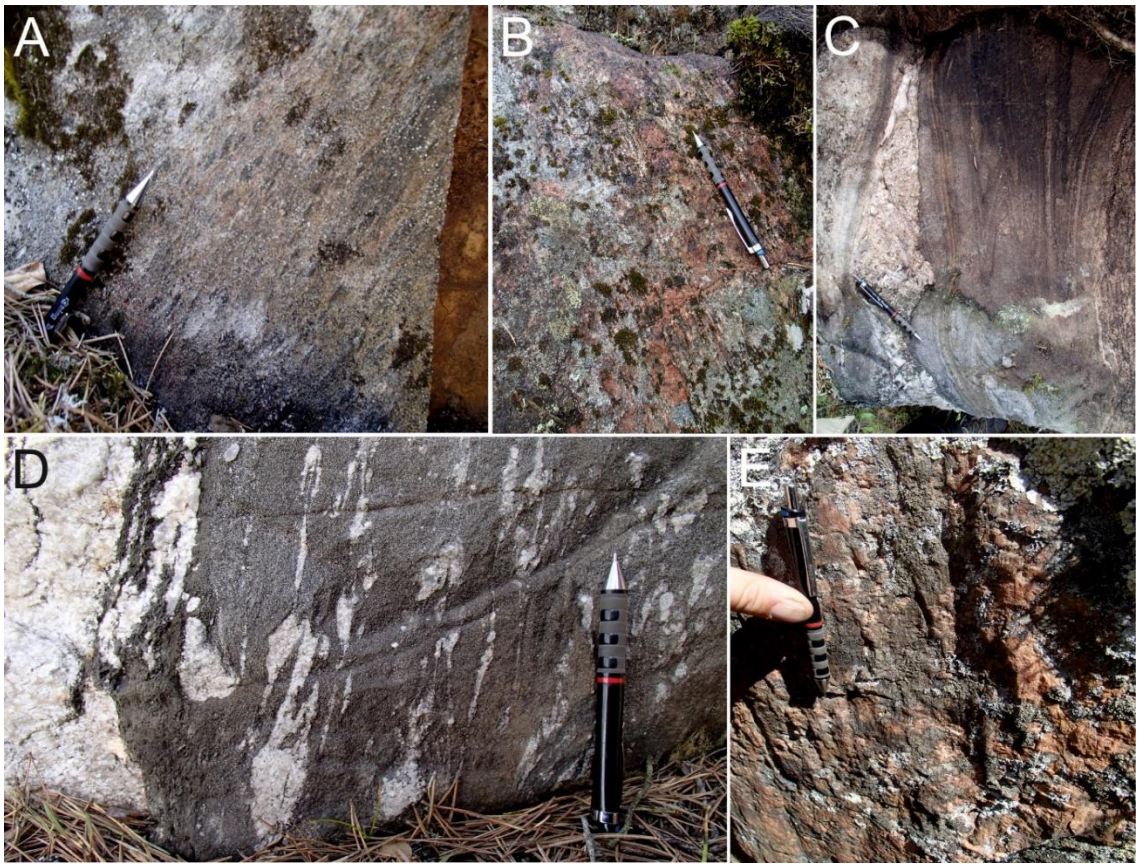

Fig. 10. Caption overleaf

Fig. 10. A: Strong aggregate lineation in amphibolite (view to SW) (IJPI-2017-22.1, N: 6752621, E: 264279). B: Strong lineation in amphibolite (L-tectonite) (view to E) (IJPI-2017.13, N: 6750592, E: 265425). C: Intrafolial isoclinal folding in mafic volcanic rock (pen points north) (IJPI-2019-19, N: 6751844, E: 263788). D: Folded leucosome in intermediate volcanic rock (view to NE) (IJPI-2017-20, N: 6753146, E: 264460). E: Subvertical slickenlines in pegmatite (view to E) (IJPI-2017-21, N: 6752641, E: 264275).

4.2.2 D2 subarea

The NE-SW striking structures of the D1 area become transposed into N-S trending shear zone within the subarea D2 (Fig. 11). Most of the measurements are from the southern and eastern part of this subarea, due to amount of the available outcrops. N-S and NNE-SSW striking foliations are dominant within D2 area (Fig. 11), but some exceptional NW-SE striking foliations were also observed. Dip direction of the N-S and NNE-SSW trending structures is mainly towards west with the full range of orientations observed between WSW and NW. The deviating NW-SE trending foliations are dipping towards NE with an angle of 60°. Measured planar features are mostly steeply dipping between 53° and 90°. Regional-scale gentle folding is observable in aeromagnetic map and field observations in the central part of the D2 area, which causes the development of NNE-SSW and NW-SE structural trends. Folding starts when foliation trend changes from NW-SE to N-S in the central part of the D2 area.

Foliations within the shear zone are generally more steeply dipping (70°-90°) than the backround foliations (53°-90°), but have similar dip directions. Lineations are plunging a bit more gently than in the D1 area (Fig. 11A). The dominant set of lineations cluster around the stereoplot with subvertical and vertical plunges. Lineations show major deviation in orientations, especially in the southeastern and eastern part of the D2 area, where lineations are mainly plunging subvertically (44°-73°) towards W, but also approximately towards SW and N. In central part, where the folding is observable, the measured lineation (55°) is plunging towards SSW. No lineations were measured from the northern part of D2. Lineations marked on the map are the most representative ones. Outcrop scale fold axis measured from central part also plunges towards SSW like nearby lineation, but with gentler angle (32°). Lineations have no major variation in their plunging angles between backround and the shear zone areas.

Backround foliations are mainly pervasively occurring penetrative foliations, but gneissic and compositional banding, schistosity and zonal foliations were also observed. Foliation parallel compositional banding occurs locally in medium-grained volcanic rocks and

medium- to fine-grained sheared paragneisses (Fig. 12B). Zonal foliations occur in mafic volcanic rocks in areas where post tectonic pegmatite granite veins and lenses are bending the foliation. Foliation intensity is weak or moderate in the central area, where folding has affected the bedrock, while foliations in the southern, eastern and northern parts have mainly strong intensities. In aeromagnetic map, these foliations occur in an area controlled by strong negative magnetic anomaly. Lineations of the backround area are characterized by weak to strong alignment of minerals, such as biotites. Similar with foliations, the lineation intensities are weak in central part and moderate or strong in the east near the shear zone. Fold axis was measured from isoclinal symmetric outcrop-scale fold from the central part, where tight to isoclinal folding occurs in medium-grained granite and gneiss. Semi-brittle features were also common within the D2 area. Semi-brittle faults have caused sinistral displacement (Fig. 12A) and tension fractures in volcanic rocks and some brittle fracture systems have developed in cubic fracture patterns in granite.

Outcrops best characterizing the shear zone deformation occurred within the eastern and central parts of the D2 within areas known as Ladonmäki, Vuori and Huhtamonmäki (Fig. 11). Rocks of these outcrops have smaller grain size than rocks farther away from shear zone and have been intensely sheared (Fig. 12C), and some of them have visible mylonitic textures. Shear zone deformation has occurred in ductile and semi-brittle conditions, and stretching lineations were observed from ductile retrograde mylonitic zones (Fig. 12D) and semi-brittle faults. Measured stretching lineations from two semi-brittle faults in mafic volcanic rock (Fig. 12E) in the Huhtamonmäki area plunge steeply (65°) towards west with down-dip geometries, indicating purely dip-slip type of displacement. Only half a kilometer towards north in the Vuori area the ductile deformation becomes dominant and is represented by sheared paragneisses (Fig. 12B) and mylonitic bands in pegmatite and intermediate volcanic rock. Half kilometer more towards north in Ladonmäki area the observed ~10 m wide mylonitic zone is located in the contact area of mafic volcanic rock and granite (Fig. 12F). In these outcrops the quartz grains have been recrystallized and formed the lineation, which plunges 64° towards SW, indicating oblique-slip displacement. Observed kinematic indicators include dextral sigmoids on leucosome along horizontal plane (Fig. 12G). However, sinistral indicators were more common along vertical plane. These vertical sinistral indicators, steep down-dip- and oblique stretching lineations and west dipping mylonitic foliations are indicating a west-block up shear sense with a weaker dextral strike-slip component. Garnets are locally

present within the shear zone (Fig. 12H), where they occur in mylonitic volcanic rocks and granites and also in mafic and leucosome parts of the sheared paragneisses. Shear bands in outcrops are biotite rich and have undergone minor chloritization.

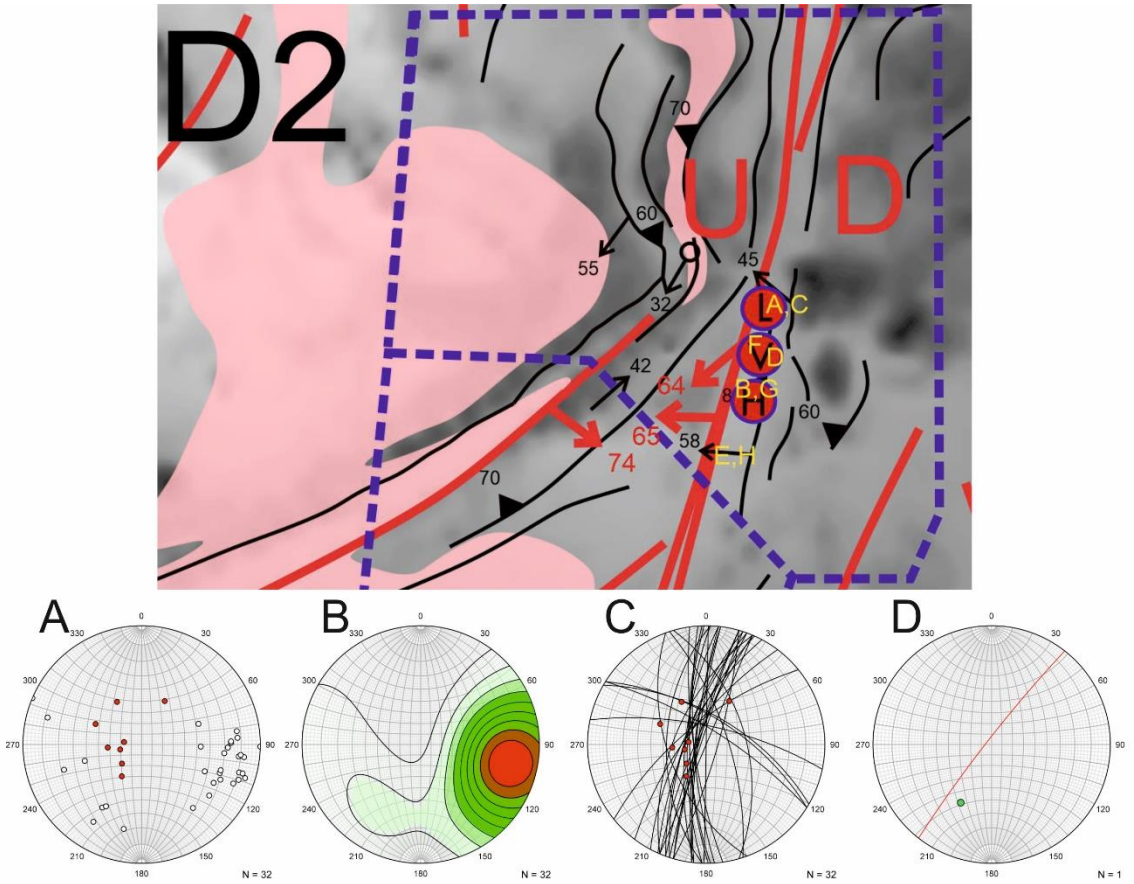

Fig. 11. D2 subarea. Top: An overview and structural interpretation of subarea D2. The letters refer to the field photos in Fig. 12. “U” and “D” refer to the up and down movements of the blocks on the opposing sides of the shear zone. “L”, “V” and “H” refer to the most important locations (red circles with blue outlines on map, L= Ladonmäki, V= Vuori, section 5.1 and H= Huhtamonmäki). Greyscale aeromagnetic anomaly map provided by GTK. Below: The lower hemisphere stereographic projections of the structural data. A: White dots = pole to foliation, Red dots = lineations. B: Densities of the pole to foliation. C: Black lines = foliation as great circles, Red dots = lineations. D: Red line = axial surface as a great circle, Green dot = fold axis.

Fig. 12. A: Intermediate volcanic rock cut by sinistral semi-brittle fault (IJPI-2017-6, N: 6753701, E: 266756). B: Sheared paragneiss with compositional banding (IJPI-2017-136, N: 6753021, E: 266370). C: Intensely foliated granite (IJPI-2017-8, N: 6753769, E: 266672). D: Retrograde mylonite in pegmatite (view to N) (IJPI-2017-3, N: 6752919, E: 266446). E: Overview of two semi-brittle faults on mafic volcanic rock (IJPI-2017-179, N: 6752301, E: 266323). F: Contact of mylonitic granite and mylonitic volcanic rock (IJPI-2017-43, N: 6753743, E: 266665). G: Dextral sigma clast in leucosome part of the paragneiss (IJPI-2017-136, N: 6753021, E: 266370). H: Garnets in pervasively foliated mafic volcanic rock layer (IJPI-2017-179, N: 6752301, E: 266324). Pen or handle of the hammer are pointing north in A, B, C, E, F, G and H.

4.2.3 D3 subarea

D3 (Fig. 13) is the third subarea within Alastaro SZ and is located west of the large magnetite bearing granite intrusion described in section 2.4. Most of the measurements were made from outside the main shear zone, and hence reflect the regional N-S and NNE-SSW structural trends. Measured planar structures have similar deviation in

orientations as in D2 area. In aeromagnetic map, the shear zone (negative anomaly) seems to turn towards NNW-SSE trend in the north. However, like in D2 area the measured N-S and NNE-SSW striking foliations were most common. In contrast to the D2 area, the N-S and NNE-SSW foliations are mostly dipping towards E or ESE. These foliations are mainly steeply dipping 53°-87°, which is similar with every other subarea within Alastaro SZ. Few observed E-W and NE-SW striking foliations are dipping with nearly horizontal angles (15°-26°) towards N or NW. Like in D2 area, the NW-SE striking foliations are dipping subvertically (53°-75°) towards NE especially in the southern part of the D3 area. Folding, which started at the central part of the D2 area is likely bending foliations within D3 area as well causing the deviation in structural trends. Lineations were only observed in the central and northern parts of the D3 area. In central part, the lineation plunges gently (~20°) towards N-NNE, which is much more horizontal compared to other subareas. In northern part, the lineation plunges towards NNW with steeper angle of 63°. Fold axes measured from southern and northern parts, plunge towards north with gentle to moderate angles (21°-54°). Measured axial surfaces are N or NNW striking and dip steeply (77°-80°) towards E and ENE.

Most of the observed foliations are pervasively occurring penetrative foliations or gneissic bandings, but zonal foliations were also measured. Foliation instensity varies from moderate to strong. Most intensely foliated rocks are the coarse- to medium-grained granodiorites in the central part and medium-grained gneissic quartz diorites and granites in the northern part. Zonal foliations are observed from medium- to small-grained granites and granodiorites, where post-tectonic unfoliated pegmatite veins are cutting the host rocks. Lineations are weakly represented in outcrops, but the ones measured are weak to moderate mineral lineations. Folding continues from south all the way to the northern part of the D3 area. Folds are mainly sinistral, and have gentle to open tightness, occurring in the migmatitic felsic gneisses (Fig. 14A), in quartz- and granodiorites and in granites in the northern and southern parts of the subarea. In the northernmost part of D3, the hinges of these folds have been intruded by a syntectonic granite at some locations (Fig. 14B), and therefore the U-Pb age sample for Alastaro SZ was collected from this area. Wavelength of the folds vary between ~10 cm to ~7 m and most of the folds are asymmetric (Fig. 14C). The largest observed outcrop scale fold structure (Fig. 14A), is a 7 m wide open synform, where the foliation on the fold limb dips steeply (53°) towards NW and E, and gently (26°) towards N in the hinge. Outcrops from the main shear zone deformation area were not observed. Some thin shear bands are bending the N-S foliation

in the coarse- to medium-grained granodiorites (Fig. 14D) and granites in the central part. In northern part, the intensely foliated granites have sheared appearances and mafic minerals are bending around feldspar grains (Fig. 14E), resembling mylonitic texture. These granites are probably located very close to the main shear zone. Conjugate brittle fractures (Fig. 14F) are observed from these granites at some areas.

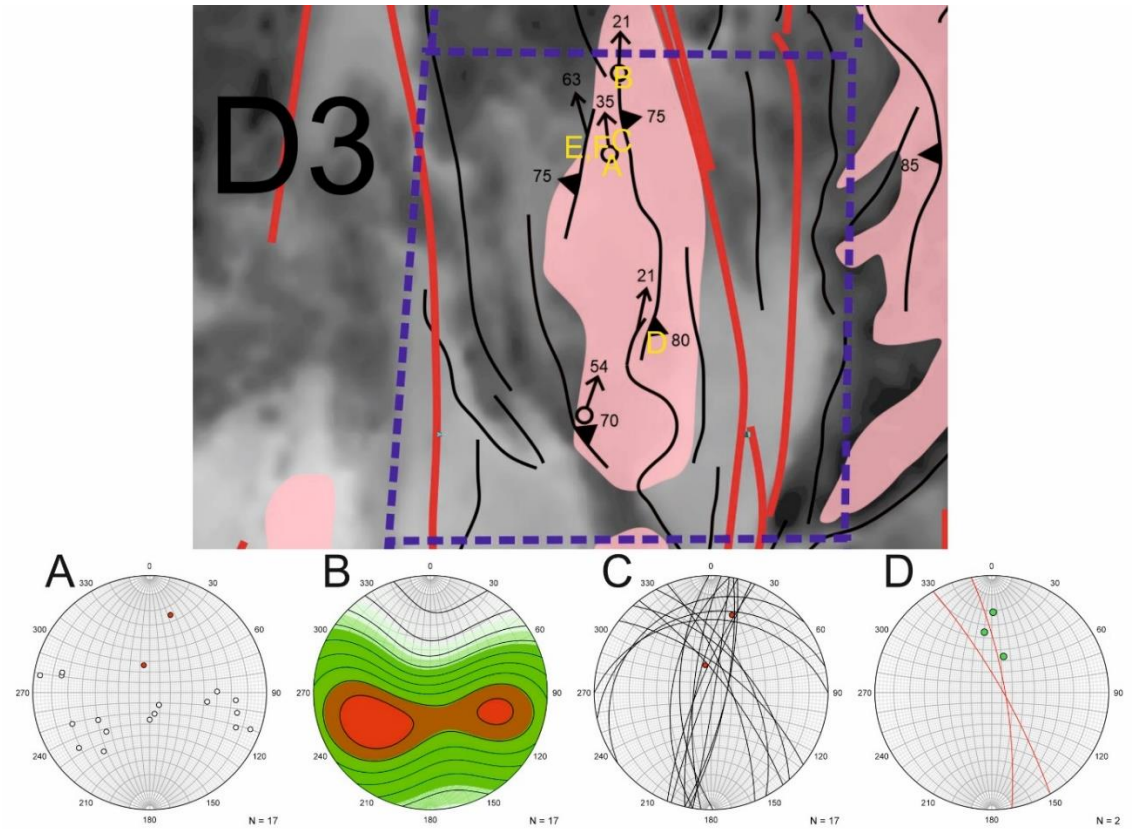

Fig. 13. D3 subarea. Top: An overview and structural interpretation of subarea D3. The letters refer to the field photos in Fig. 14. Greyscale aeromagnetic anomaly map provided by GTK. Below: The lower hemisphere stereographic projections of the structural data. A: White dots = pole to foliation, Red dots = lineations. B: Densities of the pole to foliation. C: Black lines = foliation as great circles, Red dots = lineations. D: Red lines = axial surface as great circles, Green dots = fold axes.

Fig. 14. A: Hinge of an open 7 m wide synform (view to NNE) (IJPI-2017-29.1, N: 6760979, E: 265278). B: Folding in mesosome and leucosome of the gneiss cut by syntectonic foliated granite (IJPI-2017-35, N: 6762089, E: 265548). C: Sinistral open asymmetric folding in gneissic granite (IJPI-2017-33, N: 6761253, E: 265412). D: A thin shear band is bending the foliation in granodiorite (IJPI-2017-84, N: 6759279, E: 265832). E: Foliated sheared granite (TALE-2017-199, N: 6761294, E: 265296. F: Conjugate fractures on sheared granite (IJPI-2017-178, N: 6761327, E: 265293). Compass, pen or handle of the hammer are pointing north in B, C, D, E and F.

4.2.4 D4 subarea

The D4 subarea (Fig. 15) is the northernmost part of the Alastaro shear zone. In D4 area the strike of the shear zone and planar structures of the backround have been turned to NNW-SSE, which is supported by the aeromagnetic map and field observations. Foliations are mainly NNW-SSE or NW-SE striking and dipping steeply (64°-78°) towards ENE or NE. However, some NNE-SSW striking foliations, which are steeply

dipping (88°) towards WNW were also observed from the eastern part of the D4 area. Lineations observed from central and eastern part of the D4 area have less scatter in their orientations than in D1 and D2 areas, and plunge moderately or steeply (37°-71°) towards N, NNE or NE. Axial surfaces are steeply dipping towards NNE (75°) and SSE (85°), and fold axes plunge towards ENE. Both the planar and linear structures within the shear zone are steeper, than the backround structures. Shear zone foliations are dipping towards WNW, which is contrasting to the dips of the backround foliations.

Foliations are mainly of moderate intensity, types ranging from penetrative foliations to gneissic banding. Penetrative foliation occurs especially in tonalitic and granodioritic ortogneisses (Fig. 16A) Some strong zonal foliation occurs in tonalites, in areas where tonalite and intensely migmatized gneisses are occurring variably. Epidote alteration along foliation causes locally compositional banding to intermediate volcanic rocks in the southern part of the D4 area. These rocks also have brittle fracture systems and minor faults filled with epidote (Fig. 16B), which are cutting the host rock. Lineations are characterized by moderate or strong alignment of minerals. Strongest mineral lineation occurs in medium-grained tonalitic gneiss (Fig. 16C) in the central part of the D4. This is the only area within Alastaro SZ where rocks have L-tectonite appearance, except the rocks in eastern part of D1 subarea. Open symmetric folding in small-grained paragneisses (Fig. 16D) was observed from the eastern part of D4. Orientations of the axial surfaces is significantly variable between nearby outcrops, where foliation and leucosomes are folded. Thin quartz veins occur in the hinges of the folds along axial surfaces. Fold axes have approximately the same trend, but plunges range from 37° to 71°. Foliation with dip direction of 049 and Dip of 33° (NW-SE striking), was determined to be the pretectonic (to shear zone deformation) planar orientation and envelope surface of the fold hinges (m-symmetry method). Folds have likely formed, when the shear zone deformation has affected the preexisting planar structures of the paragneiss.

Within D4 subarea the Alastaro SZ is interpreted to consist of two deformation zones. This assumption is derived from aeromagnetic map and the field observations from Ruskonkallio (Fig. 15). Separation of these two zones has likely started from subarea D2 or D3. In central part the NNW-SSE striking negative magnetic anomaly continues across the D4 area to the North fold area (Section 4.4.3). No outcrops, which represents this shear zone deformation were found. In eastern part, the N-S or NNE-SSW striking deformation zone is best represented in the outcrops of Ruskonkallio. Mylonite zone was observed from this area, and part of the zone was classified as protomylonitic, due to

amount of grain size reduction. The granodiorites and tonalites of the area have strong, nearly vertically (78°-88°) towards WNW dipping mylonitic foliations. Streching lineations are plunging ~40° towards N. Sinistral ductile shear bands deform the pervasively foliated granodiorite (Fig. 16E-F). Steep mylonitic foliations, subvertically towards N plunging lineations and sinistral kinematic indicators in horizontal plane are supporting the oblique E-block-up shear sense. Trend of the lineation is however, contrasting to slickenlines within D1 area and stretching lineations and semi-brittle faults within D2 area, which also have steeper plunge. Shearing within Ruskonkallio is also more pervasive than in other outcrops within the Alastaro SZ.

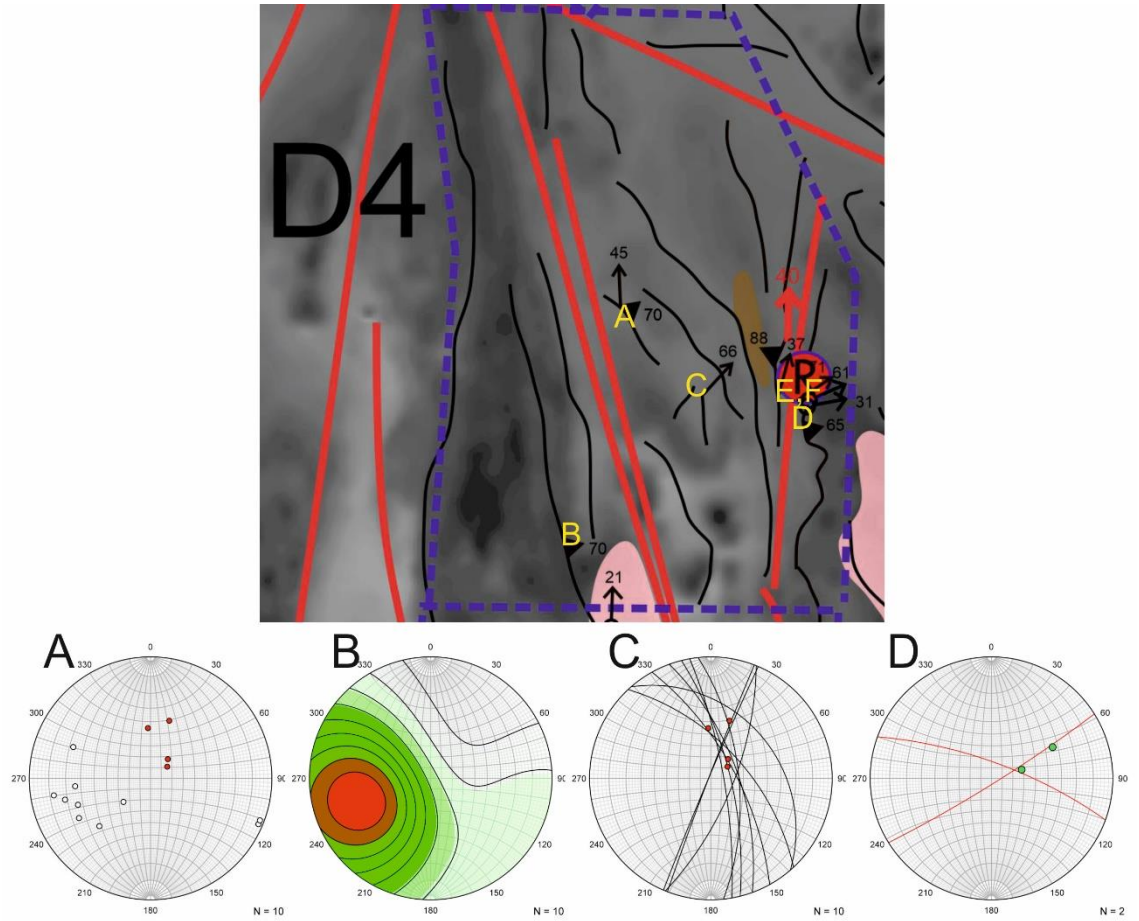

Fig. 15. D4 subarea. Top: An overview and structural interpretation of subarea D4. The letters refer to the field photos in Fig. 16. “R” refer to the location of Ruskonkallio (red circle with blue outline). Greyscale aeromagnetic anomaly map provided by GTK. Below: The lower hemisphere stereographic projections of the structural data. A: White dots = pole to foliation, Red dots = lineations. B: Densities of the pole to foliation. C: Black lines = foliation as great circles, Red dots = lineations. D: Red lines = axial surface as great circles, Green dots = fold axes.

Fig. 16. A: Penetrative foliation in ortogneiss (IJPI-2017-23, N: 6766090, E: 265723). B: Epidote altered intermediate volcanic rock cut by minor epidote filled sinistral fault (IJPI-2017-28, N: 6763146, E: 265016). C: Intense lineation in gneiss (TALE-2017-102, N: 6764985, E: 266519). D: Overview of the symmetric folding in paragneiss (IJPI-2017-25, N: 6764977, E: 267790). E & F: Sinistral shear bands deforming granodiorite (TALE-2017-59, N: 6765147, E: 267695). Pen or handle of the hammer are pointing north in each of the pictures.

4.3 Kankaanranta shear zone

The ENE-WSW striking Kankaanranta shear zone (C in Figs. 6 & 17) begins from north of Uunimäki deposit in the west and continues towards ENE outside of the present study area. Like in Alastaro SZ, most of the observations were made from outside the main shear zone and hence reflect the regional backround structures.

Measured planar features are showing less variation in their orientations than in Alastaro SZ. Most of the measured foliations are ENE-WSW to E-W striking, especially near the assumed core of the main shear zone. However NW-SE, NE-SW and WNW-ESE striking foliations also occur, especially in the backround area some distance away from the shear zone. All foliations within Kankaanranta SZ are steeply dipping (60°-90°), with dip directions both to NNW and SSE present. Split to eastern and western part from the middle, SSE-dipping foliations are more common within the eastern part of the Kankaanranta SZ and NNW-dipping foliations are more common within the western part, especially in areas just north and northeast of Uunimäki. Lineations within the Kankaanranta SZ scatter around the stereoplot with mostly vertical (58°-80°) orientations (Fig. 17A), but some moderately and even close to horizontally (19°) plunging lineations were observed. Most of the lineations are plunging towards ENE, WSW or N. Axial surfaces were only measured from two outcrop scale folds from eastern and western parts of Kankaanranta SZ. They are ENE-WSW striking and thus following the major foliation trends. In western part the axial surface dips towards SSE and in eastern part towards NNW. Observed fold axes plunge towards ENE with steep angles (65° and 76°), and are therefore following the most common lineation trend. Shear zone foliations are a bit steeper than the observed backround foliations (78°-90°) and are dipping towards NNW or SSE, but also towards N, S and SE. Lineations associated to the shear zones commonly have similar steep (58°-80°) plunges with the backround lineations, except one subhorizontal 19° slickenline lineation in the western part, near Uunimäki. Similar with backround lineations, the most common shear zone lineation trends are ENE and WSW, but SE plunging lineation was also observed from the central part.

Most of the foliations observed outside of the main shear zone are penetrative foliations or penetrative gneissic bandings. Foliation intensities vary between weak and strong being mainly moderate. Strongest foliations occur near the main shear zone. Most of the foliations occur pervasively in volcanic rocks, ortogneisses, quartz diorites, granodiorites or tonalites (Fig. 18A), but some zonal foliations were observed from areas where post-tectonic pegmatite veins are cutting the foliated ortogneisses and amphibolites. Foliation-parallel compositional banding in intermediate volcanic rock, where some layers contain uralite porphyroblasts, was also observed from eastern part. In the central area the primary bedding of the aluminum rich volcanic sediment (Fig. 18B) has likely been preserved, as shown by the variation of intermediate and mafic layers. Backround lineations are characterized by moderate or strong alignment of minerals. These mineral lineations are

generally stronger near the shear zone. Fold axis and axial surface were measured in the west from migmatitic psammitic gneisses, where two leucosomes of different generations are observable (Fig. 18C). The older generation of leucosomes is folded with the mesosome and the younger of generation leucosomes intrudes along the axial surface. In east, the fold axis and axial surface were measured from folded granitic vein in mafic volcanic rock.

The main shear zone deformation structures occur in gabbros, quartz diorites, granodiorites, tonalites or paragneisses. The shear zone foliations have mainly strong intensities and they occur zonally within shear bands. Some larger scale pervasive mylonitic foliations were also observed. Shear zone lineations are moderate or strong stretching lineations or slickenlines. In westernmost part of the Kankaanranta SZ, north of Uunimäki the mylonitic contact of gabbro and garnet-biotite-paragneiss shows dextral asymmetry of the leucosome aggregate (Fig. 18D). In this area, the secondary structures thought to be caused by the shearing crosscut the folded areas. Dextral folding of leucosomes occurs within horizontal plane in outcrop just 20 m away in sheared mica gneiss (Fig. 18E), which also contains highly altered quartz vein fragments (Fig. 18F). From this area the slickenline lineation within NNW dipping foliation plane surface was measured to plunge towards ENE with subvertical angle (073/73°). Dextral folding combined with steep ENE-plunging slickenlines are indicating oblique S-block up movement. In area just about 100 m towards south and immediately south of the main shear zone, in border of the Uunimäki gabbro area, the fault with dextral fault markers has been developed (Fig. 18G) to the quartz diorite. However with fault plane dipping towards NE (050/75), and down-dip lineation also plunging towards NE (045/68), this fault is not exactly in same orientation with shear zone structures. In northeast of Uunimäki the stretching lineation in mylonitic contact of mafic volcanic rock and mica gneiss is plunging towards SW with steep angle (230/80°), and slickenlines in sheared tonalite from other nearby outcrop are nearly horizontally plunging towards WSW (252/19°). Difference of these two plunges is baffling, but the nearly horizontal slickenlines appear to be dominant linear structures of the area. Kinematic indicators within this area are supporting dextral strike-slip shear sense, especially in local contact between mafic volcanic rock and feldspar-quartz-schist, where tension fractures in mafic volcanic rock have dextrally deflected and in schist there are dextral folds and dextral leucosome aggregates (Fig. 18H). In the central area of the Kankaanranta SZ the stretching lineation measured from granodiorite is plunging towards SE with a steep angle

of 80°. Mylonitic foliation of the granodiorite is also steeply dipping (80°) towards SE. These features indicate almost pure dip-slip type of movement, but no kinematic indicator were observable within this area. Approximately 5 km towards ENE the shear zone deformation is represented by dextral shear bands in intensely deformed granodiorite (Fig. 18I). Lineation could not be measured from this point though. Just 1 km more towards ENE the core of the main shear zone is represented at local outcrop (Fig. 18J). The mylonite within this outcrop could be classified as mesomylonite or ultramylonite. Foliation measured from shear band is dipping vertically towards NNW (343/85°). Lineation could not be precisely measured, but it was estimated to plunge steeply towards E. Sinistral and dextral indicators were both represented in this outcrop. Orientations of the recrystallized quartz grains suggests sinistral shear sense, but the crosscutting pegmatite dike and other markers around shear band are suggesting a dextral shear sense. The easternmost kinematic indicators were observed from 5 cm shear band within heavily deformed intermediate volcanic rock. Some quartz veins and fragments (Fig. 18K), which have a strike parallel to the shear band are showing dextral asymmetries.

In summary, based on the field observations, dextral shear sense is clearly dominant in outcrops within the Kankaanranta SZ and the amounts of dip-slip and strike-slip types of motions variate in the western part. However, the steeply plunging lineations are indicating a major dip-slip component in central and eastern parts of the shear zone. Kinematic indicators from the western part are suggesting that, the shear sense variates between south-block-up and dextral strike-slip. The NW-SE striking foliations are probably related to the splays of the shear zone. Based on the lineation plunges the block movement in splays are likely dip-slip type as well.

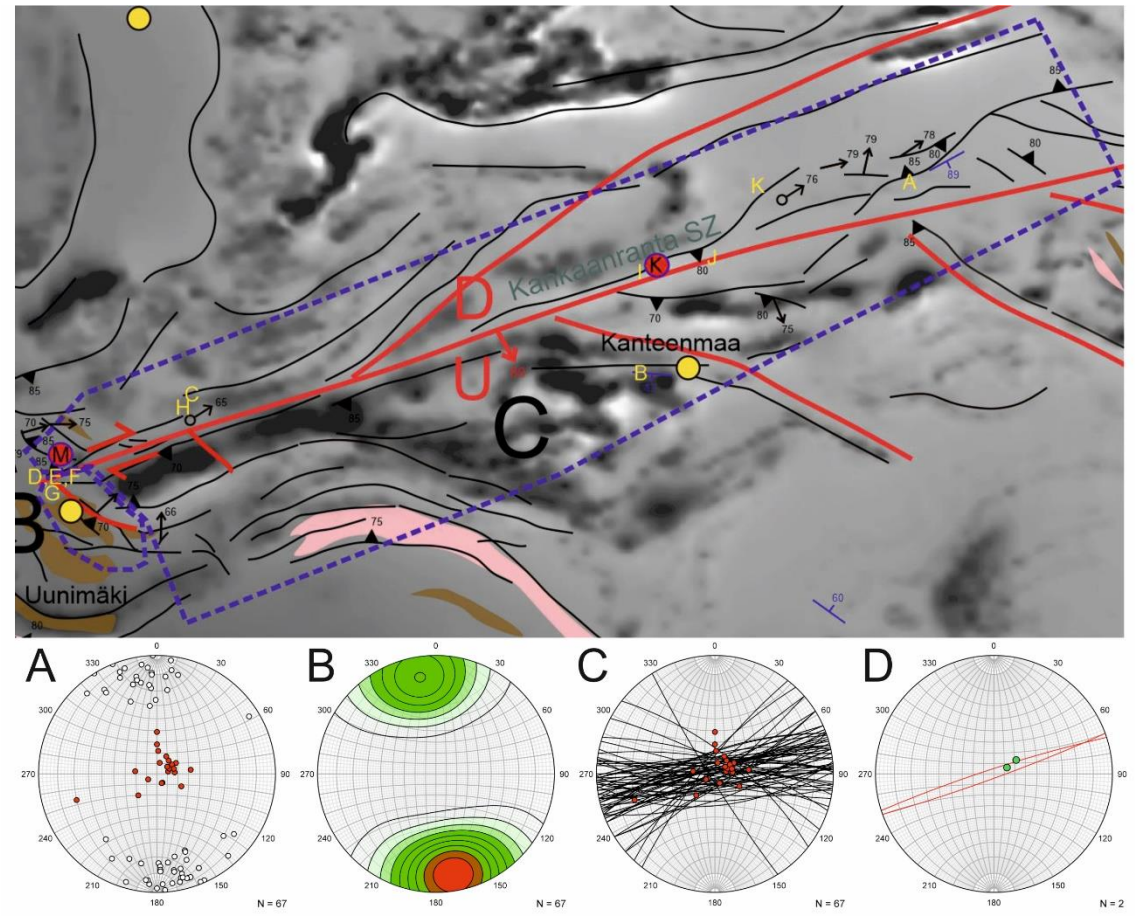

Fig. 17. Kankaanranta SZ. Top: An overview and structural interpretation of the subarea C. The letters refer to the field photos in Fig. 18. “U” and “D” refer to the up and down movements of the blocks on the opposing sides of the shear zone. “K” and “M” refer to the thin section locations (red circles with blue outlines on map, K= Kankaanranta, M= Metsäsiankallio, section 5.2). Locations of the Uunimäki, Kanteenmaa and Korvenmaa gold prospects as yellow circles with black outlines. Greyscale aeromagnetic anomaly map provided by GTK. Below: The lower hemisphere streographic projections of the structural data. A: White dots = pole to foliation, Red dots = lineations. B: Densities of the pole to foliation. C: Black lines = foliation as great circles, Red dots = lineations. D: Red lines = axial surface as great circles, Green dots = fold axes.

Fig. 18. A: Penetrative foliation (right) and strong mineral lineation (left) in tonalite (view to SSW) (TALE-2017-146, N: 6777749, E: 288924). B: Bedding of the aluminum rich volcanic sediments (TALE-2017-3, N: 6774341, E: 285008). C: Leucosomes of two different generations in psammitic mica gneiss (TALE-2017-7, N: 6773364, E: 275572). D: A leucosome aggregate as dextral sigma clast in mylonitic contact between gabbro and garnet-biotite-paragneiss (TALE-2017-182, N: 6772845, E: 274195). E: Dextral folding of leucosome veins in mylonitic mica gneiss (IJPI-2017-158, N: 6772714, E: 273445). F: Alterated quartz vein fragment in mylonitic mica gneiss (IJPI-2017-158, N: 6772714, E: 273445). G: Dextral fault in quartz diorite (TALE-2017-16, N: 6772195, E: 273382). H: Asymmetric dextral folding in contact of feldspar-quartz-schist and mafic volcanic rock (TALE-2017-11, N:6773370, E 275570). I: Dextral shear bands in intensely sheared granodiorite (TALE-2017-28, N: 6776050, E: 284400). J: Overview of the sampled exposed mylonite zone (visible strike has ENE-WSW orientation) (TALE-2017-33, N: 6776585, E: 285675). K: Shear band in intermediate volcanic rock and parallel quartz vein and some dextral fragments (IJPI-2017-126, N: 6777616, E: 286780). Compass, pen or handle of the hammer are pointing north in B, C, D, E, F, G, H, I and K. Figures C, D, H, I and J are published with permission from Tuomas Leskelä.

4.4 Regional fold patterns

The folded domains include the Oripää fold, Alastaro fold and the North fold. The Oripää fold in southwestern part is a regional scale single synform. In central area the fold patterns are intervened with the younger shear zone deformation structures causing a very complex crustal structure. The Alastaro fold is also quite a heterogeneous entity compared to the Oripää fold or the North fold and thus it is not clear whether the fold is a synform or antiform. In northwestern part the North fold is actually consisting of three interpreted regional scale folds: from two antiforms and from one synform in the middle.

4.4.1 Oripää fold

The Oripää fold (F in Figs. 6 & 19) is located in the southeastern part of the study area. In aeromagnetic map, the hinge area of the regional scale fold appears to be located in the western part of the F area, while limb sites are located in northern and southern part of the F area (N-limb and S-limb). In N-limb side, the foliations are ENE-WSW or NE-SW striking and steeply (62°-84°) dipping towards SE or SSE, except in the northernmost part of the N-limb, where foliations dip steeply (78°-86°) towards NW and NNW. ENE-WSW foliations bend to NE-SW striking in eastern part, close to the hinge area. The ENE-WSW striking foliations are also most common in stereoplots, because most of the observed outcrops are located in N-limb side. In S-limb side, the foliations are E-W striking, but dip direction varies. In southern part of the S-limb side, the foliations dip towards N, with angles between 68° and 87°, while in northern part of the S-limb, the foliations are dipping towards S, with angles between 70° and 80°. Closer to the hinge area, the E-W foliations bend to NW-SE striking and steeply (62°) towards NE dipping. In hinge area, the foliations have turned to N-S striking, and are dipping towards E, with angles between 58° and 88°. Lineations were not observable in many outcrops, except from a few in the N-limb and the hinge area. In the N-limb area, the lineations have steeper plunges (60°-80°) than in hinge area, and trend towards WWS in north and towards SSE in east. In the hinge area, the lineation is locally plunging towards NE with moderate 47° angle. Axial surface was observed only in N-limb area, where it dips subvertically (81°) towards NW, which is homologous with foliations. From a nearby outcrop the fold axis was also measured from asymmetric tight microfold, which is plunging towards SSW with moderate 52° angle. Major E trending fold axis for the regional scale Oripää fold was derived from foliation orientations and is steeply plunging

towards east (086/69°). Oripää fold is suggested to be tight asymmetric synform, which likely turns into an overturned position when followed the axial trace towards east.

Foliation intensities varies from weak to strong. N-limb foliations are mainly strong, especially in the northern part, where pervasively or zonally occurring penetrative foliations have been developed into granodiorites and quartz diorites. Zonal foliations occur in quartz diorites, which are cut by younger post-tectonic aplitic or pegmatite granitic veins. Some of these veins are boudinaged (Fig. 20A), and locally contain lenses of intermediate volcanic rock. Pretectonic veins also occur locally within quartz diorites (Fig. 20B). In southern part of the N-limb, close to the hinge area, the foliations are moderate penetrative foliations, which occur in intermediate volcanic rocks with compositional variation. Some weakly foliated granites were also observed. Penetrative foliation and gneissic banding with moderate intensities are most common in the hinge area. In S-limb area the foliations are weak to moderate penetrative foliations. Lineations within the N-limb are characterized by strong (northern part) or weak (eastern part) alignment of minerals, whereas the lineation observed from the hinge area can be classified as moderate crenulation lineation of the leucosome veins. Outcrop scale folding occurs in both limbs and hinge area. Within the southern part of the N-limb area, the foliation parallel granite veins in intermediate and mafic volcanic rocks are cut by younger granite veins intruding along axial surface of the folds (Fig. 20C-D) and some intermediate volcanic rocks have been intrafolially folded, to small scale isoclinal folds (Fig. 20E). In S-limb area the compressional deformation is characterized by tight to isoclinal folding within ortogneisses (Fig. 20F). In hinge area, the metasedimentary rocks with stromatic leucosomes have undergone a local outcrop-scale folding, where leucosomes are forming the aforementioned crenulation lineation to the hinges of these folds.

A ductile shear deformation has locally occurred in the southern part of the N-limb, where the local shear band is causing sinistral shear components on granitic veins within small-grained mafic volcanic rock (Fig. 20G). Semi-brittle conjugate faults were locally observed from small-grained intermediate volcanic rocks within the area between the N-limb and the hinge area (Fig. 20H). One NW-SE striking dextral fault with ~30 cm displacement is cut by two sinistral smaller faults with displacements of 1-5 cm and 5-10 cm. Faults are conjugate with an interlimb angle of 48°. The dextral fault is linked with some fault breccia and epidotization.

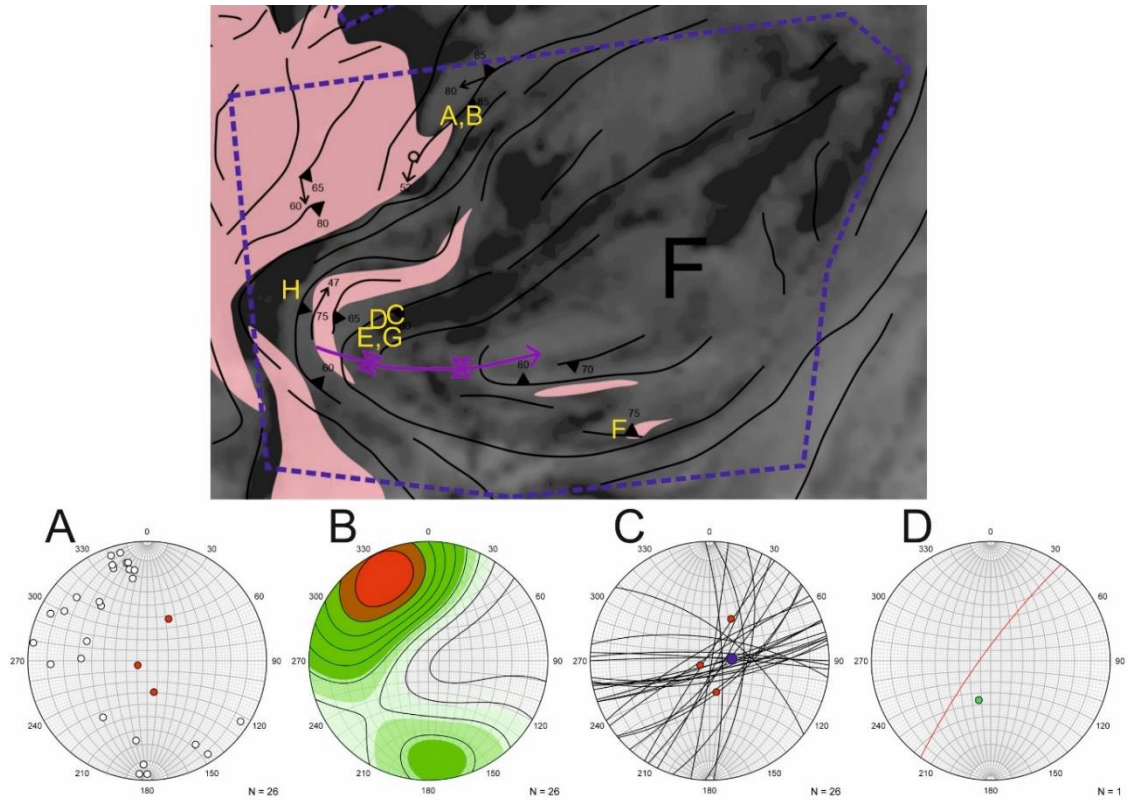

Fig. 19. The Oripää fold. Top: An overview and structural interpretation of subarea F. The letters refer to the field photos in Fig. 20. Greyscale aeromagnetic anomaly map provided by GTK. Below: The streographic projections of the structural data. A: White dots = pole to foliation, Red dots = lineations. B: Densities of the pole to foliation. C: Black lines = foliation as great circles, Red dots = lineations. D: Red line = axial surface as a great circle, Green dot = fold axis.

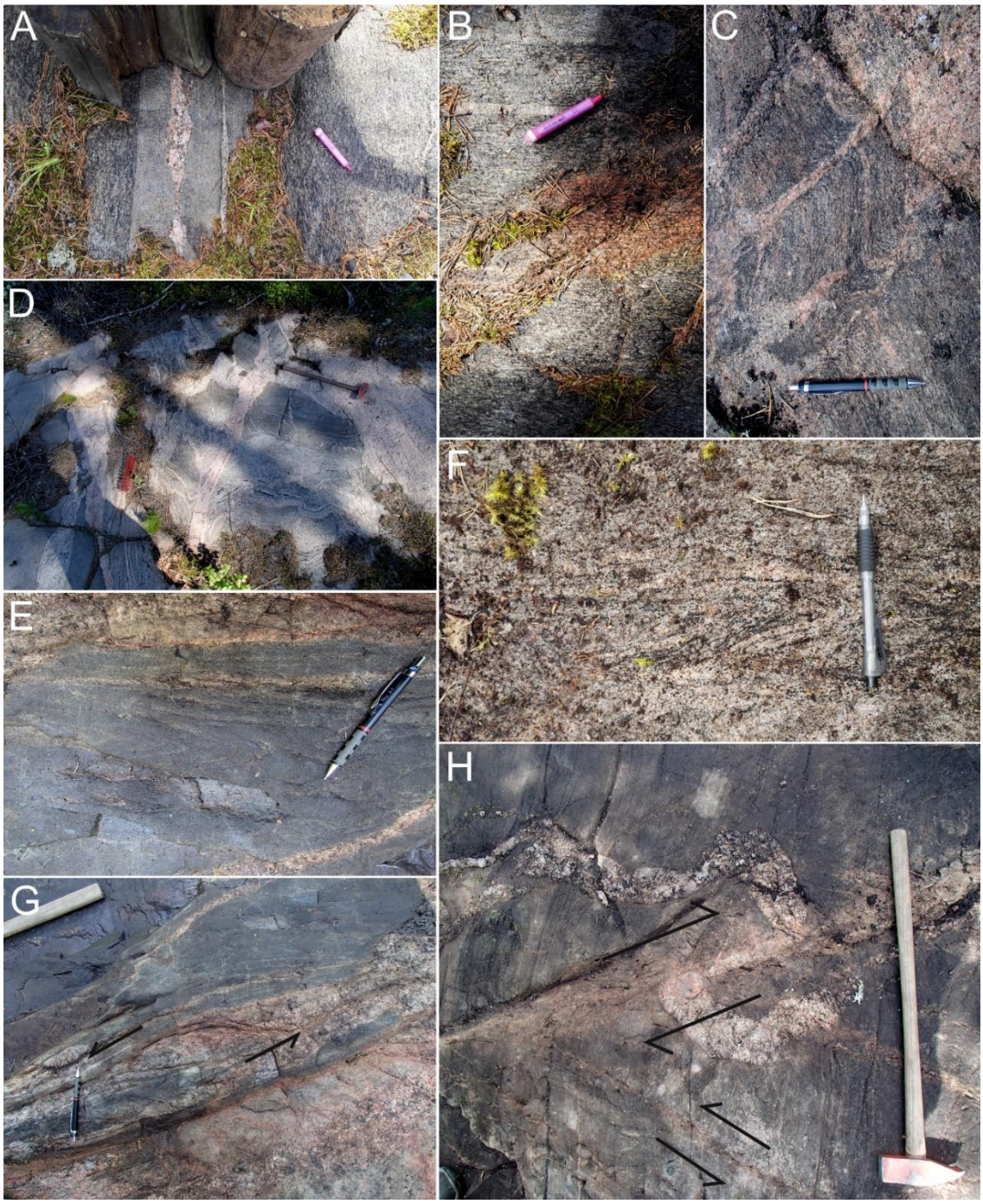

Fig. 20. A: Foliation parallel boudinaged granite vein in mica gneiss layer within quartz diorite (IJPI-2017-143, N: 6762166, E: 275192). B: Pre-tectonic granite vein in quartz diorite (IJPI-2017-143, N: 6762166, E: 275192). C: Cross folding with axial surface-parallel pegmatite veins (TALE-2017-52, N: 6758381, E: 274 343). D: Overview of the folded intermediate volcanic rock and folded granite veins cut by younger granite veins intruding along axial surface (TALE-2017-55, N: 6758194, E: 274089). E: Isoclinal intrafolial folds in intermediate volcanic rock (TALE-2017-50, N: 6758168, E: 273 778). F: Tight folding in ortogneiss (IJPI-2017-146, N: 6756045, E: 278340). G: Apparent sinistral shear in mafic volcanic rock and granite vein (TALE-2017-50, N: 6758168, E: 274089). H: Conjugate dextral and sinistral faults in intermediate volcanic rock (TALE-2017-56, N: 6758986, E: 272 061). Pen or handle of the hammer are pointing north in each of the pictures.

4.4.2 Alastaro fold

Classifying the limbs and hinge area of the Alastaro fold (E in Figs. 6 & 21) is more difficult than within the North fold and Oripää fold areas due to the complexity of the data. Most of the structural measurements were made from the western and central part of the Alastaro fold. Most of the measured foliations strike NE-SW and NNE-SSW, with dominant dip directions towards NW and WSW. However, in southeastern part ENE-WSW striking foliations are dominant with dips towards NNW. Also some WNW-ESE and NNW-SSE striking foliations are dipping towards WSW and NNE. Most of the measured foliations are steeply dipping (60°-88°) but some gently dipping (18°-27°) foliations were locally observed from two outcrops in the central part of the area. Measured lineations have similarly subvertical plunges between 57° and 62°. Lineations are plunging towards NNW/N and SSW in the northern part and towards W in southern part. Axial surface was only measured locally from one outcrop in the southern part. Contrasting to the foliations, the axial surface is dipping towards S, but with similar dip angle of 80°. The measured local fold axis from the western part is plunging towards N, and thus following the most common lineation trend. From foliations the regional scale fold axis was calculated to plunge steeply towards ENE (060/72°).

Observed foliations are mainly moderate penetrative foliations or gneissic bandings, including foliation parallel compositional banding of mafic volcanic rocks. Moderate or strong alignment of minerals is associated with the observed lineations. Strongest lineation within the Alastaro fold was observed in the southern part, where the mineral lineation in amphibolite (Fig. 22A) plunges towards W. Rocks within the Alastaro fold have been folded in many outcrops with different intensities. In southern part the small veins derived from syntectonic asymmetrically folded aplitic vein in folded mafic volcanic rock are intruding along axial surface (Fig. 22B). From the same outcrop the most gently dipping foliation (18°) was also observed. The folded leucosome- aplitic-, pegmatite- and quartz veins are quite common in mafic volcanic rocks and mica- and hornblende gneisses of the area. The dextral and sinistral nature of the folding varies in the western part (Fig. 22C-D). Open folding of the leucosome veins (Fig. 22E) and boudinaged quartz veins in hornblende gneisses are common in the southeastern part of the area. In the northwestern part of the area the granite and intermediate volcanic rock occur as foliation parallel layers and some dextral folding has developed to the granitic part (Fig. 22F).

No clear marks of the shear zone deformation was identified from the outcrops of the Alastaro fold area. Still, the shear zone deformation has possibly transposed the foliation orientations within this regional scale fold, which has made the identifying of the limbs and the hinge areas very difficult.

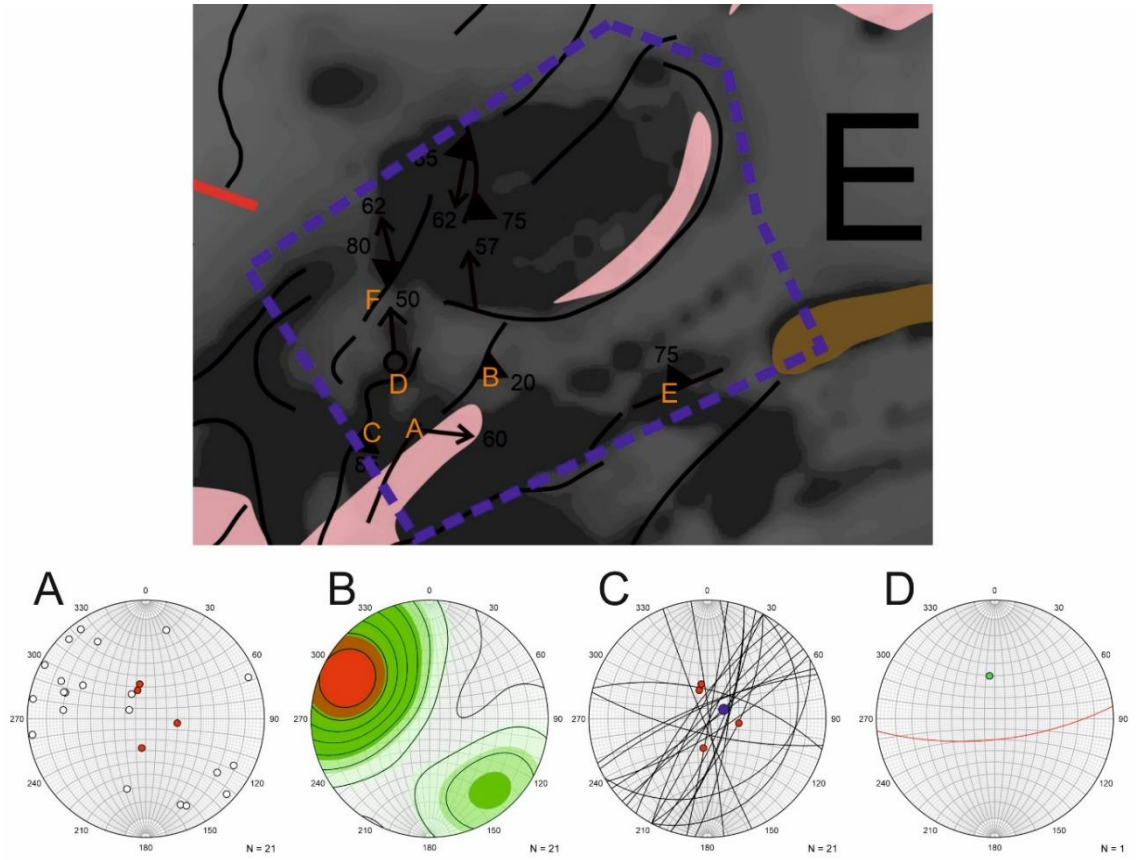

Fig. 21. The Alastaro fold. Top: An overview and structural interpretation of subarea E. The letters refer to the field photos in Fig. 22. Greyscale aeromagnetic anomaly map provided by GTK. Below: The streographic projections of the structural data. A: White dots = pole to foliation, Red dots = lineations. B: Densities of the pole to foliation. C: Black lines = foliation as great circles, Red dots = lineations. D: Red lines = axial surface as a great circle, Green dot = fold axis.

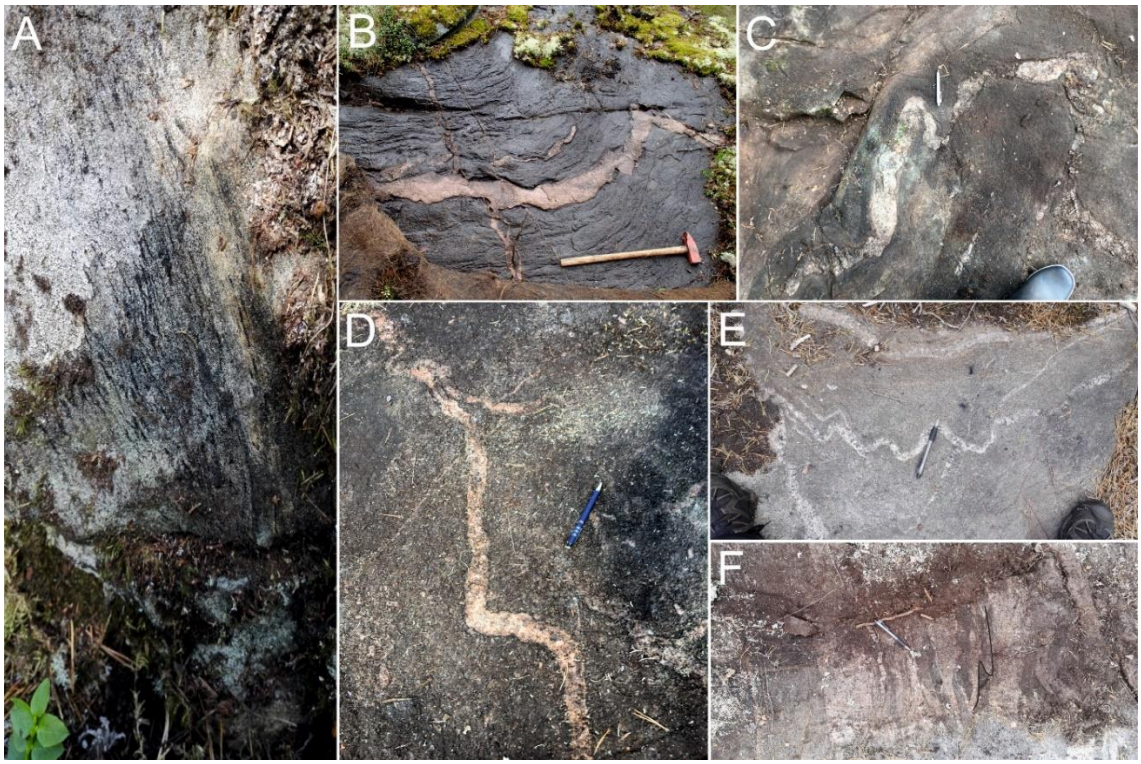

Fig. 22. A: Strong lineation in amphibolite (IJPI-2017-163, N: 6764847, E: 273061) (unknown direction of view, lineation = 98/60°). B: Nearly horizontal folded foliation in mafic volcanic rock and small aplitic veins derived from larger aplitic vein intruding along axial surface (TALE-2017-40, N: 6765261, E: 273790). C: Dextral folding of leucosome vein in mafic volcanic rock (TALE-2017-185, N: 6 764 826, E: 272760). D: Sinistrally folded granitic vein in mafic volcanic rock (TALE-2017-188, N: 6765194, E: 273083). E: Open folding of the leucosome vein in hornblende gneiss (IJPI-2017-169, N: 6765151, E: 275440). F: Foliation parallel layers of dextrally folded granite and intermediate volcanic rock (IJPI-2017-165, N: 6765985, E: 272 770). Pen or handle of the hammer are pointing north in pictures B, C, D, E and F.

4.4.3 North fold

The north fold area (A in Figs. 6 & 23) is located in northwestern part of the study area. Mapping of the north fold area had an aim of explaining the possible linkage between the Alastaro SZ and the Kynsikangas shear zone further towards NNW. Folds were identified from the aeromagnetic map and supported with field observations. It seems there are three isoclinal regional scale folds: the right fold (R-fold), left fold (L-fold) and central-fold (C-fold). Most of the observations were made from the R-fold area. Based on the field observations the R-fold and L-fold are interpreted to be antiforms and C-fold is interpreted to be a synform. Three different main foliation orientations can be identified from stereoplots. In the limb areas the foliations are N-S or NNE-SSW striking. In north the foliations start to bend towards NE-SW and NW-SE orientations and eventually in northernmost area the foliations representing the hinge, are transposed to E-W and ESE-WNW orientations. Foliations within the North fold area are dipping moderately or steeply with the full range between 42° and 90°. Foliations measured from the right limb

of the R-fold are mainly dipping steeply towards west with angles between 59° and 88°. From the left limb of the R-fold, which is also the right limb of the C-fold, the observations points are scarce but steeply (85°) towards NNW dipping foliations were measured from northern part approximately between the limb and hinge area. Foliations within the left limb of the C-fold/right limb of the L-fold are dipping towards W or WSW with steep ~75 angles. No tectonic measurements were made from the left limb of the L-fold. Lineations have subvertical or vertical orientations. Most of the lineations were also measured from the right limb of the R-fold, where they are plunging moderately or steeply (35°-71°) towards ESE, E, ENE or NE. Lineations within the hinge area of the R-fold are plunging with a bit gentler angle (35°-56°) towards ENE or E. No lineations were measured from other parts of the North fold area. Axial surfaces are showing major variation in their orientations, but are all steeply dipping. Axial surfaces measured from the right limb of the L-fold (left limb of the C-fold) are dipping towards SE and SSE with an angle of 75°. Close to the hinge area of the R-fold the axial surface is dipping towards ESE with an angle of 75° and in right limb towards SW with an angle of 80°. Measured fold axes from both limbs of the C-fold are plunging towards SW with angles of 60° and 73°. However, in left limb of the R-fold the fold axes are plunging steeply towards ENE in southern part and towards W in northern part. From observed foliations, the large scale fold axis was calculated to plunge steeply towards northeast (055/68).

Most of the foliations are pervasively occurring penetrative foliations, schistosities and gneissic bandings with mainly moderate intensities in tonalites, granodiorites, quartz diorites, intermediate and mafic volcanic rocks, calsite marble and migmatic gneisses. The most intensely foliated rocks were observed from southern side of the right limb within the R-fold, where small- to medium-grained granites, hornblende- and hornblende-garnet-gneisses have been heavily foliated. Compositional banding was also observed within paragneisses, especially in the C-fold area and in the R-fold area. In northern part of the right limb of the R-fold the pegmatite granite and intermediate volcanic rock form foliation parallel layers (Fig. 24A). Lineations are mainly characterized by moderate alignment of minerals. The most intense lineations occur in the northernmost part of the R-fold within a medium-grained tonalite. Outcrop scale folding was observable in several outcrops within the North fold area, where axial surfaces and fold axes were also measured. In the right limb of the R-fold, the open and tight folding occurs within leucosome (Fig. 24B) parts of the paragneisses and mafic volcanic rocks, but in some outcrops the rocks are more pervasively folded including the mesosome part. Dextral and

sinistral asymmetries are both represented, but dextral folds are a bit more common (Fig. 24C). Locally some thin pegmatite veins are intruding along axial surfaces of these folds. In C-fold area the folding occurs in para- and ortogneisses. In some of these areas the folding is characterized by dextral folding of the granite (Fig. 24D) and quartz veins. Locally in same areas the small granitic veins derived from larger foliation parallel pegmatite veins have formed parasitic folding on paragneisses (Fig. 24E).

The aforementioned heavily foliated rocks in the southern part of the right limb of the R-fold are likely deformed by the NNE-SSW striking shear zone splay from the Alastaro SZ. The gneisses of the area are heavily foliated and sheared (Fig. 24F). Also some narrow pseudotachylite bands have been developed. The intense mylonitic foliation is dipping towards WNW. No kinematic indicators or lineation orientation for the shear zone splay was observed from field. Outcrops which characterize the NNW continuation of the Alastaro SZ were not found, even though the continuation seems likely in aeromagnetic map within the central part.

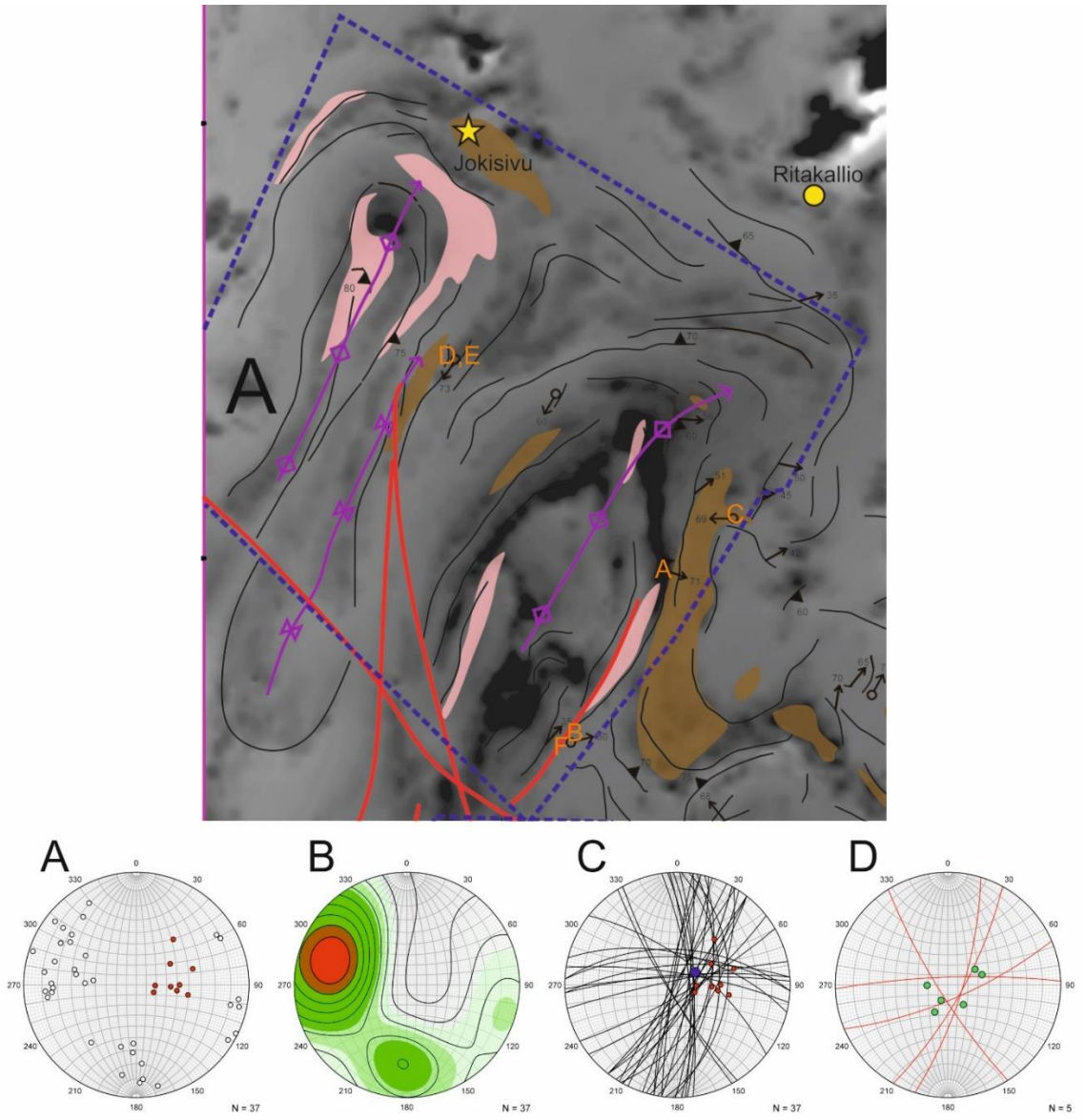

Fig. 23. The North fold. Top: An overview and structural interpretation of subarea A. The letters refer to the field photos in Fig. 24. Locations of the Jokisivu gold mine and the Ritakallio gold prospect (yellow star or circle with black outline). Greyscale aeromagnetic anomaly map provided by GTK. Below: The streographic projections of the structural data. A: White dots = pole to foliation, Red dots = lineations. B: Densities of the pole to foliation. C: Black lines = foliation as great circles, Red dots = lineations. D: Red lines = axial surface as great circles, Green dots = fold axes.

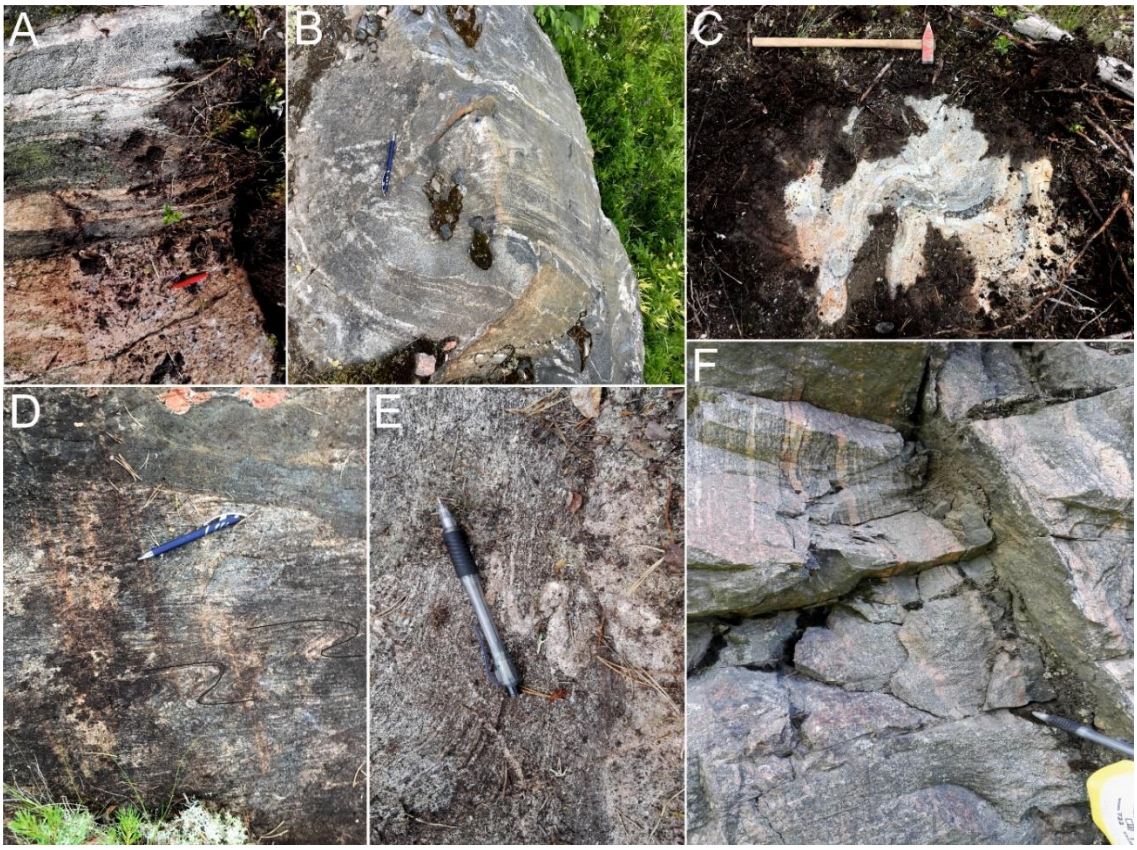

Fig. 24. A: Foliation parallel pegmatite granite and intermediate volcanic rock layers (IJPI-2017-73, N: 6774978, E: 268109). B: Isoclinal folding of the leucosome veins in garnet-mica gneiss (TALE-2017-195, N: 6771127, E: 266114). C: Dextral folding in migmatitic gneiss (TALE-2017-92, N: 6775739, E: 269546). D: Dextral folding of the felsic material in paragneiss (TALE-2017-179, N: 6779109, E: 263749). E: Parasitic folding of small vein derived from larger vein (IJPI-2017-155, N: 6779146, E: 263776). F: Mylonitic foliation in banded gneiss (IJPI-2017-170, N: 6771108, E: 266140). Pen or handle of the hammer are pointing north in each of the pictures.

5. Microscale kinematics

The micro-structural behavior of the rocks was observed to determine the kinematics and the deformation conditions of the Alastaro SZ and the Kankaanranta SZ. Based on the micro-scale asymmetric structures, the kinematic evidence within the Alastaro SZ is diverse indicating both west-block up and east block up shear senses, while in Kankaanranta SZ the kinematic evidence supports south-block up shear sense. The dynamic recrystallization of quartz indicate temperature between 480 and 530°C during the Alastaro SZ deformation, while in Kankaanranta SZ the deformation temperature was indicated between 420 and 480°C in the eastern part and somewhat lower, between 300 and 380°C in the western part.

5.1 Alastaro SZ

The best mylonite outcrops within Alastaro SZ were observed from the D2 area from local areas known as Ladonmäki and Vuori (locations in Fig. 11). Thin sections from these areas are best displaying evidence from the development of the asymmetric structures characteristic for mylonites, such as shear bands, sigma clasts and oblique foliation of quartz.

Shear bands and dynamic quartz recrystallization are common, whereas asymmetric sigma clasts (Fig. 26A) are only rarely observed. No delta clasts were observed. Some polygonised quartz grains have developed oblique foliation in Ladonmäki (Fig. 26B). The shear zone related asymmetry and sense of the shear is still best characterized by bending of the shear bands and ribbon quartz around large feldspar grains (Fig. 26C-F). Shear bands are mostly composed of micas but in some areas within Ladonmäki they are also filled with garnets, which have been broken down and transported along shear bands. Kinematic indicators from Ladonmäki (IJPI-43.1 and IJPI-43.2) are suggesting oblique west-block-up sear sense, while thin sections from Vuori area (IJPI-3.1) are suggesting oblique east-block-up shear sense within the Alastaro SZ (Fig. 25). Ladonmäki is located only half km towards N from the Vuori area. This indicates, that the block movements of rigid bodies are changing slip sense even within small area. However the rocks within Ladonmäki are more pervasively sheared and thus indicating from dominant west-block-up movement for the whole Alastaro SZ.

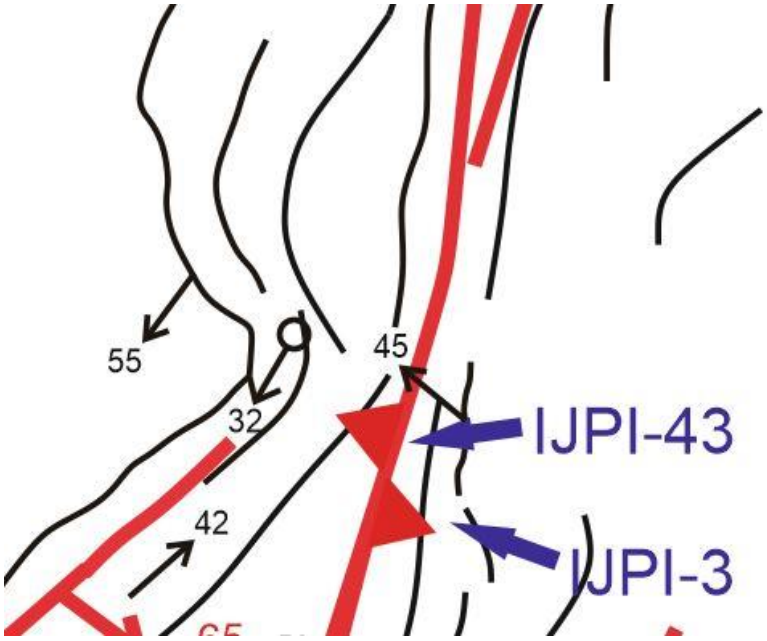

Fig. 25. Samples supporting west block up shear sense (IJPI-43, Ladonmäki) and east-block-up shear sense (IJPI-3, Vuori) in areas separated only by 0,5 km.

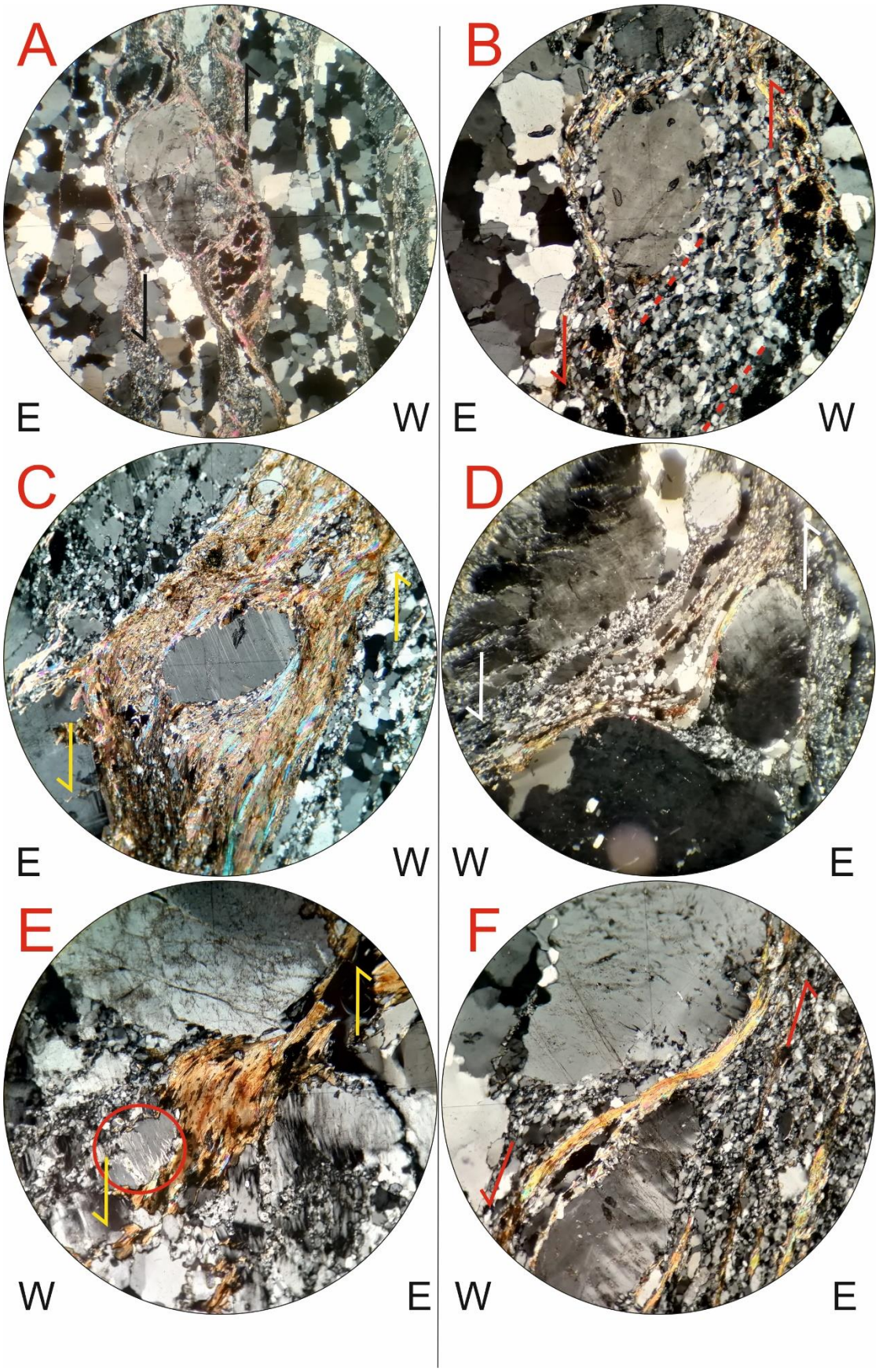

Fig. 26. Caption overleaf.

Fig. 26. Microscope photos of the Alastaro SZ observed from Ladonmäki (IJPI-43) and Vuori (IJPI-3). A: Sinistral feldspar sigma clast and garnet (black) breaking along shear band (IJPI-43.2). B: Sinistral shear band and oblique foliation of quartz (IJPI-43.1). C: Sinistral mica rich shear band (IJPI-43.2). D: Sinistral bending of the ribbon quartz within a shear band around large feldspar grains (IJPI-3.1). E: Sinistrally deflected biotite and albite lamellae within K-feldspar grain (perthite) (IJPI-3.1). F: Sinistrally deflected muscovite within shear band (IJPI-3.1)

Dynamic recrystallization of quartz was observed from the 10 m wide mylonitic zone within the Ladonmäki area in order to determine the temperature during the shear zone deformation. In some parts the quartz grains have been deformed into elongated narrow bodies known as ribbon quartz (Fig. 26D) and are completely or partially consisting of small subgrains (Fig. 28A), which are forming oblique foliation in areas near the shear bands. According to Stipp *et al.* (2002) these textures indicate subgrain rotation recrystallization (SGR). However, in other parts of the thin sections the quartz grains have been completely recrystallized forming interfingering boundaries (Figs. 28B and 28C), where evidence of the original grain boundaries are not visible and boundaries have even swept across entire grains. This indicates the highest temperature regime within the dynamic quartz recrystallization known as grain boundary migration recrystallization (GBM; Stipp *et al*. 2002). Moreover, in some parts, the completely recrystallized quartz grains have undergone the grain boundary area reduction (GBAR; Tandon *et al*. 2015, in Fig. 27), where grain boundaries have been straightened, which has led in reduction of the surface area of the grain boundaries. Quartz grains affected by GBAR are forming triple points with approximately 120° angles as seen in Fig. 28D. The presence of the SGR and GBM fabric indicates that the temperature during the shear zone deformation has been between 480°C and 530°C, which is the transition temperature zone between the two dynamic quartz recrystallization regimes (Stipp *et al*. 2002). After the shear zone deformation GBAR process has affected the quartz grains and thus the lattice has recovered into a stable structure, while the high temperature has still been present (Tandon *et al*. 2015). Based on the presence of perthite (Fig. 26E) the temperature has probably ceased slowly (Abart *et al*. 2009) compared to the strain of the shear zone deformation making the GBAR possible.

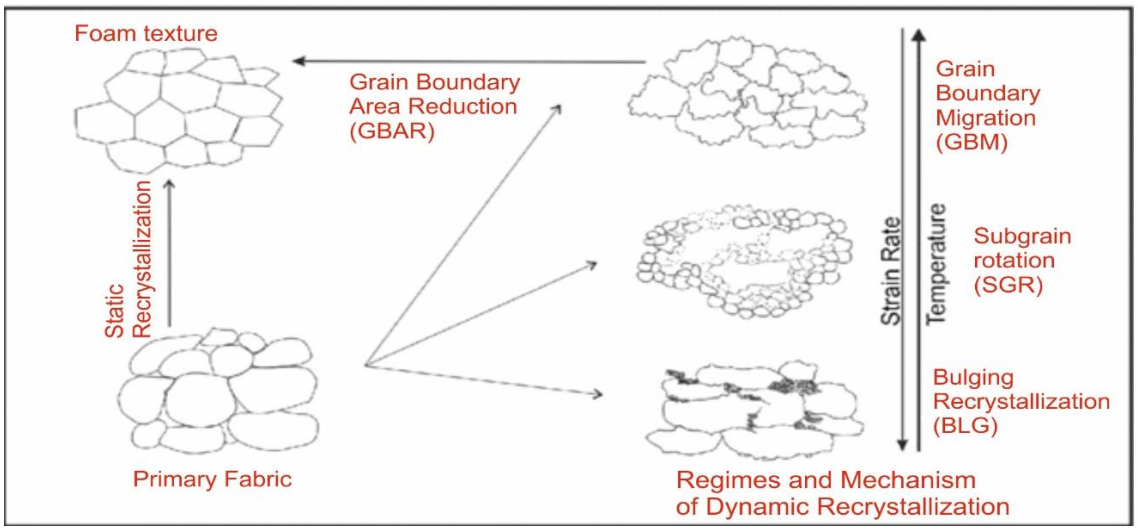

Fig. 27. Quartz dynamic and static recrystallization mechanisms, their representative microstructures and GBAR path. Modified after Tandon *et al*. (2005).

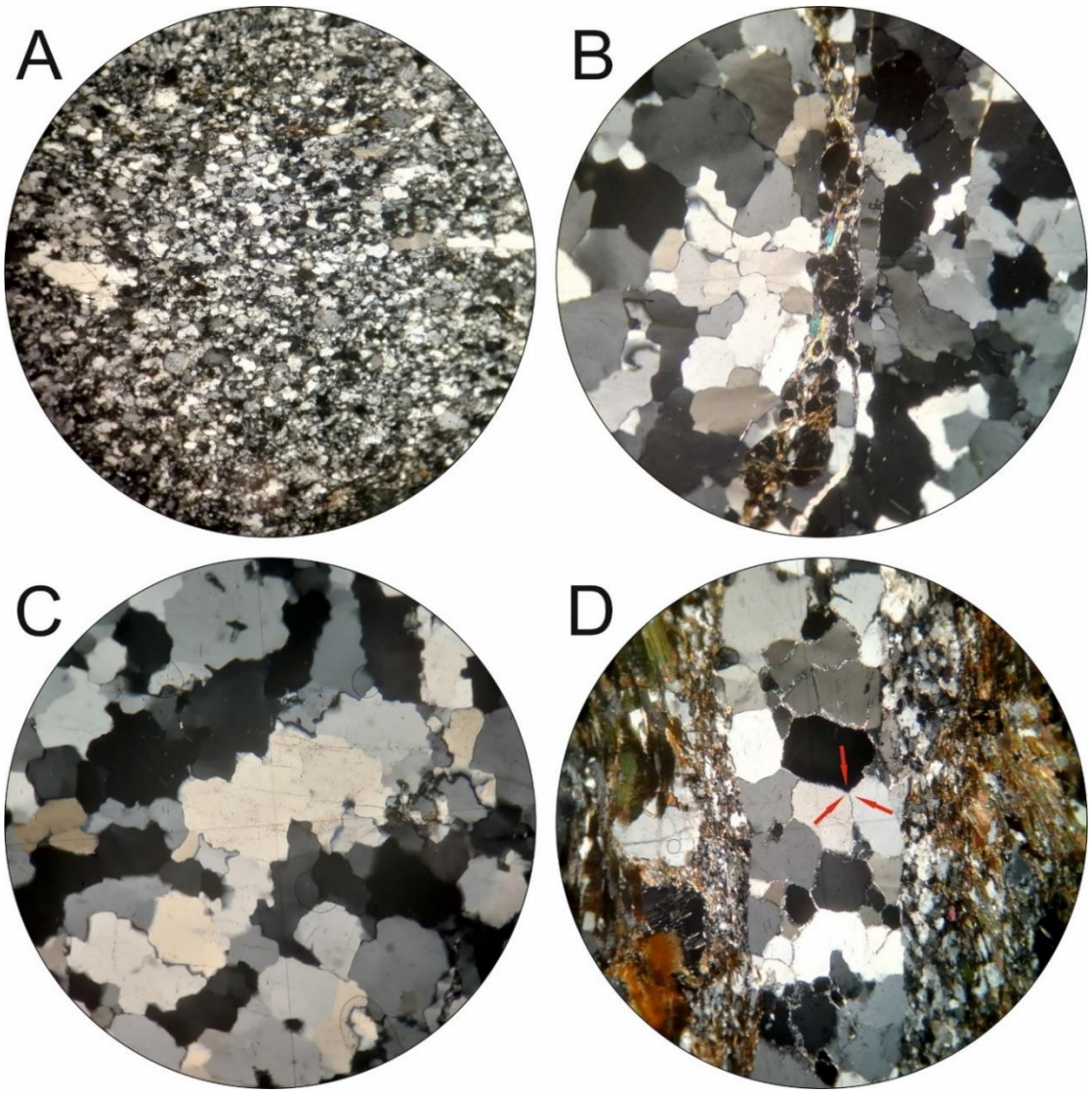

Fig. 28. Caption overleaf.

Fig. 28. Dynamic quartz recrystallization and grain boundary area reduction observed from the Ladonmäki outcrops. A: Polygonised SGR fabric with equal sized subgrains (IJPI-8.1). B: GBM fabric with larger grains with overprinting boundaries and shear band filled with garnets (small black grains) (IJPI-43.2). C: GBM fabric (IJPI-43.2). D: GBM fabric has undergone GBAR and thus the grains have formed equilibrium fabric (foam texture), where straightened grain boundaries are forming the triple junction points (indicated by arrows) with ~120° angles (IJPI-7.1).

5.2 Kankaanranta SZ.

The outcrops within Kankaanranta and Metsäsiankallio yielded the best outcrops for kinematic analysis. Kankaanranta is located in the eastern part of the shear zone, while Metsäsiankallio is located north of Uunimäki near the western termination of the shear zone (locations in Fig. 17). Evidence of the development of the asymmetric structures within the Kankaanranta SZ were best represented by the sigma and delta clasts consisting from either feldsbar or ribbon quartz (Fig. 29A-C), shear bands (Fig. 29D), oblique foliation of the polygonised quartz subgrains (Fig. 29E) and micro folds of the ribbon quartz (Fig. 29F).

Dextral kinematic evidence is observable throughout the thin sections. With the lineation plunging steeply towards ENE in Tale-2017-33 and Tale-2017-182 thin sections, the observed dextral asymmetries are supporting S-block-up tectonics within the Kankaanranta SZ, which is in line with the field observations.

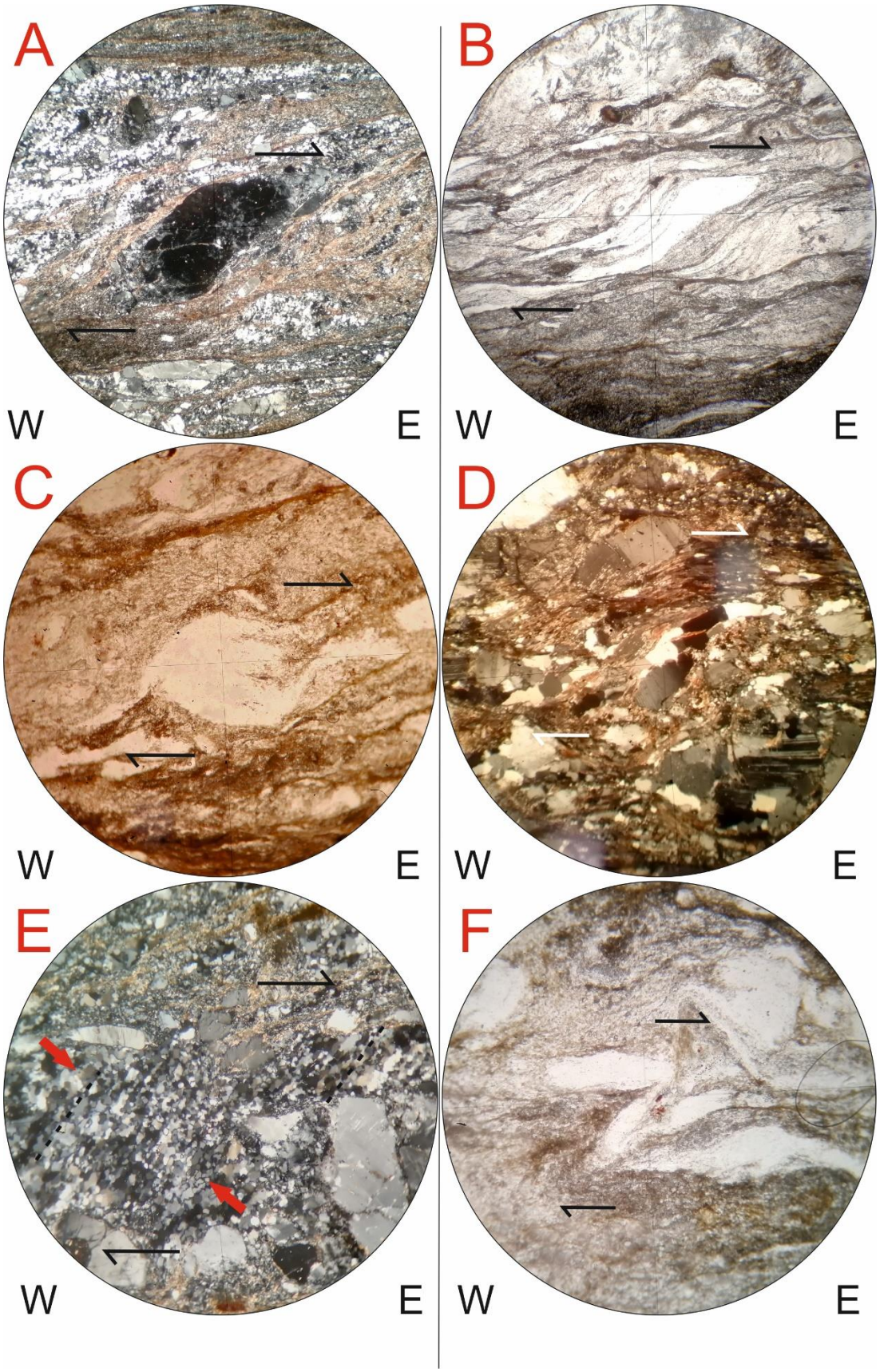

Fig. 29. Microscope photos of the Kankaanranta SZ observed from Kankaanranta (TALE-33) and Metsäsiankallio (TALE-182). A: Feldspar grain as a dextral sigma-porphyroclast (Tale-33.1). B: Ribbon-quartz as a dextral sigma-porphyroclast (TALE-33.4). C: Ribbon-quartz as a dextral delta-porphyroclast (TALE-33.4). D: Dextral shear bands cutting quartz and feldspar grains (TALE-182.3). E: Oblique foliation of the quartz subgrains between two shear planes (TALE-33.1). F: Dextral micro-folding of the ribbon-quartz (TALE-33.4).

Dynamic quartz recrystallization was observed in order to determine the temperature during shear zone deformation within the Kankaanranta SZ. Deformation related dynamic recrystallization of quartz was examined from samples from Kankaanranta and Metsäsiankallio. Different quartz behavior was recorded although their deformation in mesoscale seemed alike. Dynamic quartz recrystallization has three regimes according to Stipp *et al*. (2002). In Kankaanranta the subgrain rotation recrystallization (SGR) is dominant whereas bulging recrystallization (BLG) is the dominant type in Metsäsiankallio. Variation in thermal conditions within different parts of the Kankaanranta SZ can be constrained from differences in quartz behavior.

In oriented thin sections from the Kankaanranta, the quartz grains have developed elongated ribbon quartz textures (Fig. 30A). Quartz also exhibits polygonisation (Fig. 30B) (subgrain development) with varying degree and uniform oblique foliation with respect to the strike of the ribbon quartz has also formed. Subgrains are showing only minor undulose extinction and their boundaries are relatively straight. According to Stipp et al. (2002) this kind of quartz behavior indicates thermal conditions between 420°C and 480°C. The SGR type is indicated by the ribbon quartz. The degree of polygonisation and oblique foliation of the subgrains are suggesting higher end temperature within the SGR spectrum. The lack of grain boundary migration (GBM) features such as sutured grain boundaries suggests that the dynamic quartz recrystallization has not reached the transition temperatures between SGR and GBM (480°C-530°C) and therefore the temperature between 420°C and 480°C is suggested for the deformation within the eastern part of the Kankaanranta SZ.

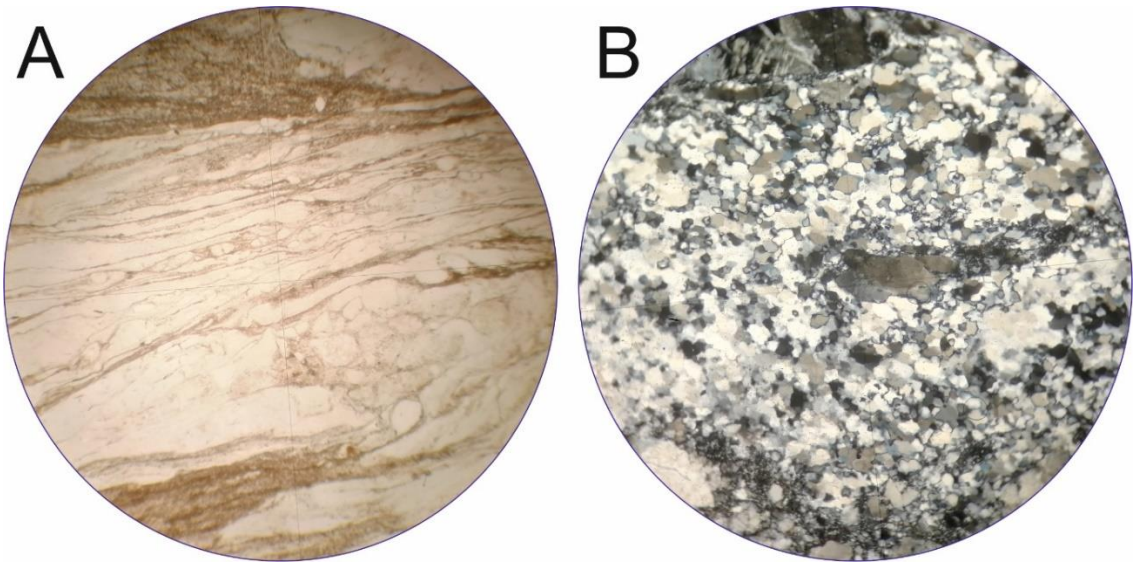

Fig. 30. Dynamic quartz recrystallization observed from the Kankaanranta (TALE-33) outcrop. A: Quartz grains appearing as stretched ribbon quartz (TALE-33.1). B: Polygonized texture related with subgrain rotation with quartz grains roughly equal in size and shape (TALE 33.3).

In Metsäsiankallio thin sections, the quartz grains have developed recrystallized bulges in the partially serrated grain boundaries (Fig. 31A-B) and have apparent undulose extinction. Micro-scale cracks are also common in quartz grains across the thin sections. Compared to the thin sections from Kankaanranta, quartz has not been developed into ribbon quartz and has not been polygonised. According to Stipp et al. (2002) the dynamic quartz recrystallization has occurred within the BLG thermal regime between 300°C and 380°C. The aforementioned quartz behavior is commonly associated within BLG. The transition boundary between BLG and cataclastic flow is approximately located at 300°C, which indicates the minimum temperature of the quartz recrystallization, since the textures related to cataclastic flow are not represented. The lack of ribbon quartz and polygonised subgrains suggests, that the thermal conditions of the BLG-SGR transition zone (380-420°C) have not been reached. These features indicate temperatures between 300°C and 380°C during the shear zone deformation.

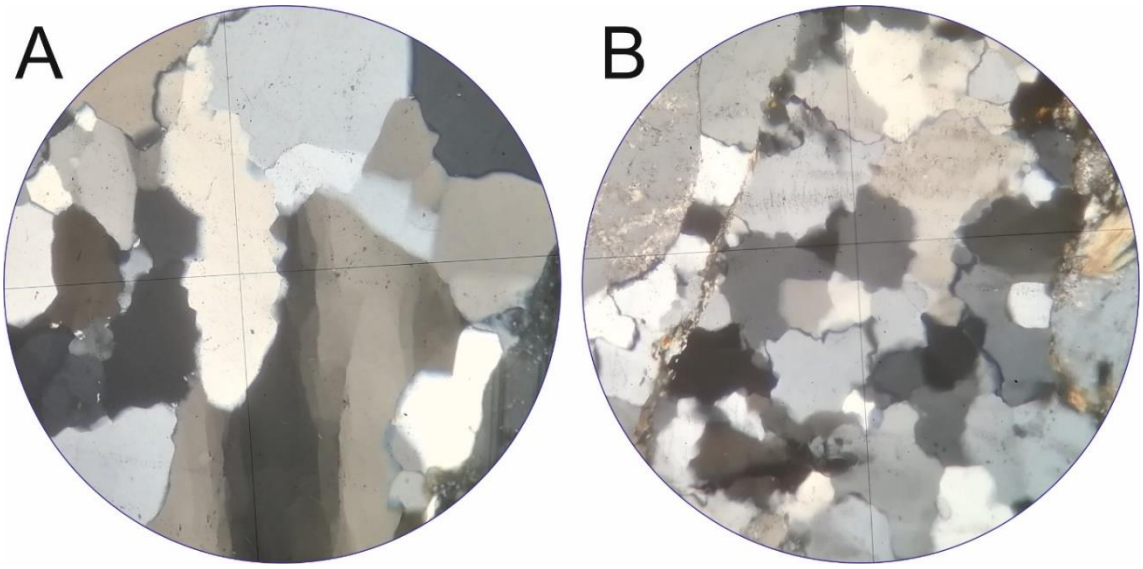

Fig. 31. Dynamic quartz recrystallization observed from Metsäsiankallio outcrop (TALE-182). A: Recrystallized bulges have developed into the partially serrated quartz grain boundaries and clear undulose extinction (TALE-182.3). B: More recrystallized bulges in partially serrated quartz grain boundaries and minor shear bands.

6. Alastaro shear zone U-Pb zircon analysis

U-Pb zircon spot analysis was made from the granite sample from the D3 area. Purpose of this sample was to determine the age of the Alastaro SZ deformation in the western part of the study area with single zircon U-Pb spot analysis. Since the granite was intruding along the hinges of the Alastaro SZ folds and it had foliation parallel to the axial surface of the folds, it was interpreted to be syntectonic to the shear zone. A total of 113

zircon grains were attached on the epoxy mount and 19 spots from 12 zircons were analyzed.

The zircons show mainly prismatic elongated shapes with their length being between 50-250μm and width between 20-90μm. However, some zircons will not fit in these average sizes such as Alastaro-101 (Fig. 33). Most of the grains are fractured and metamict at some degree. Micro fractures and zoning are also common. Homogeneous zircons were the target of interest, but only a few grains seem unaltered, such as Alastaro-82 (Fig. 33). Due to the bigger size of some metamict grains like Alastaro-101, they also contained more intact parts, which were analysed if the provided intact part was more than 25μm in diameter.

Three generations for zircon crystallisation can be distinguished (Fig. 34) after removing one discordant analysis, which had suffered lead loss and yielded deviant $^{207}Pb/^{206}Pb$ age of 1978 Ma. The first and oldest zircon generation (right in Fig. 34) yields $^{207}Pb/^{206}Pb$ ages between 1938 and 1916 Ma, which makes these zircons surely inherited. The second zircon generation (middle in Fig. 34) yields slightly younger ages of 1889-1902 Ma, which also indicates inherited nature of the second generation. The $^{207}Pb/^{206}Pb$ weighted average age of 1872±11 Ma (Fig. 35) and upper intercept age of 1868±22 Ma (Fig. 36) was obtained from six analyses from four zircons (Alastaro-32, Alastaro-82, Alastaro-98 and Alastaro-101), which represented the youngest generation of zircons (left in Fig. 34). Many analyses are reversely discordant.

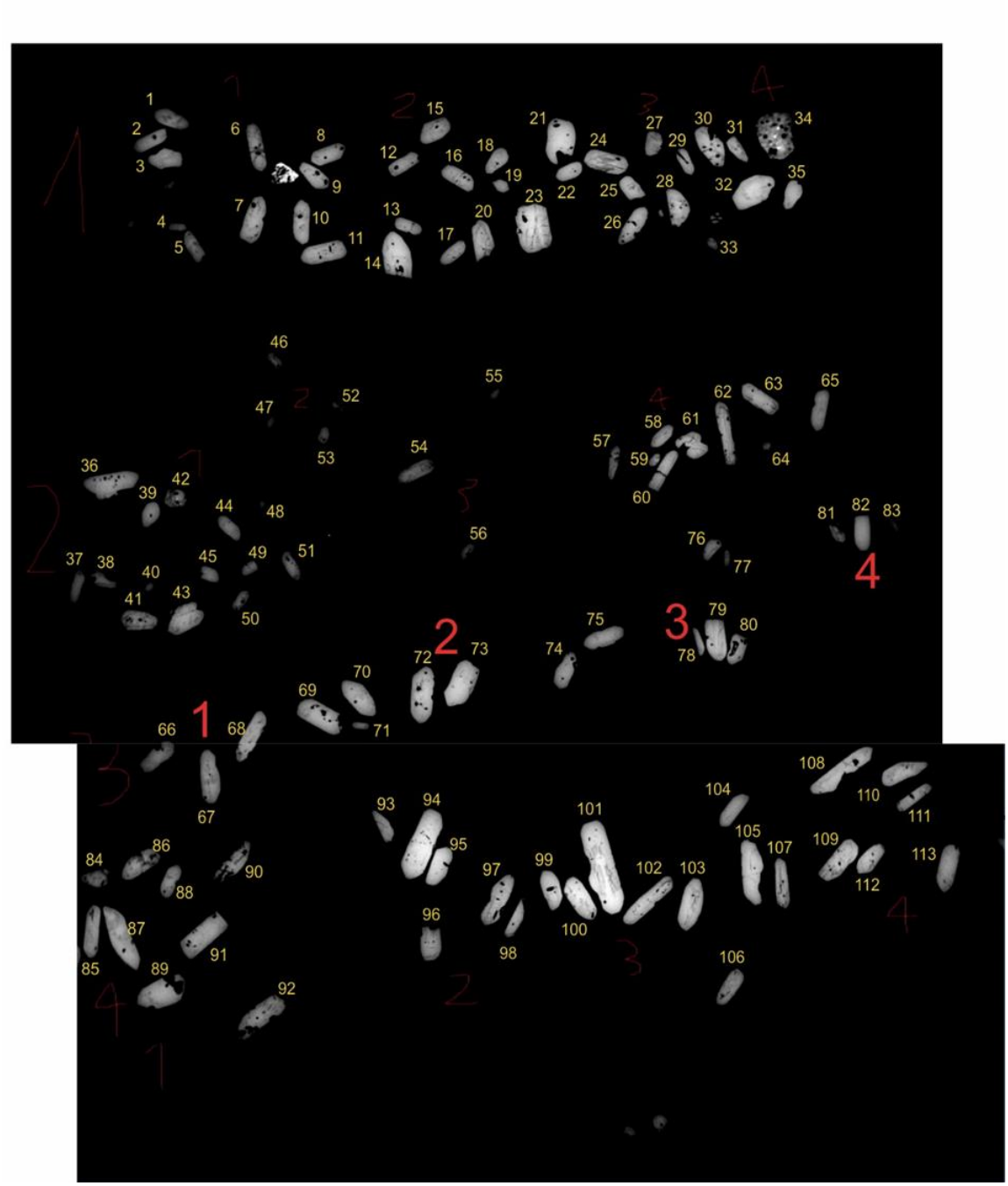

Fig. 32. All hand-picked and numbered zircons.

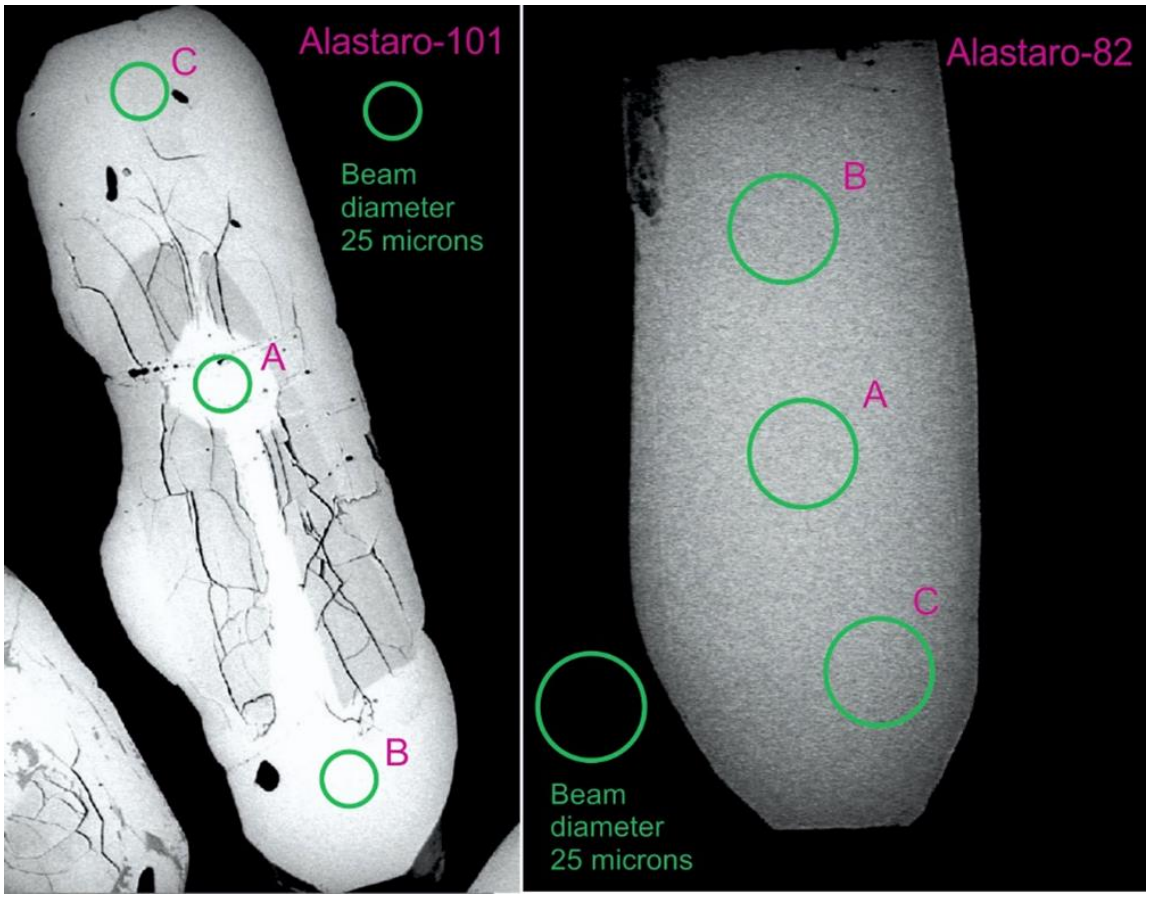

Fig. 33. Example of fractured metamict (Alastaro-101) and homogeneous (Alastaro-82) zircons.

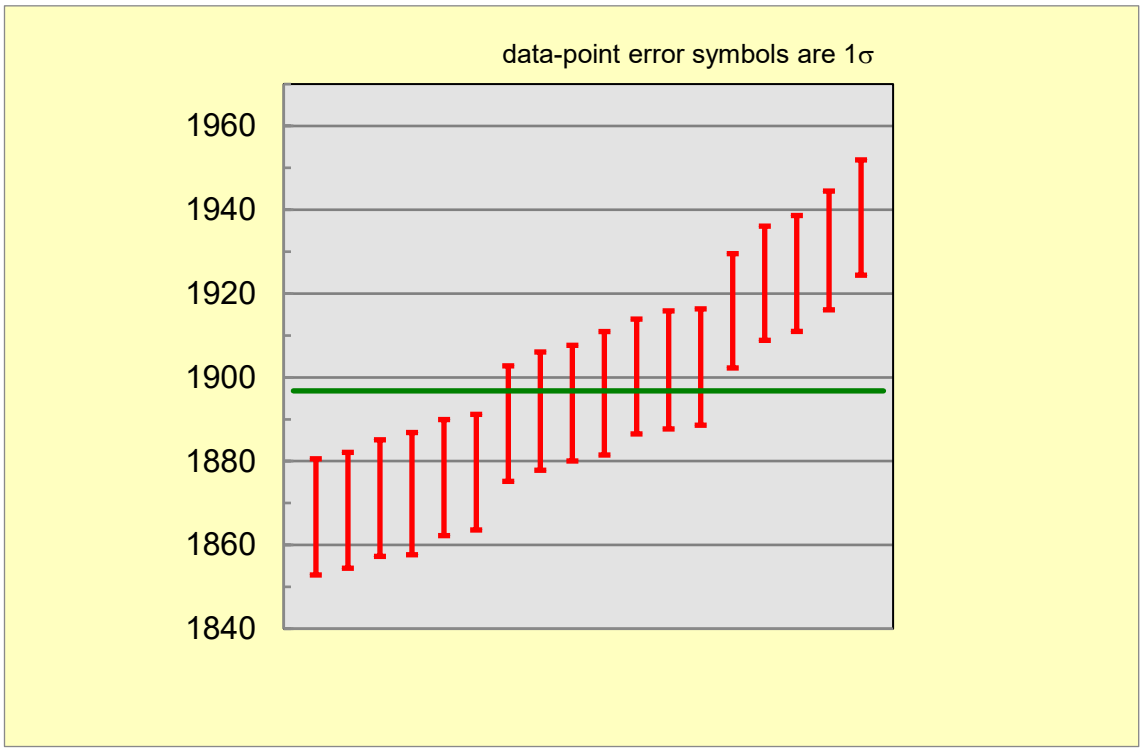

Fig. 34. Weighted average with 18 spots, displaying three generations. One discordant analysis (from Alastaro-6) was removed due to the lead loss.

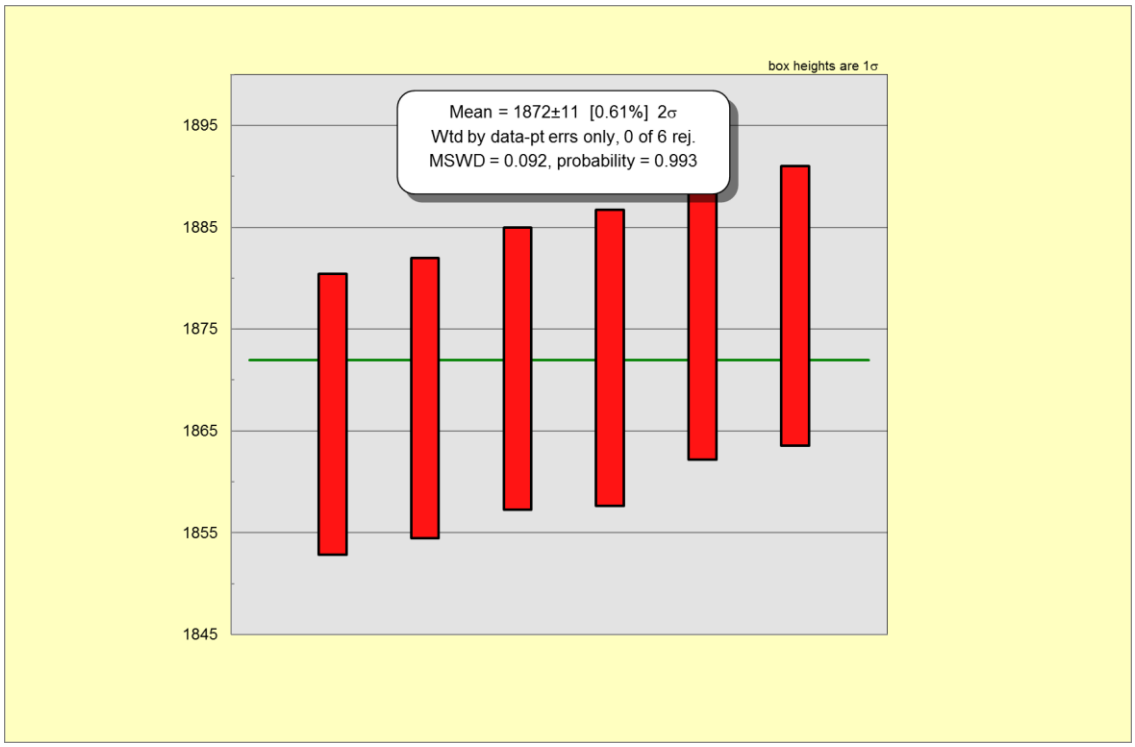

Fig. 35. Weighted average of the 6 selected spots

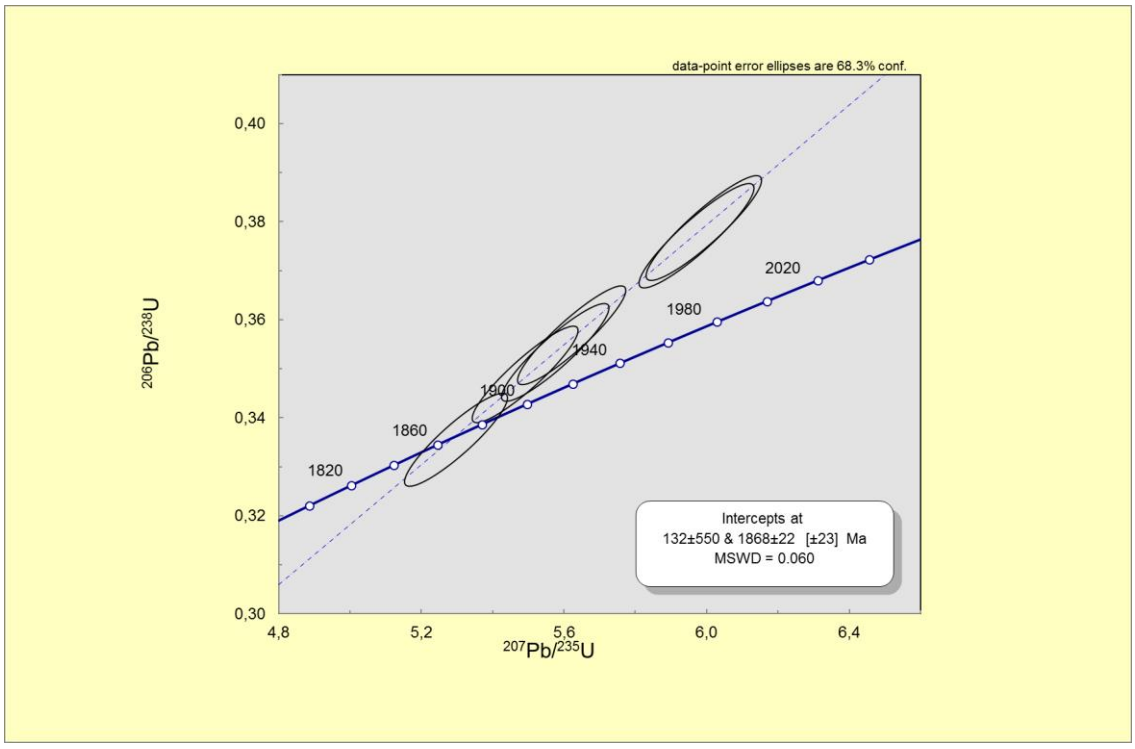

Fig. 36.Upper intercept age of the 6 selected spots

7.Discussion

7.1 Geometry and kinematics of the studied shear zones

Mesoscale and microscale indicators from the D2 area within the Alastaro SZ are suggesting reverse W-block-up dip-slip movements under ductile conditions. However, local variation exists even at half-km scale: in 10 m wide mylonite zone in Ladonmäki the kinematic evidence supports oblique west-block-up shear sense, while half km towards south, (the Vuori area) oblique east-block-up shear sense appears dominant (Section 4.2.2). Because mylonite zone is much more pervasive in the Ladonmäki outcrops, it seems to better represent the core of the shear zone. Mylonites in the Vuori area are zonal and narrower zones, and thus probably represent splays of the main zone. In the northern part the Alastaro SZ is interpreted to divide into two splays. This assumption is derived from aeromagnetic map and field observations from Ruskonkallio (D4, Section 4.2.4) where mesoscale kinematic evidence is supporting oblique east-block-up shear sense. Ruskonkallio contains more pervasively sheared rocks than other areas of the Alastaro SZ, and if added to the contrasting shear sense, it likely represents different deformation event than the Ladonmäki and Vuori outcrops. However, microscale indicators were not found in Ruskonkallio thin sections. Based on the kinematic evidence and mainly west-dipping mylonitic foliations, the west-block-up shear sense is suggested to have been dominant during the main deformation of the Alastaro SZ. Even though the deformation of the shear zone has been heterogeneous on multiple scale.

Collected data and analyses from the Kankaanranta SZ indicate a reverse ductile fault, where compression has caused the southern hanging wall to move upward in relation to the northern footwall causing crustal shortening. The south-block-up shear sense was inferred dominant based on the field observations of the western part (Section 4.3) and thin section evidence (Section 5.2). However the strike-slip- and oblique lineations were also observed in mesoscale. Dextral kinematic indicators on horizontal plane were observed from these outcrops, which are also indicative of a dextral strike-slip component within the Kankaanranta SZ. Both the reverse- and strike-slip components taken into account, the tectonic regime in the Kankaanranta shear zone has likely been transpressional. The semi-brittle, nearly horizontal slickenlines in the western part could characterize later reactivation of the shear zone. The NW-SE trending splays are likely

younger than the primary ENE-WSW trending structures within the Kankaanranta SZ and could represent the weakness zones, which have likely also evolved during reactivation of the shear zone.

7.2 Folds and their relation to the shearing observed in this study

Three types of folding can be distinguished across the study area (Fig. 37): i) Regional scale folds (area 1 in Fig. 37) containing the subareas A, E and F, ii) shear-induced folding in proximity to the Alastaro SZ (area 2 in Fig. 37), and iii) folding within the transitional area between Kolinummi and Alastaro shear zones (area 3 in Fig. 37).

The major regional-scale folds, The North fold, Alastaro fold and Oripää fold have most likely developed under ~NW-SE and NNW-SSE directed compression. Based on the tectonic measurements the folds are tight to isoclinal and are in upright to slightly overturned position. Their position, similar foliation orientations and similar major fold axes are indicating penetrative folding generating a continuous chain of folds, which has most likely developed during earlier stages of the collisional orogeny. These regional scale folds have not been transposed along Alastaro or Kankaanranta shear zones. However, a very complex structure has developed to the central part of the study area including the Uunimäki prospect, where shear zone deformation has mixed with the folds and thus overprinted the major fold structures. In North fold area the negative anomaly is seemingly causing sinistral displacement in aeromagnetic map (area 4 in Fig. 37), but field observations from this area are scarce. This magnetic anomaly might be derived from the southern continuation of Kynsikangas SZ. Still, older age for the regional scale folds in relation to the two shear zones is suggested. This interpretation is supported by the outcrop scale folds within the eastern part of the D4 area (Fig. 16D in section 4.2.4). In this area the NW-SE striking foliation (derived with envelope surface method) is interpreted pretectonic to shearing and is likely representing the hinge area of the regional scale fold. The shear zone deformation has caused the foliation to transpose into open symmetric folds. In western part of the Kankaanranta SZ (Section 4.3) the secondary structures, which are likely shear-induced are cutting the folded domain and thus also indicating, that regional scale folds are older than the shear zones.

The observed folding within the D3 area (Fig. 14A-B in section 4.2.3) is probably related to the crustal shortening of the Alastaro SZ deformation. This folding is thus suggested to be shear-induced, with the measured axial surfaces striking NNW, parallel to the

controlling shear zone. These folds have likely formed under WSW-ENE compression, which would also explain the oblique dip-slip shear sense within the N-S striking Alastaro SZ. Similar type of folding has probably affected all the subareas within Alastaro SZ, but field observations from these syntectonic (syntectonic to shearing) folds were only made from the D3 area.

Third type of folding in the central part of the D2 area is likely caused when the deformation of the Alastaro SZ transposes the preexisting NE-SW striking foliations of the Kolinummi SZ along N-S trend. This indicates younger origin for the Alastaro SZ compared to the Kolinummi SZ. These folds might also represent the possible event where Alastaro SZ and KoSZ merge into same shear zone.

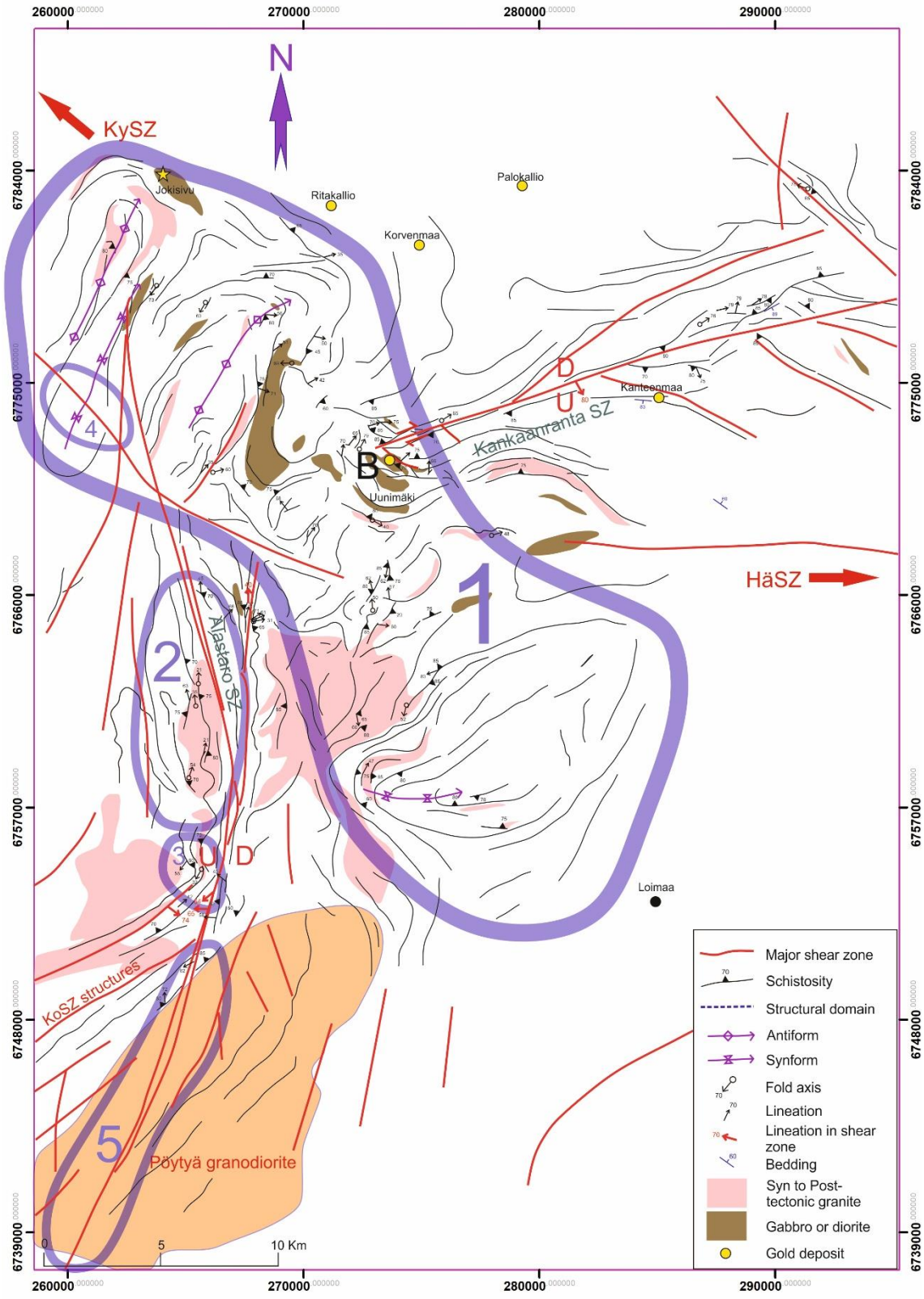

Fig. 37. Structural map of the study area and separation of the different fold phases (1-3). Sinistral displacement of the regional scale fold caused by the possible splay from the Kynsikangas shear zone (4). Continuation of the Alastaro SZ towards SSW across the Pöytyä granodiorite (5). Moreover the orientations and locations of the Kolinummi shear zone (KoSZ) structures and directions of the Kynsikangas (KySZ) and Hämeenlinna shear zones (HäSZ). “U” and “D” refer to the up and down movements of the blocks on the opposing sides of the shear zones. Coordinate system is EUREF-FIN-TM35FIN.

7.3 Correlation with the existing models of crustal evolution in SW Finland

7.3.1 Correlation of the Alastaro and Kankaanranta shear zones with other known major shear zones

The Kynsikangas shear zone and the Kolinummi shear zone (Fig. 37) were interpreted to be the same shear zone by Väisänen and Skyttä (2007). In this suggestion the Alastaro SZ would be the part connecting them. In north the connection between the Alastaro SZ and the Kynsikangas SZ is possible but evidence is too scarce. Lineations within the Kynsikangas SZ are nearly horizontal and rocks are dominantly L-tectonites (e.g. Pietikäinen 1994 & Reimers *et al*. 2018), while in Alastaro SZ the nearly vertical lineations and S- or SL-tectonites are dominant. Observed lineations from the D4 area and North fold area are not transposing to similar orientations with those of the Kynsikangas SZ. However, their connection seem likely in the aeromagnetic maps. With these things added, the northern termination of the Alastaro SZ still needs more investigation to determine the possible linkage with the Kynsikangas SZ.

The semi-brittle slickenlines and L-tectonites in the D1 area of the Alastaro SZ are interpreted to represent the deformation of the NE-SW striking Kolinummi SZ. This suggestion is supported by a negative anomaly that extends towards SSW and across the Pöytyä granodiorite in the aeromagnetic map. This anomaly is suggested to represent the continuation of the Alastaro SZ (5 in Fig. 37) outside the study area. This also suggests that the Alastaro SZ and Kolinummi SZ have been separate shear zones at first, but possible tectonic reactivation could have connected the shear zones. The reactivation of the shearing supports the interpretation of the Kynsikangas SZ, Alastaro SZ and Kolinummi SZ forming the same shear zone (Väisänen & Skyttä 2007). In addition with the magnetic anomaly, the SSW continuation of the Alastaro SZ is supported by ductile shearing and dynamic quartz recrystallization observed in the Pöytyä granodiorite area by Nironen (1999), where quartz behaviour is similar with that observed in the D2 area.

Shear zone reactivation in southern Finland has been interpreted previously by Torvela et al. (2008) who describe three distinct deformation events within the ~E-W trending South Finland shear zone, which is one of the most prominent shear zones in southern Finland along with the Somero shear zone. Separate stages of deformation within other ~N-S striking shear zones within Southern Finland have been suggested by Väisänen and Skyttä (2007), such as in the Kolinummi, Kisko, Porkkala-Mäntsälä and Jyly shear zones. In

South Finland SZ and in several N-S striking shear zones the oldest stage of deformation has happened under ductile conditions followed by later semi-brittle and brittle deformation (Väisänen & Skyttä 2007, Torvela *et al*. 2008). Since both shear zones are interpreted to belong to the same shear zone network in southern Finland (Väisänen and Skyttä 2007), it is likely that reactivation of shearing has also occurred in the other shear zones within the network including the Alastaro SZ. The younger reactivation could explain the observed semi-brittle features in the D2 area and formation of pseudotachylites in a splay of the Alastaro SZ within the North fold area.

The Kankaanranta SZ might represent the western termination of the Hämeenlinna shear zone (Fig. 37), which is located towards the east (Nironen *et al*. 2001). Near the western termination of the Hämeenlinna SZ strain has likely partitioned into ENE-WSW and NW-SE striking shear zones (at the top-right corner in Figs. 6 & 37). The Kankaanranta SZ represents the ENE-WSW continuation. The interpreted NW-SE continuation stands out from the NW-SE striking splays (Section 4.3) located in the southern side of the major Kankaanranta SZ by its longer extend and much wider negative anomaly area. Hakkarainen (1994) observed indicators from both vertical and horizontal displacement, within the Hämeenlinna SZ, which is somewhat in line with the collected evidence from the Kankaanranta SZ (Sections 4.3 & 7.1).

7.3.2 Temperature and timing of deformation

Nironen (1999) described the Alastaro SZ as a brittle shear zone. However, the outcrops in Ladonmäki, Vuori and Ruskonkallio areas show ductile conditions and outcrops in Huhtamonmäki are characterizing semi-brittle conditions. Quartz behaviour in dynamic recrystallization within mylonites of the Alastaro SZ (Section 5.1) indicated deformation temperature between 480°C and 530°C (Stipp *et al.* 2002). The development of foam/polygonal texture (similar with static recrystallization) has happened during cessation of the deformation. This indicates preserved high temperatures during subsiding shearing deformation or high concentration of fluids between grain boundaries. Other option is, that the foam texture developed after the shear zone deformation in static recrystallization (annealing; Passchier *et al*. 2005 & Tandon *et al*. 2015) and was caused by a thermal pulse from the intruding post-tectonic pegmatite granites. These suggestions are somewhat in line with the over 500°C deformation temperature and static recrystallization of quartz described by Nironen (1999) from the sheared Pöytyä granodiorite. Ductile conditions in the Ladonmäki and Vuori areas within the D2 area

likely represent the early high-temperature deformation phase within the shear zone. Even though the deformation in Ruskonkallio might be older. The semi-brittle faulting in Huhtamonmäki, also within the D2 area, represents a younger phase of deformation, where temperature has decreased. This suggestion is supported by the aforementioned inferred shear zone reactivation.

Conditions in the Kankaanranta SZ have mainly been ductile, except the semi-brittle slickenlines in the western part. Observing the quartz behaviour in mylonites within the Kankaanranta SZ (Section 5.2), the temperature between 420°C and 480°C was suggested in the eastern part (Kankaanranta) while lower temperature between 300°C and 380°C (Stipp *et al.* 2002) was suggested in the western part (Metsäsiankallio). The deformation temperature during shearing has thus been lower in the Kankaanranta SZ than in Alastaro SZ, since the grain boundary migration textures were not observed. This indicates younger origin for the Kankaanranta SZ.

The collected granite sample for dating purpose from the D3 area contained lots of inherited zircons belonging to at least two generations with $^{207}Pb/^{206}Pb$ ages of 1938-1916 Ma and 1889-1902 Ma. The weighted average age of 1872±11 Ma and upper intercept age of 1868±22 Ma (Section 6) of the youngest generation are probably not representing the deformation age of the Alastaro SZ, since those ages would make it older than the South Finland SZ (Torvela *et al*. 2008) and interpreted age of the shear activity in Southern Finland (Väisänen & Skyttä 2007). All zircon populations are probably inherited from the source, including the ~1.87 Ga population. This assumption is supported by the ~1.87 Ga granitoids within the study area (Nironen 1999) and similar age from the nearby Oripää granite (Kurhila *et al*. 2005), which was also interpreted to be inherited. Also, the older zircons are not displaying new ~1.87 Ga grain growth around the rims which is a typical phenomenon during a younger zircon growth. It is possible that the syntectonic granite (Fig. 14B) stems from a melt with temperatures not high enough for zircon or monazite crystallization.

7.3.3 Inferred tectonic model

The mafic- and intermediate volcanic rocks (the Loimaa suite) observed in all the subareas have likely formed during volcanic-arc magmatic phase (Sipilä & Kujala 2014), which has likely taken place between 1.90-1.88 Ga (Lahtinen *et al*. 2005 & Saalman *et al*. 2009). The emplacement of the pervasively foliated tonalites and granodiorites could

represent the oldest observable plutonic activity within the study area. These plutonic rocks might have the same genesis with the tonalites and granodiorites observed from partially overlapping study area by Nironen (1999), who described these rocks to be 1.89-1.87 Ga old. However, the 1891±5 Ma age of the Uunimäki gabbro by Leskelä (2019) suggest, that some gabbroic magmatism took place even before the emplacement of tonalites and granodiorites. The continent-continent collision stage, which in its entirety lasted from 1.87 Ga to 1.79 Ga (Lahtinen *et al*. 2005) resulted in pervasive planar orientations of the aforementioned supracrustal and plutonic rocks in early stages of the orogeny (1.87-1.84 Ga). Orientation trends of this phase are not represented within the study area because these orientations were folded into the observable regional scale folds (subareas A, E and F) during NW directed thrusting at approximately 1.84 Ga, when Sarmatia collided with Fennoscandia (Lahtinen *et al*. 2005; Väisänen & Skyttä 2007). After this the Alastaro SZ and the Kankaanranta SZ developed in late orogenic phases most likely between 1.84–1.79 Ga (Väisänen & Skyttä 2007; Torvela *et al*. 2008). According to Väisänen and Skyttä (2007), the most active contractive shearing occurred between ~1.81 Ga and ~1.79 Ga when crustal unit between the South Finland SZ and the Somero SZ was transported westwards and deformed along N-S shear zones. In this study the similar but less voluminous second contractional crustal unit is interpreted to have been formed between the Hämeenlinna SZ and the Somero SZ during the same orogenic stage. Contraction within this second crustal unit has likely formed the Alastaro SZ and the shear- induced folding observed in the D3 area. This would explain the similar steep structures of the Alastaro SZ within other N-S oriented reverse faults in southern Finland (Väisänen & Skyttä). The Kankaanranta SZ, which was suggested to be a part of the Hämeenlinna SZ, has likely formed during later reactivation of the Hämeenlinna SZ under ductile conditions, which would explain the lower deformation temperature and thus interpreted younger age compared to the Alastaro SZ. The Alastaro SZ is also suggested to have been reactivated under ductile conditions, which would explain the folding in the merge area with the Kolinummi SZ structures and compatibility to the Kynsikangas SZ in aeromagnetic map. The semi-brittle to brittle structures and post-tectonic granites and pegmatites are representing the youngest phases of defomation within the study area. They are most likely formed or emplaced at/or after 1.80 Ga, such as in the case of the SFSZ (Torvela *et al*. 2008).

7.4 The sources of error

It is not clear whether the density of the field observations is enough to create a fully trustworthy structural model of the study area. Also, there are only few outcrops, which can be thought to represent the cores of the two shear zones, which make the kinematic interpretations to be based only on these outcrops. The soil and permanent vegetation are covering main parts of the areas with most intense shear zone deformation.

8. Conclusions

- A continuous chain of the regional scale folds were formed during the peak stage of the continent-continent collision prior to the generation of the Alastaro and Kankaanranta shear zones. The NW directed thrusting caused the folding of older planar features of the study area into their current orientations
- The Alastaro shear zone and the Kankaanranta shear zone evolved during late orogenic phases when highest strain was partitioned into ~E-W and ~N-S striking shear zones. The foliations in proximity to the shear zones have also transposed into the present day E-W and N-S trends.
- Both the studied shear zones characterize principally oblique dip-slip shear sense and have been reactivated at least once, most likely several times. In the Alastaro shear zone the ductile oblique west block-up shear sense has been dominant. In the Kankaanranta shear zone the ductile south block-up shear sense appears dominant apart in the westernmost part, where semi-brittle dextral strike-slip component appears dominant. Shear zones are thus oblique reverse faults.
- The Alastaro shear zone has likely been merged with the Kynsikangas shear zone in the northwest and with the Kolinummi shear zone in the southwest during reactivation, and has thus formed one major shear zone. The reactivation is perhaps also related to the split-up of the shear zone into two parts within the D4 area.
- The Kankaanranta shear zone is likely a western appendage of the Hämeenlinna shear zone. The lower deformation temperature within the Kankaanranta shear zone indicates, that it has been formed during a later reactivation of the Hämeenlinna shear zone. NW-SE trending splays characterize the weakness zones during reactivation of the Kankaanranta shear zone.

- The zircons in the syn-tectonic granite within the Alastaro shear zone are most likely inherited.
- The syntectonic folding observed in the D3 area along with the oblique uplift of the western block within the Alastaro shear zone are caused by the late-orogenic WSW-ENE compression.

9. Acknowledgements

In the first place, I want to thank the Geological Survey of Finland for funding this project. I want to thank geologists Hanna Leväniemi, Markku Tiainen and Janne Hokka at the GTK, for offering supervision and support during the project. I also want to thank these people for providing the needed GIS- and geophysical materials. I want to thank Hugh O'Brien and Yann Lahaye at the Finnish Geosciences Laboratory for teaching the use of the mass spectrometer during the zircon U-Pb analysis. I want to thank Professor Pietari Skyttä, university lecturer Markku Väisänen and MSc Jaakko Kara at the University of Turku for offering introduction, guidance and expertise in geological field work and knowledge related to structural geology. Their support continued in the writing process as well. Thanks go to Jaakko Kara for performing the data reduction for the U-Pb geochronological data. I'd like to thank MSc Niklas Tenovuo for preparing the thin sections used in this study and Arto Peltola for preparing the zircon mount for the BSE and mass spectrometer studies. Finally, I want to thank my mapping partner BSc Tuomas Leskelä for his contribution during field work, structural analysis and thesis writing.

References

Abart, R., Petrishcheva, E., Wirth, R., Rhede, D. 2009: Exsolution by spinodal decomposition II: Perthite formation during slow cooling of anatexites from Ngoronghoro, Tanzania. American Journal of Science, 309, 450-475.

Belousova, E.A., Griffin, W.L., O'Reilly, S.Y. 2005: Zircon crystal morphology, trace element signatures and Hf isotope composition as a tool for petrogenetic modelling: examples from eastern Australian granitoids. Journal of Petrology, 47, 329-353.

Daly, J. S., Balagansky, V. V., Timmerman, M. J., Whitehouse, M. J., De Jong, K., Guise, P., Bogdanova, S., Gorbatschev, R., Bridgwater, D. 2001: Ion microprobe U-Pb zircon geochronology and isotopic evidence for a trans-crustal suture in the Lapland–Kola Orogen, northern Fennoscandian Shield. Precambrian Research, 105, 289-314.

Fossen, H. 2010: Structural geology. Cambridge University Press. Cambridge. 463 pp.

Fossen, H., Cavalcante, G. C. G. 2017: Shear zones–A review. Earth-Science Reviews, 171, 434-455.

Gebre-Mariam, M., Hagemann, S. G., Groves, D. I. 1995: A classification scheme for epigenetic Archaean lode-gold deposits. Mineralium Deposita, 30, 408-410.

Gorbatschev, R., Bogdanova, S. 1993: Frontiers in the Baltic Shield. Precambrian Research, 64, 3-21

Goldfarb, R., Baker, T., Dube, B., Groves, D. I., Hart, C. J., Gosselin, P. 2005: Distribution, character and genesis of gold deposits in metamorphic terranes. Society of Economic Geologists. Economic Geology 100th Anniversary Volume, 407-450.

Groves, D. I. 1993: The crustal continuum model for late-Archaean lode-gold deposits of the Yilgarn Block, Western Australia. Mineralium Deposita, 28, 366-374.

Groves, D. I., Goldfarb, R. J., Gebre-Mariam, M., Hagemann, S. G., Robert, F. 1998: Orogenic gold deposits: a proposed classification in the context of their crustal distribution and relationship to other gold deposit types. Ore Geology Reviews, 13, 7-27.

Grönholm, S., Kärkkäinen, N. 2012: Gold in Southern Finland: Results of GTK studies 1998-2011. Geological Survey of Finland, Special Paper, 52, 276 pp.

Hakkarainen, G. 1994: Geology and geochemistry of the Hämeenlinna-Somero volcanic belt, southwestern Finland: a Paleoproterozoic island arc. Geochemistry of Proterozoic Supracrustal Rocks in Finland, 19, 85-100.

Hermansson, T., Stephens, M. B., Corfu, F., Page, L. M., Andersson, J. 2008: Migratory tectonic switching, western Svecofennian orogen, central Sweden: Constraints from U/Pb zircon and titanite geochronology. Precambrian Research, 161, 250-278.

Homberg, C., Schnyder, J., Roche, V., Leonardi, V., Benzaggagh, M. 2017: The brittle and ductile components of displacement along fault zones. Geological Society, London, Special Publications, 439, 439-21.

Huhma, H., Mänttäri, I., Peltonen, P., Kontinen, A., Halkoaho, T., Hanski, E., Hokkanen, T., Hölttä, P., Juopperi, H., Konnunaho, J., Lahaye, Y., Luukkonen, E.,

Pietikäinen, K., Pulkkinen, A., Sorjonen-Ward, P., Vaasjoki, P., Whitehouse, M. 2012: The age of the Archaean greenstone belts in Finland. Geological Survey of Finland, Special Paper, 54, 74-175.

Hölttä, P., Heilimo, E. 2017: Metamorphic Map of Finland. Bedrock of Finland at the scale 1:1000 000 – Major stratigraphic units, metamorphism and tectonic evolution. Geological Survey of Finland, Special Paper, 60, 77-128.

Jackson, S. E., Pearson, N. J., Griffin, W. L., Belousova, E. A. 2004: The application of laser ablation-inductively coupled plasma-mass spectrometry to in situ U–Pb zircon geochronology. Chemical Geology, 211, 47-69.

Korsman, K., Koistinen, T., Kohonen, J., Wennerström, M., Ekdahl, E., Honkamo, M., Idman, H., Pekkala, Y. 1997: Suomen kallioperäkartta–Berggrundskarta över Finland–Bedrock map of Finland. Geological Survey of Finland, Espoo, Finland.

Kurhila, M., Vaasjoki, M., Mänttari, I., Rämo, T., Nironen, M. 2005: U-Pb ages and Nd isotope characteristics of the lateorogenic, migmatizing microcline granites in southwestern Finland. Bulletin-Geological Society of Finland, 77, 105 pp.

Kähkönen, Y. 2005: Svecofennian supracrustal rocks. In: Lehtinen, M. & Nurmi, E.A. The Precambrian Geology of Finland- Key to the Evolution of the Fennoscandian Shield. Elsevier B.V., Amsterdam, 343–405.

Lahtinen, R. 1994: Crustal evolution of the Svecofennian and Karelian domains during 2.1–1.79 Ga, with special emphasis on the geochemistry and origin of 1.93–1.91 Ga gneissic tonalities and associated supracrustal rocks in the Rautalampi area, central Finland. Geological Survey of Finland, Bulletin 378, 128 pp.

Lahtinen, R. 1996: Geochemistry of Palaeoproterozoic supracrustal and plutonic rocks in the Tampere–Hämeenlinna area, southern Finland. Geological Survey of Finland, Bulletin 389, 113 pp.

Lahtinen, R., Korja, A., Nironen, M. 2005: Paleoproterozoic tectonic evolution. Developments in Precambrian Geology, 14, 481-531.

Leskelä, T. 2019: Geochemistry, age and structural character of the Au-hosting Uunimäki gabbro, SW Finland, 84 pp.

Ludwig, K. R. 2003: User's manual for IsoPlot 3.0. A Geochronological Toolkit for Microsoft Excel, 71 pp.

McCuaig, T. C., Kerrich, R. 1998: P—T—t—deformation—fluid characteristics of lode gold deposits: evidence from alteration systematics. Ore Geology Reviews, 12, 381-453.

Mertanen, S., Karell, F. 2011: Rock magnetic investigations constraining relative timing for gold deposits in Finland. Bulletin of the Geological Society of Finland, 83, 75-94.

Mertanen, S., Karell, F. 2012: Paleomagnetic and AMS studies on Satulinmäki and Koijärvi fault and shearzones. Gold in Southern Finland: Results of GTK Studies 1998-2011. Geological Survey of Finland, Special Paper, 52, 195-226.

Mäkitie, H., Kärkkäinen, N., Sipilä, P., Tiainen, M., Kujala, H., Klami, J. 2016: Hämeen vyöhykkeen granitoidien luokittelua. Geological Survey of Finland, Archive Report 33. 146 pp.

Nironen, M. 1999: Structural and magmatic evolution in the Loimaa area, southwestern Finland. Bulletin of the Geological Society of Finland, 71, 57-71.

Nironen, M., Korja, A., Heikkinen, P. 2006: A geological interpretation of the upper crust along FIRE 2 and FIRE 2A. Finnish Reflection Experiment FIRE, 2005, 77-103.

Nironen, M., Kousa, J., Luukas, J., Lahtinen, R. 2016: Geological Map of Finland: Bedrock 1: 1,000,000. Geological map of Finland.

Ojala. V. J. 2008: Geological Survey of Finland (GTK). Hankeraportti. Hanke 2801008 Suomen kultaesiintymien tutkimus. Loppuraportti, 16 pp.

Patchett, P.J., Kouvo, O. 1986: Origin of continental crust of 1.9-1.7 Ga age; Nd isotopes and U-Pb zircon ages in the Svecokarelian terrain of South Finland. Contributions to Mineralogy and Petrology, 92, 1–12.

Passchier, C. W., Trouw, R. A. 2005: Deformation mechanisms. Microtectonics. Springer Science & Business Media. 25-66.

Pietikäinen, K. J. 1994: The geology of the Paleoproterozoic Pori shear zone, Southwestern Finland, with special reference to the evolution of veined gneisses from tonalitic protoliths. Ph.D. thesis, Michigan Technological University. 129 pp.

Ramsay, J.G., Huber, M.I. 1987: The Techniques of Modern Structural Geology. Folds and Fractures, London: Academic Press, 2, 391 pp.

Rasilainen, K., Eilu, P. 2016: Assessment of undiscovered mineral resources of copper, zinc, nickel and gold for the Häme Belt. Geological Survey of Finland, Archive Report 94, 58 pp.

Reimers, S., Engström, J., Riller, U. 2018: The Kynsikangas shear zone, Southwest Finland: Importance for understanding deformation kinematics and rheology of lower crustal shear zones. Lithosphere 2018: Tenth Symposium on Structure, Composition and Evolution of the Lithosphere. Programme and Extended Abstracts, Turku, Finland, Nov. 14th-16th. Institute of Seismology, University of Helsinki, Report S-62, 95-99.

Saalmann, K., Mänttäri, I., Ruffet, G., Whitehouse, M. J. 2009: Age and tectonic framework of structurally controlled Palaeoproterozoic gold mineralization in the Häme belt of southern Finland. Precambrian Research, 174, 53-77.

Saalmann, K., Mänttäri, I., Peltonen, P., Whitehouse, M. J., Grönholm, P., Talikka, M. 2010: Geochronology and structural relationships of mesothermal gold mineralization in the Palaeoproterozoic Jokisivu prospect, southern Finland. Geological Magazine 147, 551-569.

Singer, D. A., Menzie, W.D. 2005: Statistical guides to estimating the number of undiscovered mineral deposits: an example with porphyry copper deposits. In: Cheng, Q. & Bonham-Carter, G. (eds). Proceedings of IAMG – The annual conference of the International Assoc. for Mathematical Geology. Geomatics Research Laboratory, York University, Toronto, Canada. 1028–1033.

Sipilä, P., Kujala, H., 2014: Hämeen vyöhykkeen vulkaniittien geokemia. Geological Survey of Finland, Archive Report 119, 23 pp.

Stipp, M., Stünitz, H., Heilbronner, R., Schmid, S. M. 2002: The eastern Tonale fault zone: a 'natural laboratory'for crystal plastic deformation of quartz over a temperature range from 250 to 700 C. Journal of Structural Geology, 24, 1861-1884.

Tandon, R. S., Gupta, V., Sen, K. 2015: Seismic properties of naturally deformed quartzites of the Alaknanda valley, Garhwal Himalaya, India. Journal of Earth System Science, 124, 1159-1175.

Tiainen, M., Kujala, S., Ahtola, T., Eilu, P., Grönholm, S., Hakala, O., Istolahti, P., Jumppanen, A., Kärkkäinen, N., Rasilainen, K., Törmä, H. 2017: Kanta-Hämeen potentiaalisten kaivosten aluetaloudelliset vaikutukset. Summary: Regional economic impacts of potential mining in Kanta-Häme. Geological Survey of Finland, Report of Investigation, 229, 124 pp

Torvela, T., Mänttäri, I., Hermansson, T. 2008: Timing of deformation phases within the South Finland shear zone, SW Finland. Precambrian Research, 160, 277-298.

Vaasjoki, M., Korsman, K., Koistinen, T., 2005: Chapter 1: Overview. In: Lehtinen, M. & Nurmi, E.A. The Precambrian Geology of Finland- Key to the Evolution of the Fennoscandian Shield. Elsevier B.V., Amsterdam, 1-18.

Van Achterbergh, E., Ryan C., Jackson, S., Griffin W. 2001: Data reduction software for LA-ICP-MS, In: Laser-Ablation ICPMS in the Earth Sciences–Principles and applications. Mineralogical Association of Canada short course series, 29, St John, Newfoundland, 239-243.

Väisänen M., Mänttäri I. Hölttä P. 2002: Svecofennian magmatic and metamorphic evolution in southwestern Finland as revealed by U-Pb zircon SIMS geochronology. Precambrian Research 116, 111-127.

Väisänen, M., Skyttä, P. 2007: Late Svecofennian shear zones in southwestern Finland. GFF, 129, 55–64.